Martin Appiah Kesse

ARTIFICIAL INTELLIGENCE: A MODERN APPROACH TO INCREASING PRODUCTIVITY AND IMPROVING WELD QUALITY IN TIG WELDING

Martin Appiah Kesse

ARTIFICIAL INTELLIGENCE: A MODERN APPROACH TO INCREASING PRODUCTIVITY AND IMPROVING WELD QUALITY IN TIG WELDING

Dissertation for the degree of Doctor of Science (Technology) to be presented with due permission for public examination and criticism in room 1316 at Lappeenranta-Lahti University of Technology LUT, Lappeenranta, Finland on the 29th of July 2021, at noon.

Supervisors   Associate Professor Huapeng Wu
              LUT School of Energy Systems
              Lappeenranta-Lahti University of Technology LUT
              Finland

              DSc (Tech) Tuomas Skriko
              LUT School of Energy Systems
              Lappeenranta-Lahti University of Technology LUT
              Finland

Reviewers   Emeritus Professor Suck-Joo Na
              Department of Mechanical Engineering
              Korea Advanced Institute of Science and Technology
              South Korea

              Professor Yanhong Wei
              Lab of Welding technology
              Nanjing University of Aeronautics and Astronautics
              China

Opponent   Emeritus Professor Suck-Joo Na
              Department of Mechanical Engineering
              Korea Advanced Institute of Science and Technology
              South Korea

Abstract

Recent years have seen the welding industry facing demands for improved productivity and efficiency together with simultaneous enhancement of the quality of welded structures. The welding industry has met these challenges by developing novel alloys, increasing the level of automation, and expanding the use of dissimilar welding. The utilization of materials with complicated chemical composition necessitates a detailed understanding of material behaviour and how the materials can be combined while ensuring structural integrity. Suitable joining methods for both thick and thin plates are required, as is effective control of joining processes and related technology. A key aspect of welding control is understanding of the dynamics and interactions of the various parameters associated with welding processes and procedures.

Recent developments in artificial intelligence (AI) modelling tools have led to a vision of AI removing the element of human mechanical effort from welding operations. Various AI-based methods have been developed and applied with the aim of attaining good mechanical properties and improving weld quality. These approaches include design of experiment (DoE) techniques and algorithms, conventional regression analysis and the use of computational networks, including neural networks and fuzzy logic. In welding technology, these methods have primarily been used to optimise different welding parameters. Although researchers have found neural networks to be a better approach for optimisation than other available alternatives, it is, however, a black box approach. Consequently, it is difficult to ascertain how the algorithm arrives at a decision, which is knowledge of importance for human welders and future development of welding techniques and technology. The question then becomes: Can an AI model be developed that overcomes this deficiency?

This PhD dissertation aims to contribute to the state-of-the-art in terms of knowledge of the applicability of AI in welding technology by developing an AI framework using an ANFIS and fuzzy deep neural network from which it is possible to ascertain the underlying decision-making logic as an alternative method to predict welding parameters for optimisation of the welding process.

To meet the objective of the work, an in-depth understanding of different welding and optimisation processes is first required. Methodologically, a comprehensive literature

review approach and experimental work are used as the basis for suggesting the proposed AI framework. The AI framework for welding technology was designed using a fuzzy deep neural network, which is a combination of fuzzy logic and a deep neural network. The fuzzy logic and deep neural network are incorporated into the framework with a Likert scaling strategy. In normal practice, AI decision-making tools using deep learning techniques require big data from which to learn. For welding applications, obtaining this big data is challenging, because of the laborious and costly nature of welding experiments, and limited experimental data is thus available. The added value of the work in this study is that the AI approach used overcomes the limitation of the big data requirement. Where big data is not available for the algorithm to learn from, the system can mathematically manipulate the small data using its inference engine and extract its own big data from the available small data using the technique of data augmentation.

The AI framework was developed, validated and tested with the TIG welding process to predict weld bead geometry. The results showed a predictive accuracy of 92.59% when compared to results from a real experimental welding data set.

It is expected in the future that this created model will help the welder to bypass trial and error during the selection of welding parameters when welding. This model can be part of the standard welding procedure document to help the welder when performing welding works. This tool will also be useful for industries in the welding sector and can be used for educational purposes.

Acknowledgements

Finally, my sincere appreciation is expressed to my immediate family, my treasured wife, Zita Appiah Kesse, for all the encouragement, forbearance and understanding exercised during this research.

I feel blessed, thank you all.

Martin Appiah Kesse
July 2021
Lappeenranta, Finland

To Dedication

Dedicated to God almighty and to my mother Salome Appiah and my late father Daniel Kesse for teaching me love, respect, honesty, the value of hard work and belief in God, and in recognition of their devotion and efforts keeping the family on the right track.

Contents

List of publications

This dissertation is based on the following papers. The rights have been granted by publishers to include the papers in dissertation.

I. **Kesse Martin**, Kah Paul, Martikainen Jukka. Investigations into enhanced TIG welding processes (2015), International Conference Mechanika 2015, proceedings of 20th International Scientific Conference, Kaunas

II. **Kesse Martin Appiah**, Gyasi Emmanuel Afrane, Kah Paul. Usability of Laser-TIG Hybrid Welding Processes (2017) Proceedings of the Twenty-seventh (2017) International Ocean and Polar Engineering Conference

III. Gyasi Emmanuel Afrane, Kah Paul, Wu Huapeng, **Kesse Appiah Martin**. Modelling of an artificial intelligence system to predict structural integrity in robotic GMAW of UHSS fillet welded joints (2017), International Journal of Advanced Manufacturing Technology

IV. **Kesse, M.A.**; Buah, E.; Handroos, H.; Ayetor, G.K. Development of an Artificial Intelligence Powered TIG Welding Algorithm for the Prediction of Bead Geometry for TIG Welding Processes using Hybrid Deep Learning. Metals 2020, 10, 451.

Author's contribution

I was the principal author and investigator in papers I, II and IV. In paper III, I was the co-author and I assisted in performing the experiments and the evaluation of the findings of the experiments, as well as reviewing and improving the paper.

Other scientific publications

➢ Layus, P., Kah, P., **Kesse, M.,** Gyasi, E.A. (2017). Submerged arc welding productivity in welding thick high strength steel plates used for Arctic applications. Proceedings of the Twenty-seventh (2017) International Ocean and Polar Engineering Conference, San Francisco, USA, June 25-30, pp. 92-98.

➢ Sammy-Armstrong Atta-Agyemang, **Martin Appiah Kesse,** Paul Kah and Jukka Martikainen (2015). Improvement of strength and toughness: The effect on the weldability of high-strength steels used in offshore structures. Proc IMechE Part B: J Engineering Manufacture 1–8, IMechE 2015, DOI: 10.1177/0954405415600366

➢ Gyasi, E.A., Kah, P., Ratava, J., **Kesse, M.A.,** Hiltunen, E. (2017). Study of adaptive automated GMAW process for full penetration fillet welds in offshore steel structures. Proceedings of the Twenty-seventh (2017) International Ocean and Polar Engineering Conference, San Francisco, CA, USA, June 25-30, pp. 290-297.

- G. K. Ayetor, Albert K. Sunnu & **M. A. Kesse** (2019). Engine performance and emissions of fuel produced from palm kernel oil. Biofuels, DOI: 10.1080/17597269.2019.1672006.

Nomenclature

In the present work, variables and constants are denoted using *slanted style*, vectors are denoted using **bold regular style**, and abbreviations are denoted using regular style.

Latin alphabet

A	area	m^2
c_p	specific heat capacity at constant pressure	J/(kgK)
c_v	specific heat capacity at constant volume	J/(kgK)
d	diameter	m
$\mathbf{F}$	force vector	N
f	frequency	Hz
g	acceleration due to gravity	m/s^2
h	heat transfer coefficient	$W/(m^2K)$
h	enthalpy	J/kg
$\mathbf{j}$	flux vector	m/s
L	characteristic length	m
l	length	m
M	torque	Nm
m	mass	kg
N	number of particles	–
$\mathbf{n}$	unit normal vector	–
p	pressure	Pa
r	radius	m
T	temperature	K
t	time	s
q_m	mass flow	kg/s
V	volume	m^3
v	velocity magnitude	m/s
$\mathbf{v}$	velocity vector	m/s

Greek alphabet

α	alfa
β	beta
Γ	capital gamma
γ	gamma
Δ	capital delta
δ	delta
ε	epsilon
ϵ	epsilon variant
ζ	zeta
η	eta

Θ	capital theta
θ	theta
ϑ	theta variant
ι	iota
κ	kappa)
λ	lambda
μ	mu
ξ	xi
π	pi $\pi = 3.14159...$
Σ	capital sigma
σ	sigma
τ	tau
Φ	capital phi
ϕ	phi variant
φ	phi
Ψ	capital psi
ψ	psi
Ω	capital omega
ω	omega

Abbreviations

AC	Alternating Current
AI	Artificial Intelligence
ANFIS	Adaptive neuro fuuzy inference system
ASME	American Society of Mechanical Engineers
ANN	Artificial Neural Network
BM	Base Metal
CFD	Computational fluid dynamics
CMT	Cold Metal Transfer
CTWD	Contact Tip to Work Distance
2D	Two dimensional
3D	Three dimensional
DC	Direct Current
DCEN	Direct Current Electrode Negative
DCEP	Direct Current Electrode Positive
DHAZ	Depth of heat affected zone
DoE	Design of Experiment
DNN	Deep Neural Network
DP	Depth of Penetration
FCAW	Flux Cored Arc Welding
FZ	Fusion Zone
GBF	Grain Boundary Ferrite
Gfr	Gas Flow Rate
GMA	Gas Metal Arc Welding

HAZ	Heat Affected Zone
HD	Hydrogen Concentration
HFDL	Hybrid Fuzzy Deep learning
HFDNN	Hybrid Fuzzy-Deep Neural Network
LES	Large eddy simulation
LTHW	Laser TIG Hybrid Welding
MF	Membership Function
MMA	Manuel Metal Arc Welding
MIG	Metal Inert Gas Welding
MLP	Multi- Layer Perception
PDF	Probability density function
TIG	Tungsten Inert Gas
PA	Flat (fillet weld)
PB	Horizontal (fillet weld)
UHSS	Ultra High Strength Steel
WHAZ	Width of Heat of Affected Zone
WPS	Welding Procedure Specification
Wfs	Wire Feed Speed
Ws	Welding speed
WZ	Weld Zone

1   Introduction

This doctoral dissertation work presents findings of investigations at the Department of Mechanical Engineering of Lappeenranta-Lahti University of Technology LUT which formed a part of efforts to promote research on the applicability of artificial intelligence in welding technology with the long-term aim of using AI to improve welding outcomes.

The goal of this introductory chapter is to present the research context and research problem that led to this doctoral study. The chapter is divided into two sections. The first part presents the research background, research problem, motivation for the research, research objectives and research questions. The second section consists of an overview of the work, the impact on society and the environment, the limitations of the work and an outline of the thesis.

1.1   Background

The demand to simultaneously improve productivity, efficiency and weld quality of welded structures has presented the welding industry with many challenges. Additionally, the many different production methods used and the many different materials with complicated chemical compositions have made it necessary to gain a proper understanding of how these materials can be joined while maintaining and enhancing structural integrity. Welding of both thick and thin plates is widely used in industry and has become an essential aspect of the modern world. Welding processes and procedures thus need to respond to the trend of new developments in welding technology, new metals and alloys, and new applications for welded structures. Quality welding is a challenging task because of the dynamics and interactions of the many factors involved. These challenges are usually encapsulated in the issue of how to control the various parameters associated with the welding process.

Characteristically, a welding setup either allows the welder to choose the parameters, which places a significant burden on the welder to program the setup, or the setup is partly pre-programmed with the welder having limited access to the process parameters. Both approaches create challenges for the welder. In both cases, there is an assumption that the welder has sufficient knowledge about the physical science of welding to make necessary changes to welding parameters during welding to correct any unwanted situation; however, such knowledge cannot always be guaranteed. Moreover, systems that are easy to program generally do not provide the adaptability necessary to correct undesirable situations during welding (Smart, 1993).

(Clark, 1985) investigated the effects of welding heat input per unit length on the weldability of low carbon steel geometry. In his findings he noted that heat input can be used as an independent variable for controlling the dimensions of the weld bead geometry. In addition, with the same value of heat input the weld has an identical cooling time and an identical microstructure of HAZ. However, other researchers (Chen S. Z., 2016) (Liu

Y. K., 2013) (Kiaee, 2014) are of the view that welding variables such as current, voltage and travel speed have a specific influence on output variables of the weld, namely HAZ dimensions, weld bead geometry and microstructure.

Various methods have been tested and applied in the search for a solution to challenges related to the mechanical properties of welded joints and in efforts to achieve excellent mechanical properties. These approaches include Design of Experiment (DOE) techniques and algorithms, and the use of computational networks such as neural network and fuzzy logic. Design of Experiments is a technique that is used to generate the information required with a minimum amount of experimentation by applying experimental limits and specific experimental conditions and mathematical investigation to predict the response at any point (Harold, 2014).

The primary aim of the various methods is optimisation of the different parameters in the welding process. For example, (Dutta, 2007), who carried out modelling of a Tungsten Inert Gas (TIG) welding process using conventional regression analysis and neural network-based approaches, concluded that the neural network approach is superior to conventional analysis since neural network-based approaches can carry out interpolation within a certain range. As mentioned earlier, the black box nature of neural networks has been a fundamental limitation. It was claimed that the cause of the better performance lies in the neural network-based approach being able to carry out interpolation within a certain range.

However, the neural network approach has a significant limitation, in that it is a black box algorithm, and it is thus difficult to ascertain how it reaches a decision, which is important information for human welders. This problem can be overcome by using fuzzy deep learning (also known as fuzzy-deep neural networks). In fuzzy deep learning, fuzzy logic is incorporated into the learning process of multiple neural network algorithms to form what is called a Deep Neural Network (DNN) (Buah, 2020).

Despite widespread awareness of the weaknesses of black box approaches, to the best of my knowledge, contributions in the field of welding have to date focused predominately on fuzzy logic, neural networks, neuro-fuzzy logic and deep neural networks. In research of these approaches, it has been found that neuro-fuzzy technology is able to address the interpretability-accuracy trade-off, but neuro-fuzzy systems are shallow networks and limited in terms of their ability to capture the complexities in a process, unlike current-state-of-the-art deep neural network algorithms. It is in this regard that this doctoral study aims to contribute to advancing the state-of-the-art of AI techniques. The objective is to build an AI model based on Hybrid Fuzzy-Deep Neural Network (HFDNN) architecture. This hybridisation leads to an AI model that is not only accurate but inherently interpretable for human welders to aid them in carrying out their tasks efficiently and effectively.

1.2   Research problem

In welding operations, the challenges encountered are usually related to improper control of various parameters associated with the welding process. Generally, a welder, based on experience gained over several years of welding, selects a set of parameters that could produce fairly good results. The trial and error inherent in this approach can be averted if an appropriate automation tool can be created that can predict the output from a set of defined parameters. Such a tool can help improve weld quality by improving the predictability of weld outcome and thus limiting defects in welded joints.

In welding research, the aim when applying earlier mention methods is for optimisation of the different parameters. Scholars have attempted to solve the issue of the nature of black box by using neuro-fuzzy logic. This approach has its merits, but it is a shallow network, and evidence has shown that such networks can be improved by increasing their depth. However, when the problem becomes complex, the accuracy of neuro-fuzzy logic diminishes. An alternative method is to use a deep neural network, but the use of deep neural networks makes it difficult to explain how the algorithm reaches a decision, which is an important information for a human welder. Furthermore, the combination of welding processes (hybrid welding) to improve the welding process performance creates complexity as regards the process variables. The complexity of the combination creates more welding parameters. In view of these challenges, the research problem can be formed as a question of how the welding process can be improved by applying artificial intelligence to control welding parameters?

1.3   Research objectives and motivation

The objective of this dissertation started with the aim of investigating variants of TIG welding processes and the benefits they bring regarding the weldability of non-ferrous and ferrous metals and examining possible ways to increase the productivity and quality of TIG welding. The study then moved on to applying the findings experimentally in investigation of the viability of utilising AI in modelling of the structural integrity of welded joints. Finally, AI was used in building a model that can help a human welder predict welding parameters and produce good welding output.

The motivation for this research came about due to recent developments in sensing systems for advanced welding technology and a desire to use AI to reduce the role of trial and error when welders select welding parameters. Accurate selection of welding parameters will go a long way to improving weld quality.

1.4   Research questions

The research objectives and motivations led to the formulation of the following research questions:

1. Why is there a need for different variants of the TIG welding process and what are their benefits as regards the weldability of non-ferrous metals? This question is reviewed and addressed in Publication I. The findings to this question led to the next question:
2. Where can the Laser-TIG Hybrid Welding (LTHW) process best be used and why? After critical analysis and investigation into the use of LTHW, presented in Publication II, a need arose to look at the important issue of the structural integrity of welded structures in terms of weld quality, which led to the next research question:
3. How can AI be used in welding modelling to predict the structural integrity of the welded structure? This topic is addressed in Publication III, and the findings led to the final question:
4. How can an AI model based on Hybrid Fuzzy-Deep Neural Network (HFDNN) architecture help human welders avoid the use of trial and error during selection of welding parameters? This topic is addressed in Publication IV.

1.5   Scope and limitations of study

The scope of this dissertation can be considered as being in the area of the productivity benefits of different variants of the TIG welding process, their applicability in welding of ferrous and nonferrous metals, and the possibility of using AI approaches to enhance productivity and weld quality. Welding productivity can simply be defined as the ability to weld faster with more arc-on time and less welding. Given that it is a cost-effective manufacturing process, several factors can increase cost effectiveness and productivity in welding. Factors ranging from operational efficiency to the use of consumables may affect welding productivity. To reduce welding cost and increase productivity the following must be considered: employing automation, applying the right welding processes, arrange materials properly, prepare joints and gaps properly and control the use of consumables. Recent adaption of automation and enhancement of technology through autonomous systems that are powered by machine learning and data plays an important role in improving on welding productivity. The study is limited to the following:

i. The literature review is limited to variants of the TIG welding process and their benefits; additionally, new developments and their applicability are discussed.

ii. The study of hybrid welding is limited to the Laser-TIG Hybrid welding (LTHW) process and its usability.

iii. The study on AI in modelling structural integrity is limited to robotic GMAW on UHSS fillet joints.

iv. The experimental simulation study on the applicability of AI in control parameters is limited to the effect of control parameters on predicting weld bead geometry using hybrid fuzzy deep neural networks. In addition, investigation into how adaptive neuro fuzzy systems can model and predict welding output is examined.

v. Testing the algorithm to validate its effectiveness compared to real welding experimental data.

1.6   Overview of the work

Industries like the aerospace, shipping, construction, and oil and gas industries have in recent years been looking for new ways to maximise profit. One way is using lighter materials in their products, which enables energy savings, improved safety and enhanced performance. Consequently, industries are making more use of thin sheets (less than 10mm) in their production, e.g., adoption of UHSS, greater use of dissimilar welding etc. however, producing welded structures from thin sheets is challenging. TIG welding is known to weld thin sheets with better results than for example GMAW, but one major challenge is low productivity. The relatively low productivity of the TIG welding process has led to the development of variants of the TIG welding process that attempt to address the issue.

This study is divided into two main parts: Firstly, investigation of variants of the TIG welding process such as TIP TIG, TOPTIG and A-TIG, and secondly, the issue of productivity improvement, which is investigated by looking at methods such as control algorithms and optimisation of the process using artificial intelligence. Figure 1 illustrates the framework of the dissertation. The optimisation and control of parameters are investigated by applying a Hybrid Fuzzy-Deep Neural Network (HFDNN) that combines information from both fuzzy logic and neural networks. Knowledge gained from study of the two elements of TIG welding and optimisation with a HFDNN are fused together to generate the findings of the study.

The principle of the TIP TIG welding process is that the preheated and oscillating filler wire are guided directly into the weld pool to optimize and control heat input and improve degasification. This drastically enhances weld quality and considerably increases welding speeds. The main advantage of the TIP TIG hotwire process compared to those using a fusible electrode lies in the fact that TIP TIG welding allows a managed separation of the quantity of arc energy and the quantity of filler material introduced into the welding pool.

TOPTIG is a new TIG robotic welding process that combines the high weld quality of TIG process and the productivity of the MIG welding process. The defining characteristic of the process is the configuration of the torch: the weld wire which is fed directly into the arc zone at higher temperatures which ensures continuous liquid-flow transfer as well as high deposition rate.

The principal of the A-TIG welding process involves a method of increasing the penetration capability of the arc in TIG welding process (Lucas, 1996). This is achieved by depositing a thin coating of activating flux material on the workpiece surface before welding. The effect of flux is believed to constrict the arc which increases the current density at the anode and the arc force action on the weld pool and to generate a positive temperature gradient of surface tension which induces an inward surface flow of liquid metal and hence increases the depth of penetration (Touileb, 2020).

The optimisation and control of parameters are investigated by applying a Hybrid Fuzzy-Deep Neural Network (HFDNN) that combines information from both fuzzy logic and neural networks. Knowledge gained from study of the two elements of TIG welding and optimisation with a HFDNN are fused together to generate the findings of the study.
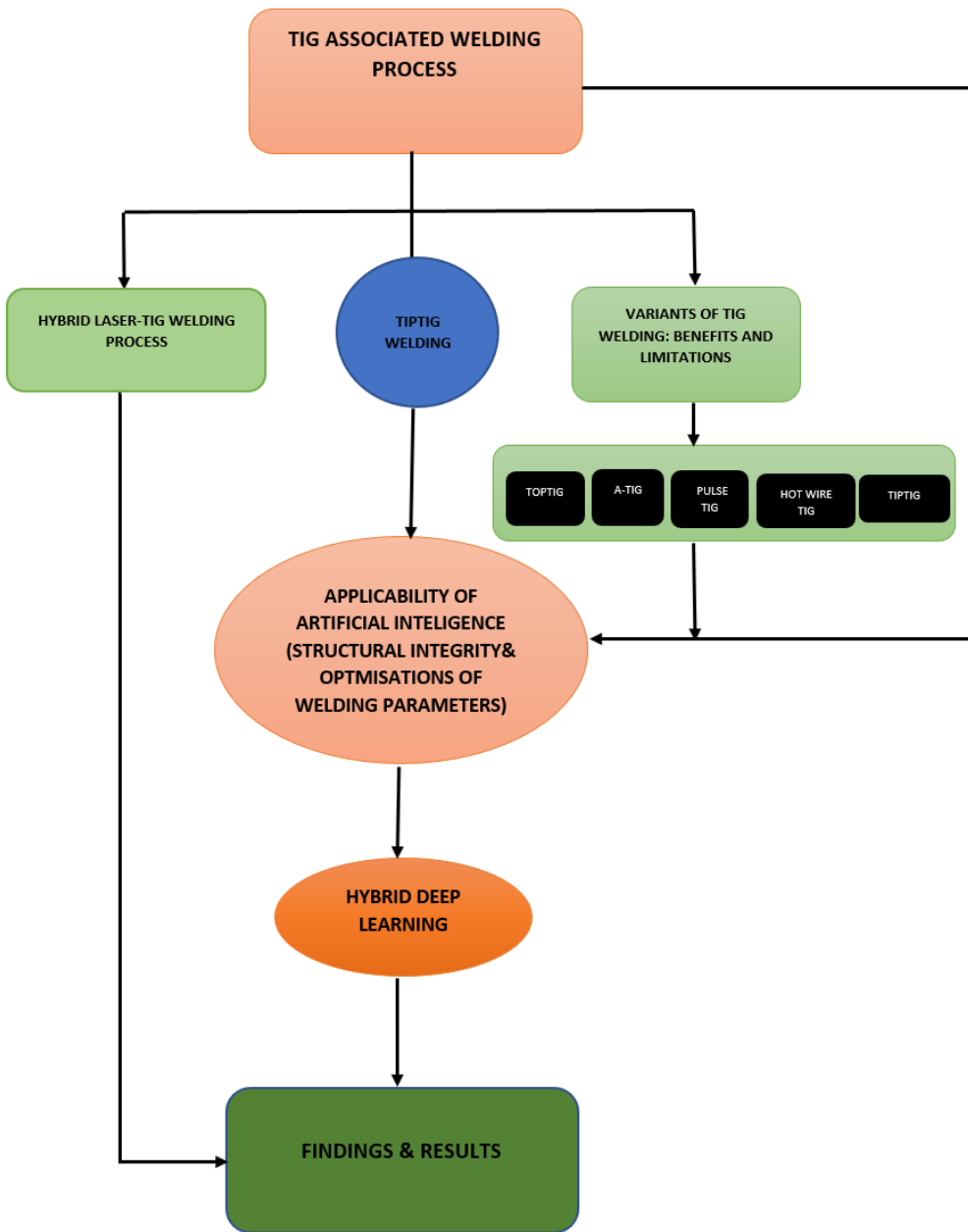
Figure 1.Illustrating Dissertation Framework.

1.7 Novelty value and scientific contribution

The AI-based method in this work is designed to use fuzzy deep learning incorporating Likert scaling. In normal practice, AI decision-making tools using deep learning techniques require big data from which to learn. For welding applications, obtaining this big data is challenging, because of the laborious and costly nature of welding experiments, and limited experimental data is thus available. The added value of the work in this study is that the AI approach used overcomes the limitation of the big data requirement. Where big data is not available for the algorithm to learn from, the system can mathematically manipulate the small data using its inference engine and extract its own big data from the available small data. The flexibility of using both small and big data is built on the inspiration from technique of data augmentation.

Additionally, the strength of the model used in this work is that it can explain its output. this therefore leads to an explainable AI system where the output of the decision is not only accurate but also interpretable. Hence, its application in the field of welding helps the welder to interpret how the algorithm arrived at a particular decision.

Another contribution to the state of the art is that the developed method is not deterministic, unlike traditional neural network and regression methods commonly used in the field of welding. For example, in a traditional system where a human welder selects the control parameters, a specific output is given. The proposed novel technique goes beyond this by giving the control parameter a maximum and minimum range in which a specific output can be achieved, which is discussed in more detail in Publication IV.

Also, the errors which occur as a result of applying the adaptive neuro fuzzy system (ANFIS) in the welding industry can be compensated for by applying ANFIS and DNN, which was tested in this study. Since ANFIS uses linear functions to generate the outputs, combining it with the DNN model helps to eradicate the issues of linearity functions, given that the welding industry uses non-linear parameters.

The work serves as background information for further research into building an AI model using HFDNN architecture as an aid to weld parameter prediction. As a contribution to the field of science, the dissertation provides an overview and in-depth knowledge of TIG welding, and the benefits acquired from recent developments in different variants of TIG welding processes. An example is the TIP TIG welding process, which has shown to increase productivity and produce welds of high quality. In the area of artificial intelligence, the dissertation demonstrates that AI usage is no longer limited to the boundaries of computer science but can be applied to welding technology for the practical task of controlling welding process parameters to optimise the process. An additional benefit of the AI-based approach is that it can control the nonlinearity inherent in the multi- input and output nature of welding, which helps the welder to carry out their work efficiently and effectively.

1.8 Impact on society and the environment

The benefits of scientific research are found in the knowledge it generates and the impact that this knowledge has on the world and society. A particular concern of current times is mitigating deleterious effects of modern technology and lifestyles on the environment and ensuring a sustainable future.

In the field of welding, the efficiency of a welding process plays an important role in selection of the most appropriate welding process. The process selected obviously influences the weld quality and economics of the welding, but there are other secondary effects. For example, the TIG welding process is known to generate less fumes compared to manual metal arc welding (MMA), gas metal arc welding (GMAW) and flux-cored arc welding (FCAW). Regarding this study, improved understanding of the variants of the TIG welding process will increase the knowledge base and thereby extend the areas of application of welding. Greater usage of welding as a joining method will create employment opportunities. The work presented in this dissertation enables improved selection of the right welding consumables and welding parameters, which has an effect on management of heat input; appropriate heat input is key to weld quality.

The structural integrity of welded structures is of enormous significance to society. Modelling of welding systems to guarantee structural integrity in welded materials can assist in understanding of associated phenomena, in addition to providing support for practical decision making. This study provides fundamental knowledge on the modelling of structural integrity that is beneficial to manufacturing industries.

1.9 Thesis outline

This dissertation consists of two parts: a summary of the research work and the papers published in conjunction with the investigation. The study includes experimental work and a literature review.

Chapter 1 introduces the work and presents the background to the dissertation. The research problem, research objectives and motivation, research questions, novelty value and scientific contribution are briefly described. In addition, an overview of the work, its impact on society, and the limitations of the work are given, and a thesis outline provided. Chapter 2 presents the state of the art in the utilisation of AI in welding. Important aspects of AI in the welding process are also considered. Chapter 3 presents the methodology used in this study. The simulation of experimental data is also presented, as are the input parameters used in the algorithm. Chapter 4 gives an overview of the research articles published as a part of this investigation. These articles and their findings form the centrepiece of this study. The observations and inferences are discussed in Chapter 5. Chapter 6 gives concluding remarks, and Chapter 7 presents suggestions for further work in the area.

2 State of the art of Artificial intelligence in welding process

The metal industry uses different methods to join metals together. The joint can be permanent or temporary, depending on the design and type of product. The area of application also influences the joining process. The welding process is usually used when it comes to permanent joints. In recent times, the systematic progress made in construction engineering, shipbuilding, petrochemical and oil processing companies and the drive for higher productivity and reduced costs in the welding industry has increased the demand for automation and robotisation (Anand, 2018). In addition, the increasing benefits derive from the use of automation such as safety concerns and the need to free welders from strenuous and repetitive conditions. Figure 2 illustrates the technical elements needed to configure a welding system that can help improve productivity and highly consistent weld quality (Ushio, 2009).
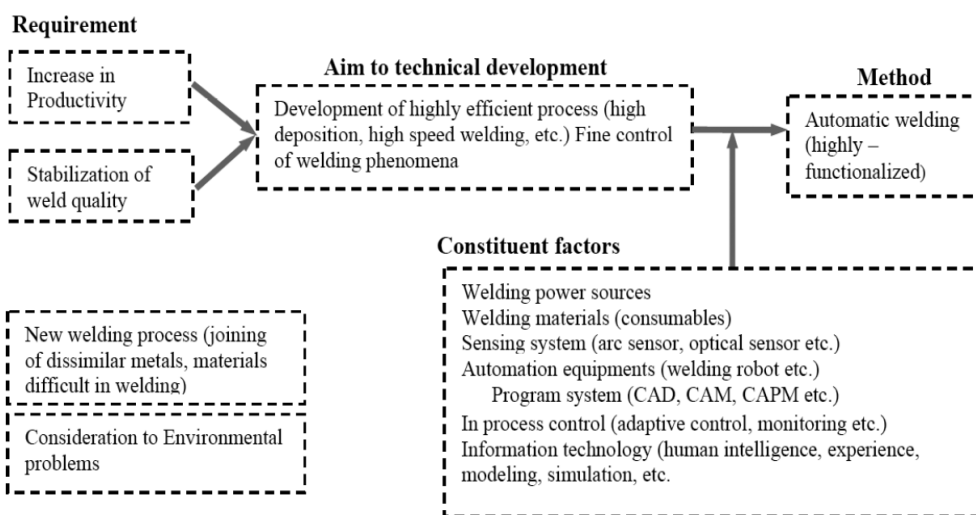
Figure 2. Requirements for welding production technology permitting its integration to automatisation (Eguchi, 1999).

To achieve high quality welds, it is important that one can choose and control the welding parameters correctly. Numerous attempts have been made by several authors to understand and evaluate the effect of welding parameters on optimal bead geometry. These comprise numerical analysis, empirical models, theoretical studies and AI technology for welding applications (Ibrahim, 2012) (Park, 2002) (Vitek, 2001) (Jeng, 2000) (Kumar A., 2013; Anand, 2018) (Pashazadeh, 2016).

2.1   Hybrid welding Processes

Hybrid is a Latin word which means anything made by putting two different things together. In a hybrid welding process, the laser beam is combined with an arc welding process, creating an interaction between the molten pool created by the first and the secondary heat source. In addition, the hybrid process creates an interaction between the two heat sources. It must be noted that both heat sources are incidents in a single weld pool (Mahrle, 2006) (Bagger, 2005).

In the laser-arc hybrid welding process, since the laser beam usually has a high energy density, it therefore serves as the primary heat source, which enables deep penetration mode welding. On the other hand, the arc that acts as a secondary heat source improves on overall productivity, cost reduction and the versatility of the process, as well as the good quality of the resultant weld seam weld (Mahrle A., 2009).

Practically, the beam from any welding laser source, such as a diode, Yb fibre, Yb: YAG disk, CO_2 Nd:YAG, etc. can be combined with any arc process (GMAW, TIG, SAW, plasma) to form a hybrid process. However, the most common combinations of hybrid welding are the laser-TIG hybrid and laser-GMAW hybrid processes.

The laser-arc hybrid welding process compensates for the disadvantages of the two combined processes. When these two processes are combined, it offers advantages such as high welding speed, reduced deformation, deeper welding penetration, the ability to bridge relatively large gaps, and a capability to handle highly reflective material (Bagger, 2005) (Ishide, 2001).

Although laser beams and electric arcs are quite different welding heat sources, both work under a gaseous shielding atmosphere at an ambient pressure that makes it possible to combine these heat sources with a unique welding technique. In the work of (Tan, 2013), a welding simulation was carried out to analyse the weldability of dissimilar and similar materials using the laser-TIG hybrid welding process.

There are two basic configurations used in laser-arc hybrid welding: the laser leading hybrid process (the laser beam precedes the arc) (Rayes, 2004) (Uchiumi, 76-85) and the arc leading hybrid process (the arc precedes the laser beam) (Arias, 2005). Figure 3 presents a schematic representation of laser-arc hybrid welding process. The arrangements of these two welding processes in the hybrid welding process are discussed in Publication II, which also reviews the usability of the laser-TIG welding process.

In the work of (Vemanaboina, 2018), a three-dimensional finite element model was developed for butt joints for SS316L. The heat flux models of a double ellipsoidal surface heat flux in the TIG process and lateral heat to the thickness face in the laser process were used to model laser-TIG hybrid and were simulated. The results showed a uniform distortion along the weld with edge deformations. In addition, residual stresses were able to maintain structural integrity with a minimum safety factor of 1.3.

In Publication II, the investigation showed that a combination of two different processes that creates the hybrid process leads to a complex phenomenon, making it challenging to optimise the process. However, the application of AI and other simulation processes in recent times have proved to create an avenue to optimise welding parameters to improve on weld quality.
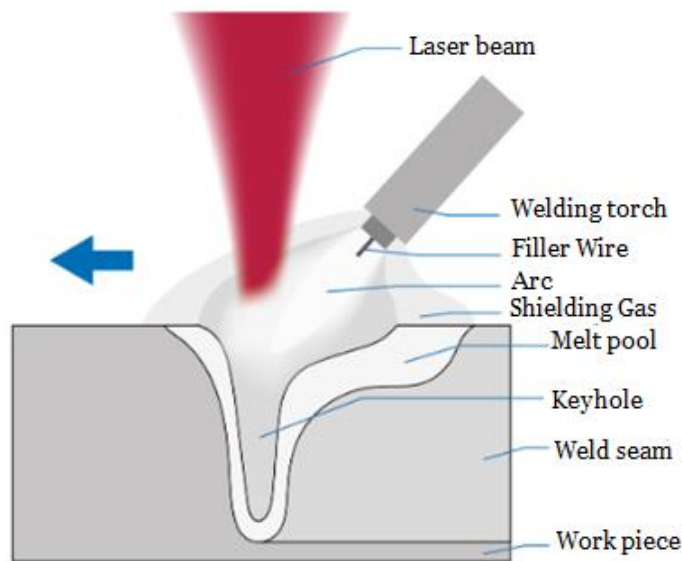
Figure 3. Schematic representation of laser-arc hybrid welding (Laserline, accessed on 3.8.2020).

2.2   Welding control system

Welding can be defined as a localised combination of weld pieces (metals or non-metals) produced by heating them to the welding temperature, either with or without the application of pressure, and filler metal can be added when needed. Figure 4 illustrates an open- and closed-loop control system. Figure 5 illustrates a schematic overview of different welding processes. In the control system a block diagram usually represents the various parts that come together to carry out an activity.
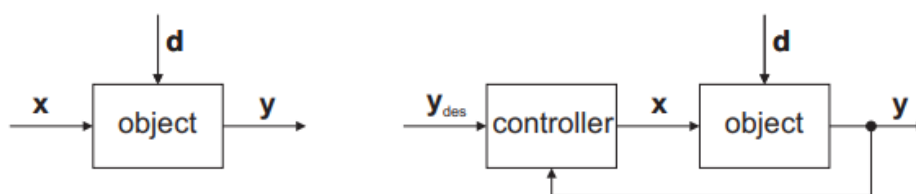
Figure 4. Illustrating an open- and closed-loop control system.

When this concept is mimicked in arc welding, the object is taken to be the welding process. The input vector x comprises all the parameters of the welding process. The parameters are welding voltage, distance between the electrode and the weld piece, electrode geometry, weld piece thickness and composition, shielding gas flow and composition, and so on (Podržaj, 2019).

Output vector *y* consists of the characteristics of the resultant weld, which is weld bead geometry, visual appearance, possible deformations, etc. The relationship between input and output can therefore be represented in theory by vector function *f* equation 1:

$$y = f(x) \tag{1}$$
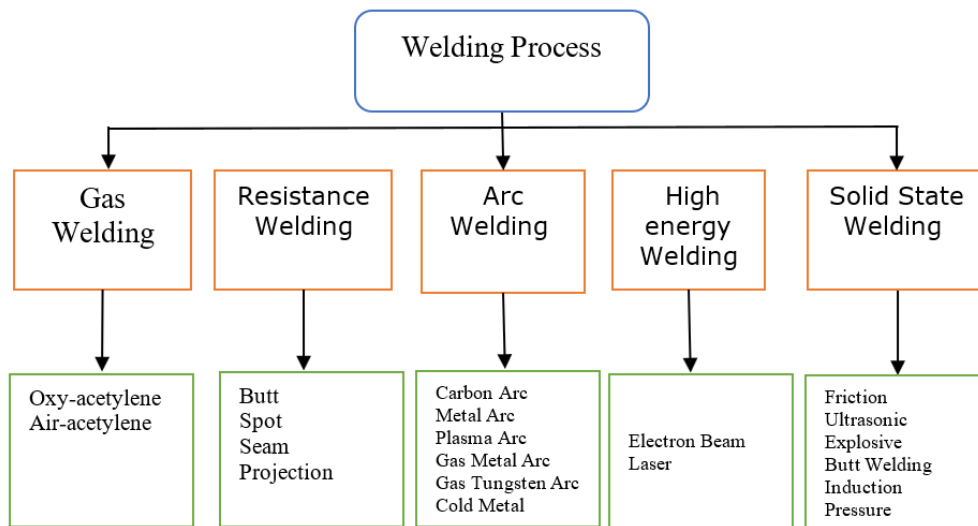
Figure 5. Overview of different welding processes (Vendan, 2018).

Although this function cannot be written, experience tells us that a proper combination of input parameters *x* usually results in an acceptable output *y*. The problem arises in situations where experience is limited or there are some signals that we cannot monitor or control due to disturbances, which are represented by *d*. Equation 2 can therefore be rewritten in the following format:

$$y = f(x, d) \tag{2}$$

In the closed-loop system, output y is measured, and the feedback is provided to the controller. The controller carries out a comparison test on the actual values y which are then transformed to the desired values y_{des} as illustrated in equation 3:

$$X = g(y_{des} - y) \tag{3}$$

In the domain of arc welding, the most used control systems algorithm is called the PID control algorithm (Henderson, 1993) (Chen, 2004) (Xu, 2012). In addition, fuzzy logic based on a control system is also used, such as neural networks (Zhao, 2001) (Wu, 2000) and the sliding mode control (Paul, 2016) .

2.3 Artificial Intelligence

AI can be described as a set of techniques that attempt to mimic the biological intelligence of humans which apply mathematics, computer science and other related subjects to enable it to reach its decision. The functions it performs include learning, reasoning and problem solving. Various techniques, such as artificial neural networks, fuzzy logic, adaptive neuro fuzzy and expert systems can be used for a variety of applications such as signal processing, the selection of nominal parameters and dynamic control. In the TIG and GMAW processes, robotic systems that integrate AI could perform functions like those carried out by human welders. AI is being utilised in many industries, such as medical technology (Holmes, AIME 2015) (Lopez, 2017), and in the area of security applications (Aikenhead, 2003). Its application is not limited to these areas but in the welding manufacturing and production industries, these data modelling approaches are gaining significance with ANN systems being popular for robotic TIG and GMAW processes. In Publication III a comparison between common artificial intelligence systems were made, showing their strength and weakness.

There has been an increase in the use of artificial neural network systems for the analysis and prediction of weld quality, as well as optimisation of welding parameters. The application of conventional adaptive control alone is not enough for the analysis and optimisation of welding parameters and quality of the welds. To improve on weld quality, various control constraints must be added for effective control of the welding process. The application of AI plays an important role in overcoming these constraints. Investigations have shown that AI can analyse data and predict the quality of welding. In the work carried out by (Hirai, 2001) on the detection of T-joint weld penetration using a hybrid neural network and fuzzy system, the results showed that the neural network system predicted the proper conditions for the weld geometry whilst the fuzzy model determined the proper welding conditions to avoid welding defects.

In general, the quality of a weld is characterised by parameters such as dimensions of penetration and structure of the material in the welded region. The structure, chemical composition and the weld pool geometry and heat-affected zone (HAZ) have a huge influence on the mechanical properties of the welded joint. The challenges and applicability AI bring to welding technology are the focus of this study.

2.4 Artificial neural network

ANNs represent a special type of machine learning algorithms that are modelled on the human brain. This implies that they learn from the data by providing responses in the

form of predictions, just like the neurons in our nervous system can learn from the past data.

This enables it to display a complex relationship between the inputs and outputs to discover a new pattern, as illustrated in Figure 6. The results at the output layer are achieved after rigorous computation by the middle layer. The output relates to the state of the neuron and its activation function (Yadav, 2015). The neuron behaves like a mapping function f (net) to produce an output y (either linear, sign, sigmoid or step function), which can be expressed as illustrated in equation 4. The use of the transfer function is for calculating the weighted sum of the inputs and the bias. One major advantage of ANNs is the fact that they can learn from the example data sets.
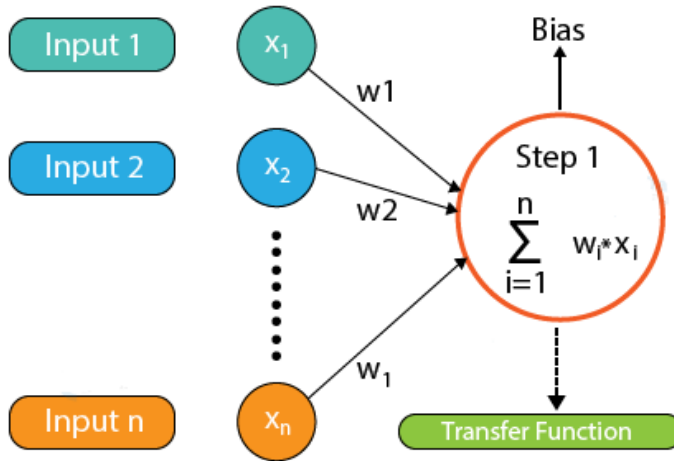
Figure 6. Illustration of input and middle layer combined with a transfer function (Team, 2019).

$$y = f(net) = f\left(\sum_{j=1}^{n} w_{ij} x_j + \theta\right) \tag{4}$$

where f represents the neuron activation function, θ represents the threshold value, xj represent the input, and wij the weight. With regards to nonlinear functions, the output y is usually expressed using a neuron transfer function, where input is mapped into values between +1 and 0 as illustrated in equation 5.

$$y = \frac{1}{1+e^{-Tx}} \tag{5}$$

In the work by (Kim, 2004), it was proven that the adjustment of the weights and biases can be derived according to the transfer function expressed in equation 6. In addition, the Levenberg-Marquardt learning algorithm provides numerical solutions that reduce error when solving complex boundary value problems, since it provides faster convergence

(Yadav, 2015). This therefore makes it more adaptable where precise welding variables and parameters are needed.

$$\Delta W = (JTJ + \mu I))^{-1} JTe \tag{6}$$

where J represents the Jacobian matrix of derivation of each error, µ represents the scalar, and e is error function.

2.4.1 Back propagation

To train the neural network, it is provided with examples of input and output data. The neural network is then trained and when it completes the training, it is tested without having been provided with the earlier data. The neural network then predicts the output and is evaluated to know which correct and various error functions are also identified. Finally, based on the result, the model adjusts its weight to optimise the system through the chain rule.

2.4.2 Types of Artificial Neural Networks

The two most important types of artificial neural networks are feedforward neural networks and feedback neural networks. In the feedforward ANNs, the flow of data moves in only one direction, which implies that the flow of information is from the input layer to the hidden layer and to the output. It should be noted that there are no feedback loops in the neural network. In the feedback ANNs, since the feedback loops form part of it, it helps create memory retention such as in the case of recurrent neural networks. These types of networks are more suitable for areas where the data is sequential or time-dependent (Team, 2019).

Other types of ANN, such as multi- layer perception (MLP), recurrent neural networks and radial basis neural networks, have also been applied in various fields. MLP, which combines the strength of feedforward neural networks and recurrent neural networks, is normally applied in the field of welding research. The MLP neural network is composed of many simple perceptron's in an ordered structure, which forms a feedforward topology creating one or more hidden layers between the input and output layers. The application of MLP utilising a neural network with a 3-3-3 system is illustrated in Figure 12 in Publication III. When MLP is used in determining an optimised set of weights, it applies learning algorithms such as resilient propagation, back propagation (BP) and Levenberg-Marquardt (Yadav, 2015).

In order to know the viability of an ANN system in welding technology, depth of penetration and bead width characteristics were predicted in an activated TIG welding process (A-TIG). The results showed that ANN can accurately predict weld bead and depth of penetration (Chokkalingham, 2010). Additionally, in the work of (Kim, 2004), weld bead width characteristics were investigated as a function of key process parameters in robotic GMAW. To verify the accuracy of the results of the ANN, it was compared

with actual robotic welding experiments in Publication III in this study. The results obtained from the ANN using a Levenberg-Marquardt learning algorithm were close to the actual values obtained from the robotic GMAW process.

2.5   Fuzzy logic

Fuzzy logic originated from the work of (Zadeh, Fuzzy set. Information and Control, 1965), which is based on the principles that there is uncertainty in small things in the world. These uncertainties are characterised by two traits, namely random and fuzzy. Zadeh came up with the term "fuzzy", which refers to something which is vague, obscure and inexact to imitate the notion of non-measurable human understanding and logic. A fuzzy set can be defined as a lot of groups that cannot be explicitly identified (Vonglao, 2017). This implies that fuzzy sets form a spine that creates more efficient and robust systems, which can resist all sorts of uncertainties and inaccuracies prevalent in the real world. The fuzzy sets are described by membership functions, fuzzy rules, fuzzification, inference system and defuzzification. Fuzzy set outputs are obtained in crisp form, as illustrated in Figure 7. The knowledge base is where the IF-THEN rules are set.
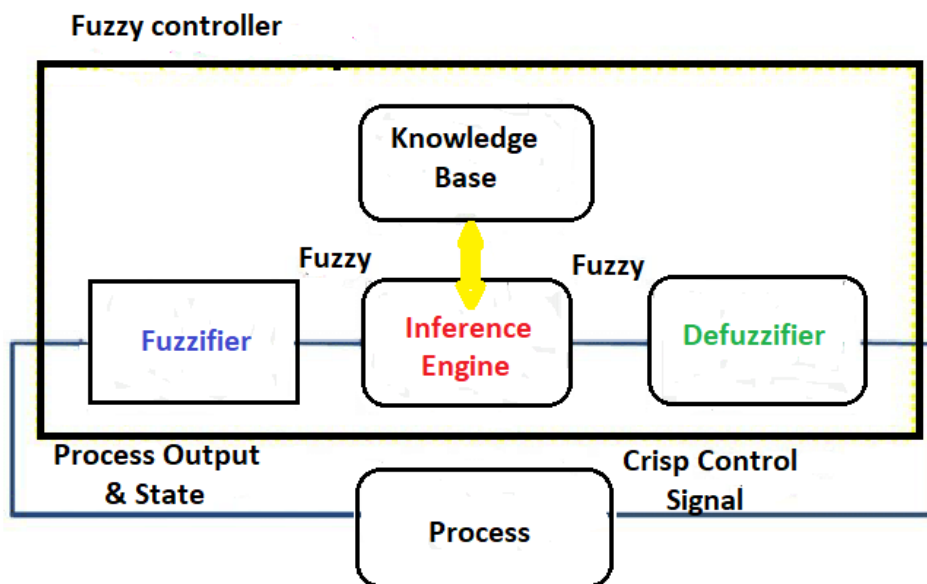

Figure 7. Block Diagram of Fuzzy Logic Controller (Zakariah, 2005)

Fuzzification:

Fuzzification is the process that transforms numerical values into a class of membership of fuzzy sets. Fuzzification converts the input or output signals into several fuzzy values

or fuzzy sets. In this stage, experts consider details concerning input, output and results. Thus, to decide how mutually the condition of each rule suits that specific input case, the fuzzification block must suit the input data with the condition of the rule. Membership function values can be set depending on the application (Patcharaprakiti, 2005).

Rule Base

The rule base usually depends on the operator's experience. In the case of welding technology, the rules are derived from the experience gained by trial and error during the welding process by the welder. As a result of the authorised relationship, both input and output changeable, based on membership function, are developed to count on that experience knowledge base. The structure of the control rule base is based on IF-THEN rules.

Defuzzification

The reverse of fuzzification is defuzzification. The transformation of fuzzified output into the normal crisp output is called defuzzification. This can be calculated as shown in equation 7 (Hon, 2013).

$$du = \left(\frac{\sum_{k=1}^{m} C(k)*W_k}{\sum_{k=1}^{n} W_k} \right) \tag{7}$$

where *du* is the change in control output, c(k) is the peak value of each output and *wk* is the weight of rule *k*.

The operation of a fuzzy system is based on a linguistic framework and its strength lies in its ability to handle linguistic information and perform approximate reasoning (Ross T. J., 2004) (Ross T. J., 2003). However, through the membership function it is possible to indicate the tendency of something to be a member of a set whose values range between 0 and 1. A membership function can be defined as a fundamental curve that defines how each point in the input crisp space is mapped to a membership. A practical clarification of an example of membership function is given by considering the speed values of a car ranging from 20 mph to 130 mph, with 20 mph and 130 mph being the extreme possibilities. The wide range of speed values of the car can only be adjudged if the speed of the car is put in the context of a fuzzy set applying the linguistic terms slow, medium and fast, which represent the sub-ranges of the car's speed (Mohammad, 2012).

Fuzzy systems operate on linguistics inputs. Therefore, in designing a fuzzy system it is important to first obtain a set of fuzzified inputs that suit the system to be designed.

It must be noted that when a membership value gets closer to 1, that can be termed high-level membership. A membership value closer to 0 is called low-level membership. If one

takes X as not an empty set, then x is any of X and A is a fuzzy set whose membership function is μ_A, so the fuzzy set A can be written in equation 8 as follows:

$$A = \{(x, \mu_A(x)) x \in X\}, \mu_A(x): X \to [0,1] \tag{8}$$

To identify the membership level for x, a membership function is used. Membership functions are of different types, but the type used in identifying the membership level usually depends on the suitability and important information from the expert (Vonglao, 2017). Membership functions can be categorised into different types, namely Gaussian trapezoidal, bell-shaped and triangular membership functions.

In the field of welding, since most welding techniques depend on process parameters applying fuzzy logic, it can learn the dependency of interaction between the process variables of the welding input and the output variables. As mentioned previously, the theory of fuzzy sets is valuable in experimental data modelling involving uncertainties that arise between the relationships of the process variables of the welding inputs and the subsequent bead geometry output.

2.6   Likert scaling

Rensis Likert introduced Likert scaling in 1932, and since then it has been the most widely used psychometric scale in survey research. In applying Likert, respondents are normally asked to indicate their levels of agreement with a declarative statement. For example, when a five-point Likert scale is applied, different agreement levels could be used for each scale point: 1=strongly disagree (SD), 2=disagree(D), 3=neither agree nor disagree (NN), 4=agree(A) and 5=strongly agree (SA). The agreement level use usually depends on what is being measured (Cheryl Quing, 2010). Various researchers have used the Likert scale to measure observable attributes. (Ohlsson, 2005) applied the Likert scale to measure fondness in music education, while (Buncher, 2006) applied it in pharmaceutics and (Seal, 2007) in patient advocacy in hospital.

The Likert scale is known to be easily constructed and modified. Additionally, the numerical measurement results acquired when Likert scales are used can be directly used for statistical inference. Lastly, the Likert scale has demonstrated a good reliability when it is used for carrying out measurements. Likert scaling can help researchers collect and analyse large quantities of data with less time and effort. Notwithstanding these advantages, Likert scales have several disadvantages (Qing, 2013).

One major problem that has been subject to debate in recent times is whether the Likert scale is ordinal or interval (Jamieson, 2004). Likert assumed that it has an interval scale quality. Interval scale can be defined as the differences between any two consecutive points which reflect equal differences in the variable measured. Researchers such as (Pett, 1997) (Hodge, 2003) considered that Likert scales are ordinal in nature. Challenges such as information loss or distortion, which occur as a result of the built-in limitations of the Likert method, have been recognised. In view of these challenges various researchers

have tried to solve these pitfalls. To solve the challenge with lost information, (Chang, 1994) discovered that when more scale points are used it may increase the measurement error due to respondents being confused by too many response categories. Additionally, (Chang, 1994) also indicated that longer responses will increase "laziness" in responding to various questionnaires.

(Albaum, 1997) also proposed a two-stage Likert scale in which the first stage measures the agreement that comprises the (agree/disagree) to a statement. On the other hand, the second stage measures the intensity of agreement, i.e., strong or weak. Even though a two-point Likert scale seems to capture more extreme positions than a traditional Likert scale, it has advantages in terms of design effectiveness, which reduces the central tendency effect. Nevertheless, it has not been proven how this method can collect more information between the extreme positions than the traditional method.

In recent decades, a novel Likert scale based on fuzzy sets theory has been proposed. This offers psychometricians a new interpretive algebra. That is ''a language that is half-verbal-conceptual and half-mathematical-analytical'' (Ragin, 2000). With this interpretive mathematical language, discrete ordinal variables can be transformed into a continuous variable that does not change its semantic meaning. This gives an advantage in capturing the interval details of ordinal variables in an open response format. This helps to reduce information loss and decreases information distortion during measurement.

2.7   Fuzzy Likert scale

As mentioned in the previous section, the Likert scale was incorporated into fuzzy logic to improve on it. The fuzzy Likert scale prevents information loss that occurs due to its ordinal nature and information distortion due to the closed response format.

Fuzzification of input variables and defuzzification of output variables forms the basis of the fuzzy Likert scale and establishes the causal relations between the input and output variables. The fuzzy Likert scale then transforms the actual response values into fuzzy values so that the fuzzy inference rules can be obtained.

The fuzzy Likert scale is design based on a set of membership functions that transforms the respondent's ideas on their agreement choices on the Likert scale. In applying a fuzzy Likert scale, the fuzzy set theory membership functions are usually developed based on empirical or expert knowledge.

In transforming the responses into fuzzy values, a set of isosceles triangular membership functions evenly distributed along the input continuum are adopted during the fuzzification procedure. A fuzzy Likert scale allows partial agreement to a scale point, and responses in this scale can be approximated to a decimal place. A fuzzy if-then rule is then applied to enable one to determine what fuzzy action to execute according to an input (Qing, 2013).

In Publication IV, a fuzzy Likert scale was applied in the field of welding technology to convert the incoming parameters into a fuzzy representation that is understood by the algorithm. Applying fuzzy logic-based technology enables the rescaling of the raw data from the human expert welder. This is then transformed into a fuzzy-driven feature as illustrated in Figure 6 in Publication IV. The advantage of applying this is that it can create the interval details that can be collected via data augmentation for training purposes.

2.8   Data Augmentation

Data augmentation is a commonly used method in deep learning to reduce the effect of overfitting, which helps to increase diversity in training data sets. Methods such generic data augmentation that includes flip, colour jittering, rotation, cropping and edge enhancement (Taylor, 2018) have been used for image classification tasks. In addition, complex data augmentation methods synthesise a new image from two training images (Inoue, 2018) or from Generative Adversarial Nets (GAN) (Antoniou, 2017).

In text classification, augmentation methods such as random insertion, random swap, synonym replacement and random deletion have been applied (Wei, 2019) and achieved the same accuracy as normal in all training data, even though only half of the training data is available.

During the application of data augmentation, value is added to the base data from the information derived from internal and external sources within the database. In addition, there is a reduction in the manual intervention required to help develop meaningful information and gain insight from the available data, as well as significantly enhancing data quality. this enables one to produce multiple copies of available data with slight variations.

To train deep learning models, typically big data sets are required, usually from manual data collection or from existing databases. However, in some cases only a limited data set is available. Therefore, to expand the size of the data set, data augmentation can be employed. In Publication IV, data augmentation was applied to expand an existing data set using only the available data so that the learning algorithm can more effectively extract those features essential to the task.

2.9   Adaptive Neuro-Fuzzy Inference System (ANFIS)

In the year 1993 Jang introduced a learning method for the inference system (FIS) that utilizes a NN learning algorithm during the construction of a set of fuzzy applying the if-then rules with suitable membership functions (MFs) from specified input–output pairs. Figure 8 illustrates the basic structure of ANFIS. ANFIS system can be described as a network structure consisting of several nodes which connects through directional links. Each node is categorized by a node function which includes an adjustable or fixed

parameter. In the Training phase of a NN the parameter values are determined in order to adequately fit the training data.
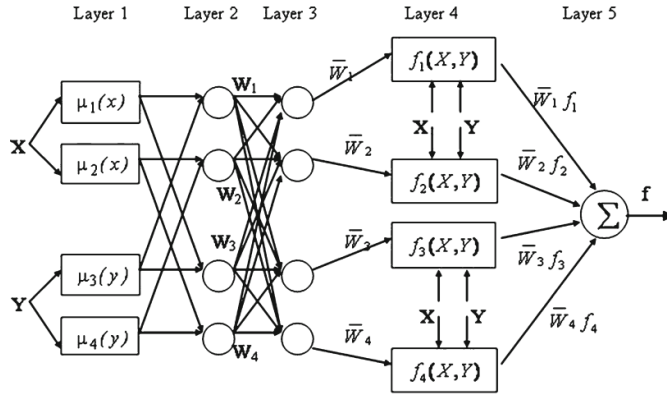
Figure 8. Basic structure of the ANFIS

In the ANFIs structure illustrated in Figure 8, x and y refer to inputs and f_2 represents the output variable, respectively. The A and B terms denote the linguistic terms of the precondition part with MF. The 'If' part of the rule 'x is A' is called the premise, while the 'Then' part of the rule is called the consequent. The p, q, r indicates the consequent parameters (Sayed et al., 2003).

Layer 1 Every node i in this layer is an adaptive node, including MFs generally described by generalized bell functions, e.g.

$$f_{1,i} = \mu_1(X) = \frac{1}{1 + |(X - c_1)/a_1|^{2b_1}}$$

(9)

where X is input to the node and a_1, b_1 and c_1 are adaptable variables known as premise parameters. The membership values of the premise part constitute the outputs of this layer.

Layer 2 This layer composes of the nodes which multiply incoming signals and sending the product out. This product represents the firing strength of a rule, as illustrated in Figure 8

$$f_{2,1} = w_1 = \mu_1(x)\mu_3(y)$$

(10)

Layer 3 In this layer, the nodes calculate the ratio of the ith rule's firing strength to the sum of all rules firing strengths.

$$f_{3,1} = \overline{w}_1 = \frac{w_1}{w_1 + w_2 + w_3 + w_4}$$

(11)

Layer 4 The nodes of this layer are adaptive with node functions.

$$f_{4,1} = \overline{w}_1 f_1 = \overline{w}_1 (p_1 x + q_1 y + r_1)$$

(12)

where w1 is the output of Layer 3 and $\{p_i, q_i, r_i\}$ is the parameter set. This layer's parameters are referred to as consequent parameters.

Layer 5 Single fixed node in this layer computes the final output as the summation of all incoming signals

$$f = \sum_{i=1}^{n} \overline{w}_i f_i$$

(13)

During the application of ANFIS the inference operations used depends on the rules applied that is the 'if-then rules. FISs can be classified into three types namely Mamdani's system (Mamdani and Assilian 1975), Sugeno's system (Takagi and Sugeno 1985) and Tsukamoto's system (Tsukamoto 1979). Although Mamdani's system is the most used Sugeno's system is known to be compact and computationally efficient.

To build-up a fuzzy system, firstly, the linguistic variables should have been provided in addition to numerical variables. Then, the system requires If/Then fuzzy rules to qualify simple relationships between fuzzy variables. A typical rule set with two fuzzy If/Then rules in first order Sugeno's system, can be shown as:

Rule 1: If x is A1 and y is B1; then $f_1 = p_1 x + q_1 y + r_1$ (14)

Rule 2: If x is A2 and y is B2; then $f_2 = p_2 x + q_2 y + r_2$ (15)

2.10 Applicability of AI in welding

ANNs have become important tools in the modelling of interrelationships between input and output variables in the field of welding technology. When ANN-controlled intelligent processes are applied in the field of welding technology, they gather information from the applied sensors to gain specific knowledge of welding conditions. To enable it to learn from the welding parameters for specific welding conditions, decision-making software

is used to evaluate the welding conditions. The decision-making tool then correlates the sensed welding condition into a trained knowledge bank to determine the optimal welding parameters. The main duty of an ANN control system is to link the relationship between the welding conditions and welding parameters.

Recent developments of the neural networks and computational technology appear to create new ideas in building AI models for predicting bead geometry under a given set of welding conditions, which was reported by (Nagesh, 2002). (Vitek, 2001) carried out an investigation into the use of neural networks in predicting weld pool shape and they concluded that a neural network model is a feasible technique for predicting weld pool shape. (Eguchi, 1999) applied neural networks in their investigation and were able to achieve the good back-bead geometry. Additionally, the wire extension and the arc length were estimated by using measurements of both welding voltage and arc current. (Kumar A., 2013), in their research work on the applicability of ANN on various welding techniques, found that artificial neural networks are beneficial when applied in the optimisation of welding process.

In an AI expert system, a set of rules is used to train the system to learn human welding knowledge. It then applies IF-THEN rules derived from welding experts to support its decision-making (Tzafestas, 2009).

Campus (2009) found that a neural network system can find patterns and relationships based on available data that would be difficult for a human being to analyse. Neural systems can then learn patterns by separating the data, building models and looking for relationships in the data. It must be noted that in applying a generic algorithm it is possible to find an optimal solution to a problem by exploring different number of solutions.

2.11 **Hybrid Fuzzy Deep learning (HFDL)**

HFDL is a much newer approach, having its first computer implementation in 2006. (Hinton, 2020) defined "Deep Learning as an algorithm which has no theoretical limitations of what it can learn", that is, the more data you give and the more computational time you provide, the better it is. Other researchers have also defined DL as a set of machines learning algorithms that attempt to learn on multiple levels, corresponding to different levels of abstraction as illustrated in Figure 9. The levels correspond to distinct levels of ideas, where higher-level ideas are defined from lower-level ones, and at the same time the lower-level concepts can help to define many higher-level concepts (Sjarif, 2019). The first few layers of the deep network are used to perform feature extraction. There are unsupervised, supervised, and hybrid DL architectures. Supervised learning uses ground truth to learn a task, whereas unsupervised learning performs a machine learning task without labels (Berman, 2019).
Since shallow neural networks have only one hidden layer, this makes it challenging to apply it to advanced feature extraction and they are unable to learn the higher-level ideas that deep neural networks are capable of learning. DL models can be trained

independently of each other. This implies that a large model with millions of parameters can be optimised in small, manageable chunks by DL. In Publication IV, a deep neural network was combined with a Likert scale to predict weld bead geometry. For further clarification on this, refer to Publication IV.
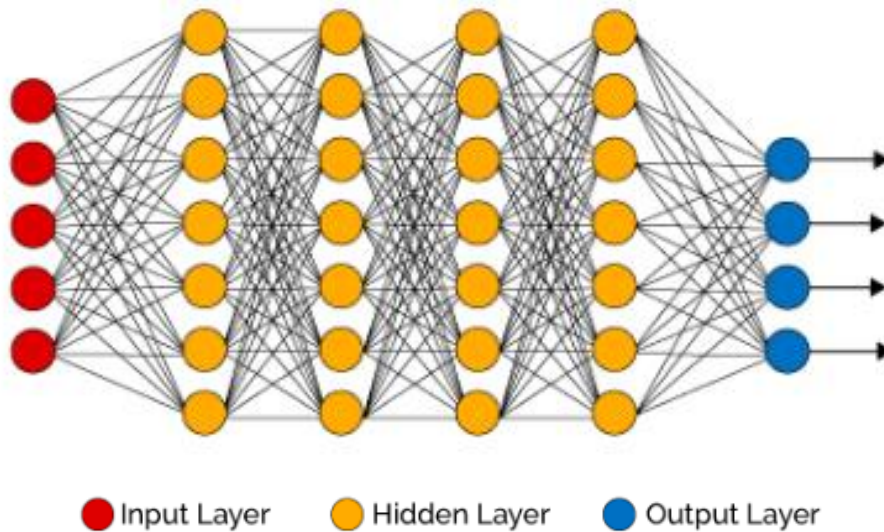
Figure 9. Illustration of a deep neural network (DNN) (Hinton, 2020).

2.12 **Welding Optimization Using Artificial Intelligence Techniques**

In recent times, welding sequence optimisation (WSO), as illustrated in Figure 10, has been applied in a few works from the perspective of quality and for minimising deformation as well as residual stress (Fu, 2016).

Despite this, welding automation has the tendency to increase efficiency in welding process, current trends in welding automation systems have major disadvantages. One major concern in automated welding is the failure to adapt effectively to changing welding conditions, which leads to inconsistent welding quality. Therefore, the more rigorous weld quality requirements of optimised structures that result from the use of thinner materials, high-strength steels and reduction of weld material are difficult to achieve (Gyasi, 2017) (Kah, 2015) (Åstrand, 2013).

To achieve a more effective and cost-efficient way in terms of quality requirements in welding is to mimic manual welding behaviour, i.e. to sense the upcoming seam and optimise the welding parameters according to the welding conditions (Chen S. B., 2014)

(Liu F. W., 2015) (Kim J. L., 2008). Figure 9 illustrates a welding sequence optimisation procedure.

(Benyounis, 2008) developed a reference guide where the works were classified basically into weld bead geometry prediction and mechanical properties. (Joshi, 2014) describes various statistical and soft computing optimisation techniques.

(Lindgren, 2007) discovered that simulation helps with the implementation of AI and ML techniques, due to the need "Do It Right First Time" and the demand for the industry to use virtual tools.
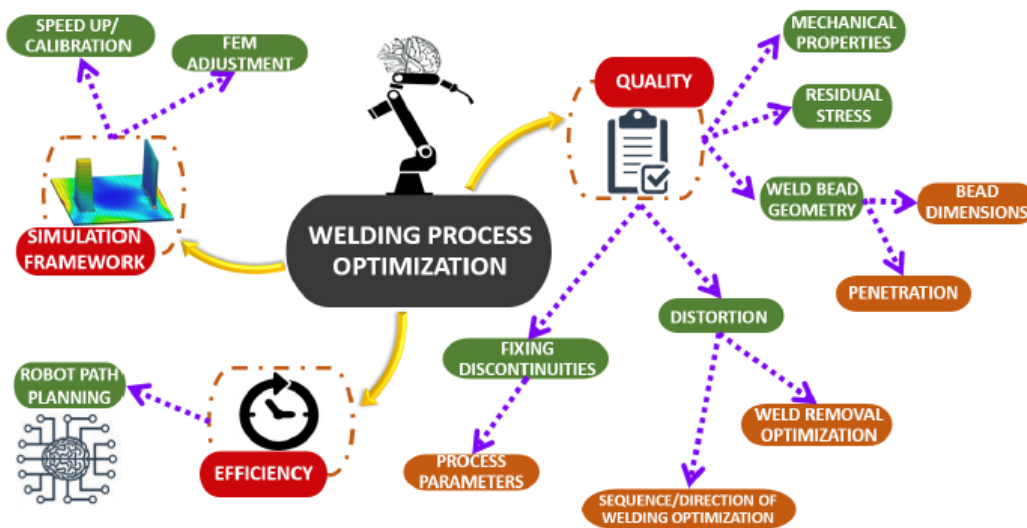
Figure 10. Welding optimisation (Romero, 2016)

In applying WSO, the usual approach is to select the best sequence based on the experience of the skilled welder, as illustrated in Figure 11. This applies a simplified DoE procedure; however, this does not usually offer the optimal sequence.
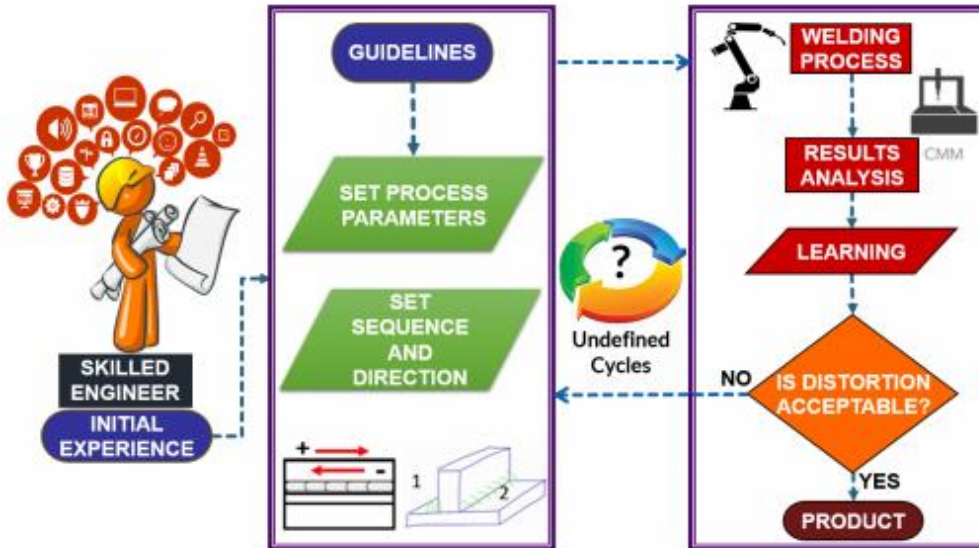
Figure 11. Conventional approach to selecting a sequence.

In Publication IV, based on the experience of the skilled welder, data was gathered and applied in developing an AI-powered hybrid deep learning algorithm system to enable one to gain a range of data to select from when a result is desired to save time. Please refer to Publication IV for more clarification.

2.13 **Concluding remarks**

This chapter discussed the state of the art of AI in welding technology and sensing control. It can be concluded that when sensing devices and the control unit are utilized properly and effectively, they can contribute considerably to reducing the burden on welders, which can create a foundation for proper adaptability. Although AI is making inroads in welding technology, its application in hybrid welding technology is currently minimal. However, its utilisation in an individual welding processes has increased considerably, and many success stories have been reported. Hybrid Deep Learning, which combines fuzzy logic and deep learning, creates an avenue for an AI system that is explainable to a human welder. This means it is easier for the welder to understand the results and apply it when needed.

3 Research Methods

The research method used in this study is discussed in this section. To achieve the objectives, a critical literature review of scientific publications and empirical experiments carried out in this field was performed, and the data collected was analysed to draw the research conclusions. Methodologically, an adaptive based neuro fuzzy inference system (ANFIS) and Fuzzy Deep learning incorporated with Likert scaling was applied in this study. The ANFIS system can be defined as a data-driven procedure which represents a neural network approach for the solution of function by approximation of problems. For the purpose of this work, the fuzzy inference system under consideration has three inputs and four outputs, which is illustrated in Figure 12. The fuzzy inference system used is proposed by Takagi, Sugeno and Kang. It formalises a systematic approach to generating fuzzy rules from an input-output data set with a built-in Gaussian membership function to emulate a given training data set. In this work, a fuzzy logic system was developed to predict the bead width, depth of penetration, depth of HAZ and width of HAZ. This is based on three inputs, namely, welding current, arc length and welding speed. The fuzzy logic toolbox that defines the input and output variables is presented in Figure 12.
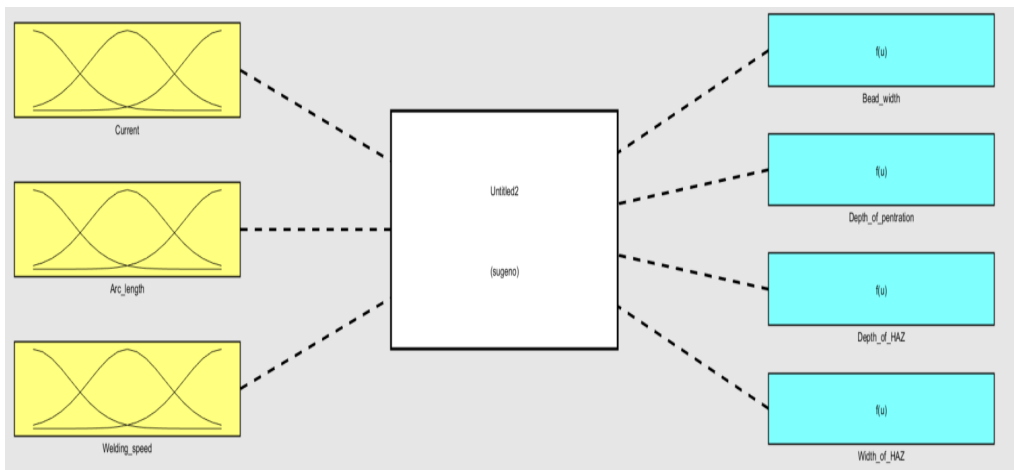
Figure 12. Illustration of fuzzy logic toolbox defining the input and output variable applied in ANFIS

After applying the ANFIS to predict the outputs, it was observed that due to limited experimental data and the shallow network nature of the ANFIS method the predictive accuracy was not so perfect. Therefore, a proposed AI framework indicated in Figure 13 was tested by using it to predict the bead geometry in order to identify means to increase the predictive accuracy using HFDNN. The proposed method was designed using fuzzy deep learning incorporated with Likert scaling applied in this study.
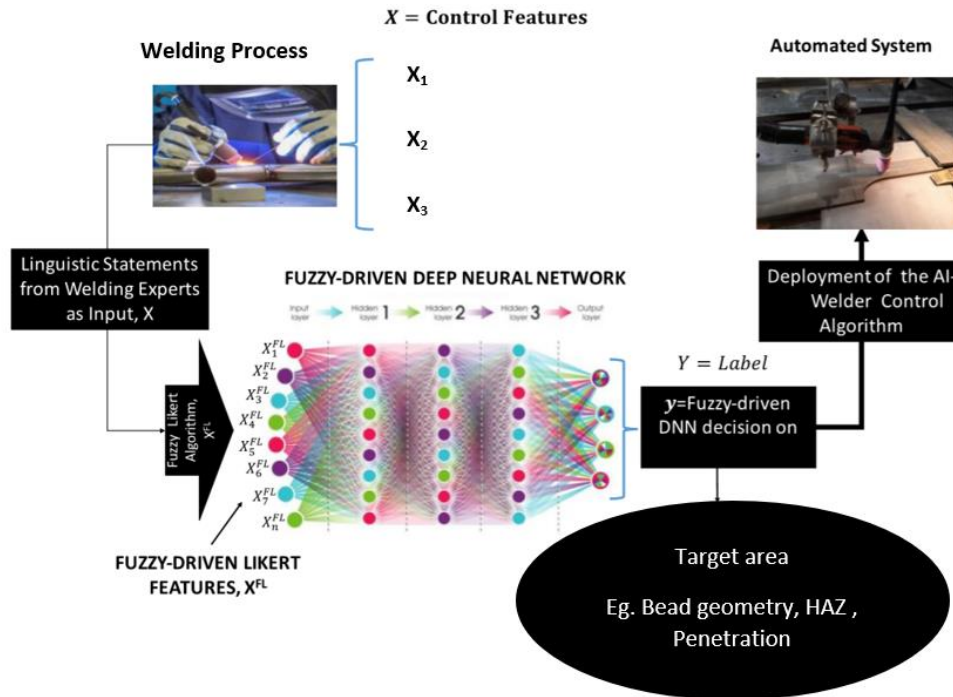
Figure 13. Proposed artificial intelligence (AI) framework

Deep machine learning can be described as a machine learning approach that simulates human intelligence by applying multiple neural networks called deep neural networks. The deep neural networks imitate the human brain's function, which enables it to learn complex structures. The learning capabilities helps to create a relationship directly from data it collects with less human influence (LeCun, 2015) (Goodfellow, 2016).

Despite these capabilities, the deep neural network model is deterministic and is a black box algorithm. Therefore, by incorporating fuzzy logic into the DNN capabilities, an explainable rule-based structure can be realised in DNN algorithms to develop a hybrid fuzzy deep neural network algorithm to alleviate the problems of strictly trading off interpretability for accuracy (Bonanno, 2017).

In the work of (Zadeh, 1975), fuzzy logic was introduced to overcome weaknesses in Boolean logical thinking. A fuzzy system consists of three parts: fuzzification, rule-base and defuzzification. Fuzzification is used to transform the responses that are the input data into fuzzy values. In doing so, an isosceles triangular membership function is evenly distributed along the input continuum. Once these values are obtained, they cannot be interpreted unless they are defuzzified to real numbers. Mostly in fuzzy logic applications, defuzzification is operated on several fuzzy IF-THEN rules (Yen, 2004). It is important to note that the IF-THEN rule is used

to determine what fuzzy actions are needed to carry out the necessary action according to the input. Using these three systems, the fuzzy logic system provides a mathematical framework to compute with words based on "degrees of truth" rather than the usual "true or false" (1 or 0) Boolean logic on which the modern computer is based. Fuzzy logic includes 0 and 1 as extreme cases of truth, but it also includes the various states of truth in between. For example, the result of a comparison between two things could not be "tall" or "short" but "somehow tall", and the height can be quantified using a mathematical curve called a Gaussian membership function (MF), which is illustrated in Figure 14.
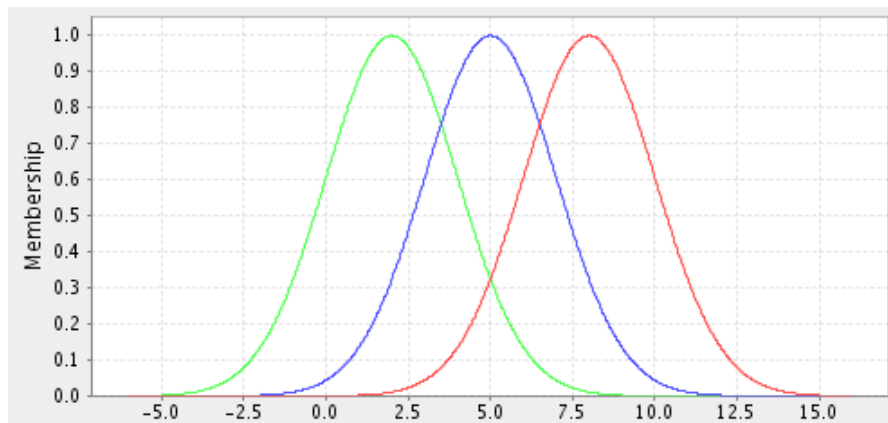
Figure 14.Illustration of Gaussian member ship function

As illustrated in the AI framework in Figure 13, X_1, X_2 and X_3 are the control parameters. These control parameters are used to predict the target area, such as weld bead, depth of HAZ and depth of penetration. After defining the parameter ranges, the next step is to learn about the control parameters and their theoretical association with the expected output from welding "experts". To accomplish this, it was important to build "expert" linguistic rules to design the fuzzy logic-based Likert algorithm. Likert scaling, which was introduced by (Likert, 1932) is the most widely used psychometric scale to measure responses. However, challenges such as distortion and loss of information, which arise from the closed form of scaling and ordinal nature when Likert scaling is used, have been recognised. To overcome these challenges a novel fuzzy Likert scale was developed which combines fuzzy logic and a Likert scale measurement technique.

Since the model architecture is a hybrid fuzzy–DNN model, it is paramount to have big data to build the model to prevent the problem of overfitting. Overfitting leads to poor generalisation and may contribute to inaccuracies (Shorten & Khoshgoftaar, 2019).

To be able to have adequate data to train the deep neural network, the X values (control parameters) were passed through a classifier called fuzzy logic-based Likert inference, which is presented in Figure 15. The advantage of the fuzzy logic-based Likert algorithm

is that it helps to rescale the raw data X. This is transformed from the human expert on a psychometric scale using traditional Likert scaling, which is then transformed to its fuzzy-driven feature denoted as X^{FL} as depicted in Figure 15. During this transformation, the human expert welder's linguistic statement is quantified by a fuzzy mathematical curve called membership function (MF) as illustrated in Figure 14.

This is the engine for transforming an input variable X to obtain its Fuzzy representations called fuzzy-driven Likert features, X^{FL}. This transformation creates a data space with interval details so that additional data can be collected via data augmentation for training the fuzzy-driven DNN model, as shown in the AI framework illustrated in Figure 13. Computationally, the X to X^{FL} transformation is performed using the fuzzy rules illustrated in Figure 15. As indicated in Figure 15, the X^{FL} is taken as the input data for a fuzzy driven neural network. The deep neural network learns the nonlinear relationship between the control features and the target. The final decision is computed in accordance with Figure 13 where Y is the target area (bead geometry (bead width and depth of penetration) and HAZ geometry (depth of HAZ and width of HAZ)).
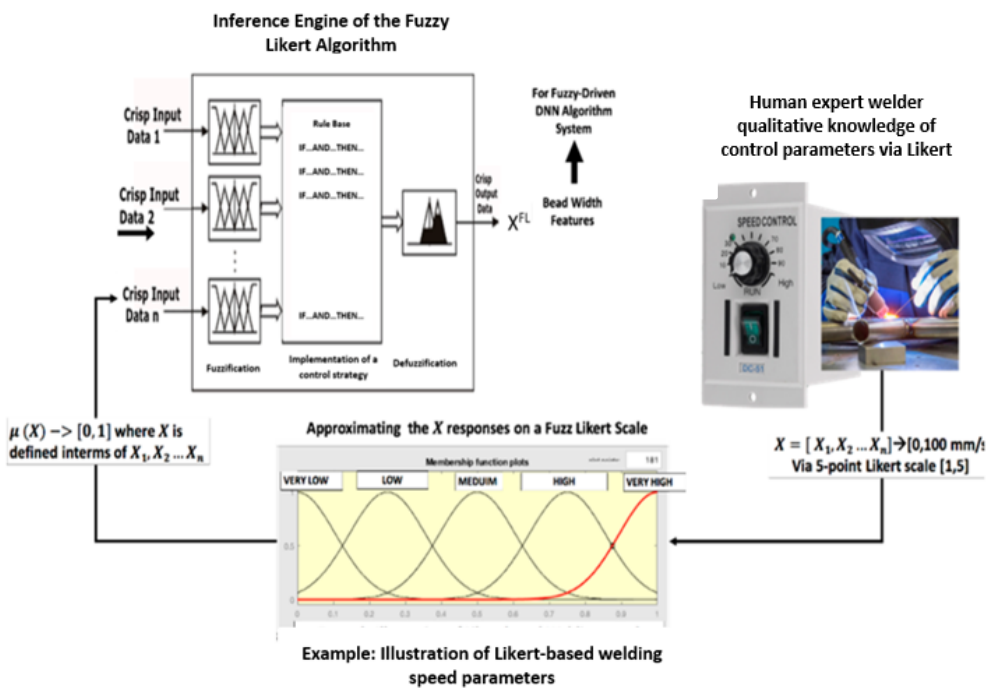
Figure 15. Fuzzy logic-based Likert inference

In real life, the fuzzy driven deep neural network can be implemented using the Keras deep learning library with the Google TensorFlow backend using the Python language. After training and optimisation, and when a well-trained module has been selected, as

indicated in the framework it can be deployed to help the human welder select the right welding parameters.

To evaluate this model a critical literature review was carried out on different welding processes to understand the control parameters and their usability. Because the general architecture was a hybrid system, in publication IV the hybrid architecture was tested to ascertain its viability.

3.1   **Welding process, training and testing of ANFIS network**

As illustrated in Figure 12, the ANFIS model was built and tested on TIG welding process. In TIG welding process, the arc is formed between the pointed tungsten electrode and the workpiece and an argon (Ar), helium (He) or a mixture of both can be used as shielding gas. The experimental setup of the TIG welding procedure was integrated with a linear variable displacement transformer (LVDT) which is illustrated in Figure 16.
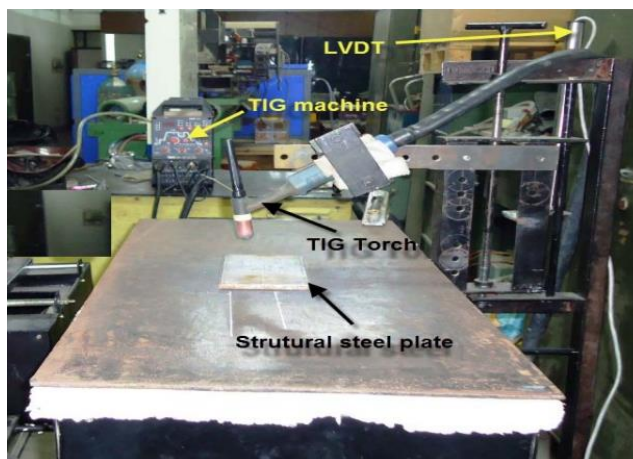
Figure 16. Experimental setup of TIG welding process

Trial runs were undertaken for the bead-on-plate welds to set the levels on welding current, traverse speed and arc length. which are the input parameters. In all, 27 experimental data on bead-on-plate welds were carried out and the results are illustrated in Table 1.

In modelling the proposed system, the Sugeno-style fuzzy logic-based methodology was applied, and it was implemented using MATLAB Simulink® and Fuzzy Logic Toolbox™. To begin the modelling process, the data obtained from the experimental (input and output) was divided into training and test data. The training data set was utilised to find the initial premise parameters for the membership functions. The training of the algorithm was carried out using 40 Epoch and tuned (optimised) with hybrid optimisation, which is a combination of least squares estimation (LSE) and Gradient descent (GD), which enables it to identify the consequent parameters that define the

coefficient of each output equation with an error tolerance of zero. To generate the rules, a fuzzy subtractive clustering (SC) method was applied to generate the rules for the algorithm and automatically generated an ANFIS-SC model. It must be noted that the model is an extension of the mountain clustering method which was proposed by Yager and Filev (1994); in this method, each data point (not a grid point) is considered a centre for potential cluster (Chiu, 1994). The model was then trained severally in order to ensure that its predictive accuracy is improved. It must be noted that the algorithm was not built using a pre-trained model; it was trained from scratch. Table 1 illustrates the 21 datasets for training and 6 for validation.

Table 1. Illustration of experimental data for training and validation (Narang, Singh, Mahapatra, & Jha, 2011)

S. N	Current (A)	Arc length (mm)	Welding Speed (mm/s)	Bead width (mm)	Depth of penetration (mm)	Depth of HAZ (mm)	Width of HAZ (mm)
1	55	2	15	5.46	1.59	1.73	1.83
2	55	2	30	4.71	1.25	1.19	1.35
3	55	2	45	4.16	1.04	1.02	1.13
4	55	2.5	15	5.77	1.76	1.94	2.20
5	55	2.5	30	4.93	1.38	1.33	1.63
6	55	2.5	45	4.46	1.18	1.16	1.33
7	55	3	15	6.09	1.91	2.13	2.45
8	55	3	30	5.03	1,42	1.51	1.84
9	55	3	45	4.55	1.23	1.23	1.46
10	75	2	15	6.12	1.99	2.48	2.25
11	75	2	30	5.13	1.39	1.46	1.72
12	75	2	45	4.59	1.16	1.22	1.39
13	75	2.5	15	6.59	2..06	2.65	2.41
14	75	2.5	30	5.26	1.5	1.65	1.89
15	75	2.5	45	4.85	1.32	1.34	1.57
16	75	3	15	7.07	2.18	2.72	2.79
17	75	3	30	5.45	1.65	1.86	2.02
18	75	3	45	5.16	1.45	1.58	1.79
19	95	2	15	6.65	2.17	3.04	2.71

20	95	2	30	5.38	1.51	1.81	1.94
21	95	2	45	4.75	1.23	1.49	1.52
22	95	2.5	15	7.19	2.23	3.3	2.89
23	95	2.5	30	6.16	1.63	1.97	2.15
24	95	2.5	45	5.2	1.32	1.56	1.75
25	95	3	15	7.64	2.51	3.21	3.15
26	95	3	30	6.31	1.74	2.15	2.70
27	95	3	45	5.11	1.41	1.74	2.16

The model employed 21 training datasets, 6 test data and 21 fuzzy rules to predict the four outputs after the training. The test data for depth of penetration and the depth of the heat-affected zone is illustrated in Tables 2 and 4. Figure 17 illustrates the welding process for fuzzy network and training process.
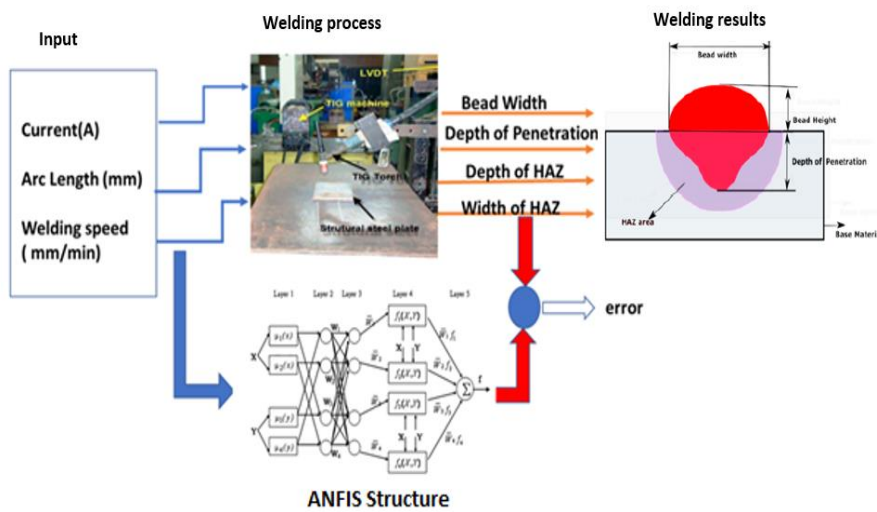
Figure 17. Welding process for Fuzzy network and training process

3.2   Results analysis and possible advanced methods, ANFIS AND DNN

This section discusses the results and possible advanced method of applying ANFIS and DNN to improve on the predictive accuracy of the model.
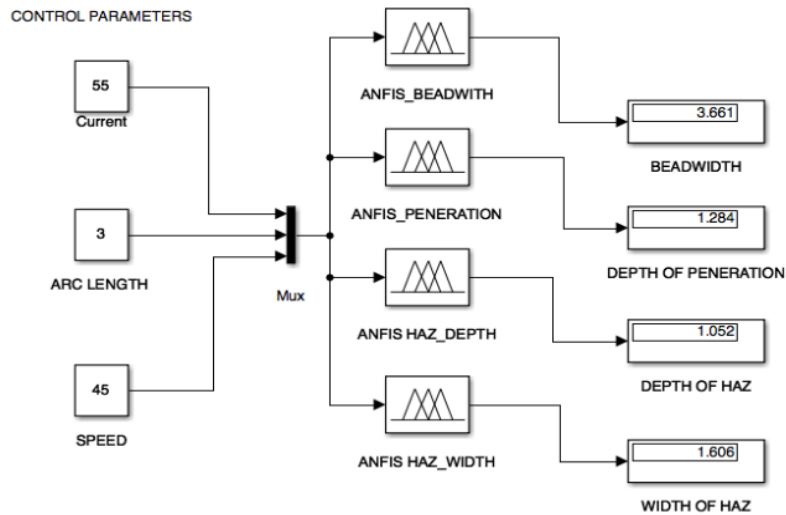
Figure 18. Illustration of the simulation model of the ANFIS model

The simulation model of the ANFIS model which shows the relationship between the input and the output variable in the applied methodology is illustrated in Figure 18 and the ANFIS model structure of the proposed approach is also illustrated in Figure 19. The ANFIS model structure shows the input, input membership function, the 21 rules, the output membership, and a single output. The membership function is generated from the ANFIS model on a fuzzy platform. Hybrid methods are applied for training ANFIS network, i.e., by using least square method to estimate the parameters in the output linear equations and by using back propagation method to train Gauss membership functions and rules.
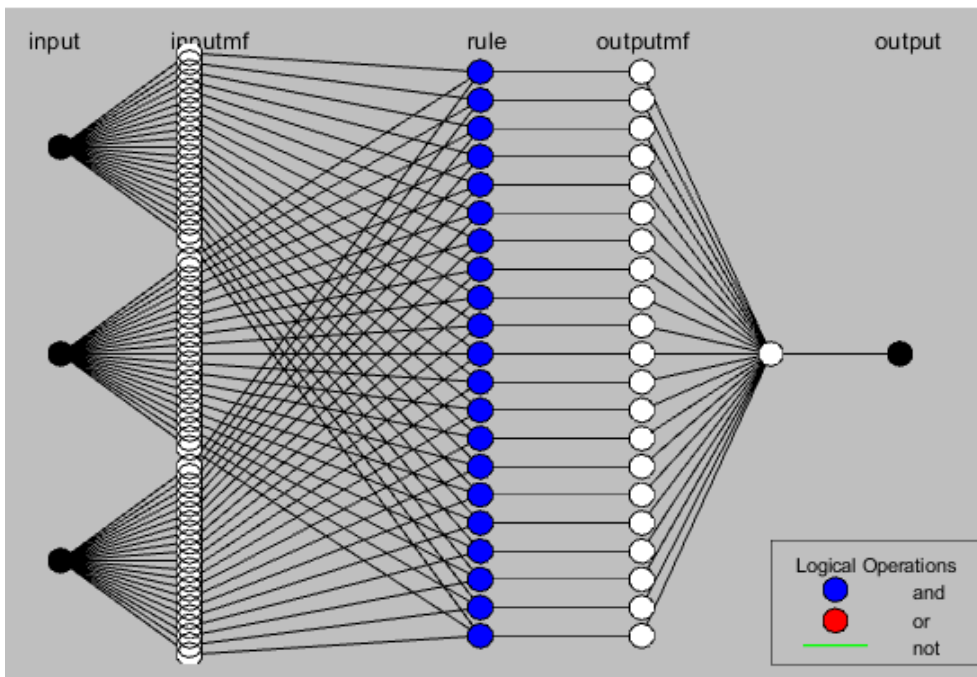
Figure 19. Illustration of the ANFIS model structure

The training data and output of ANFIS are illustrated in figures 20 ,21, 22 and 23. As the root mean square error (RMSE) values of training results are very low, the deviation was so little and hence the blue and red datapoint overlap each other.
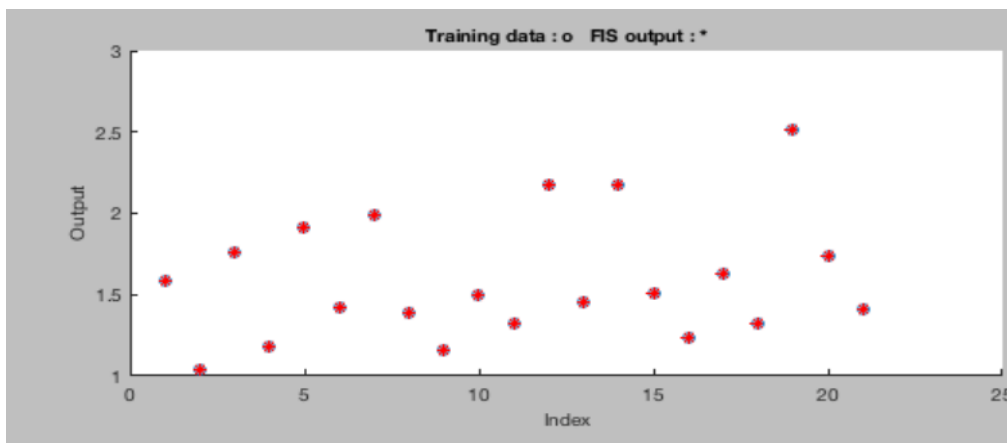
o Training data(mm)   * Training results(mm)

Figure 20. illustration of testing data vs test data for depth of prediction with RMSE (0.00004)
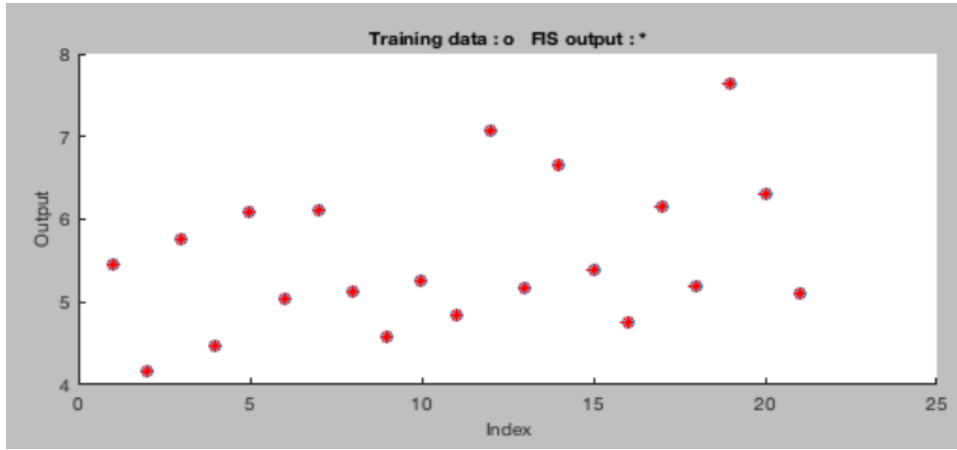
o Training data(mm)   ∗ Training results (mm)

Figure 21. Illustration of testing data vs training data for bead width showing with the RMSE (0.000012)
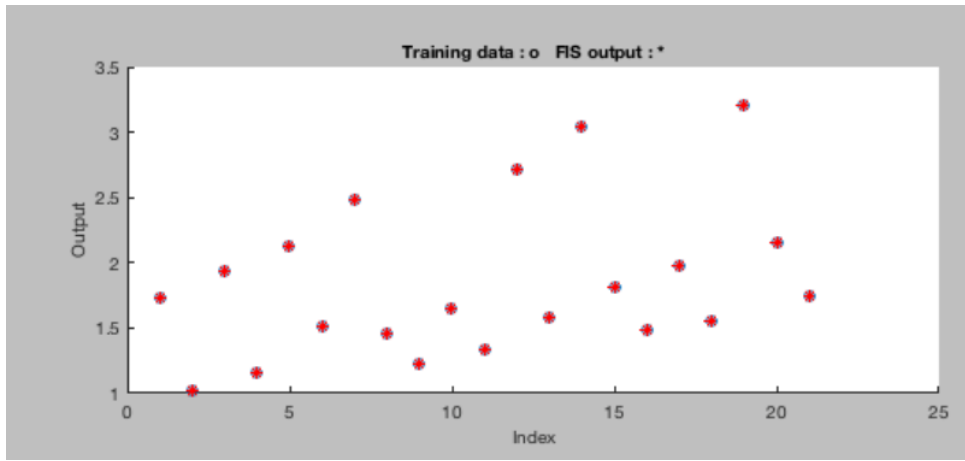
o Training data(mm)   ∗ Training results(mm)

Figure 22. Illustration of testing data vs training data for depth of HAZ with RMSE (0.000001)

o Training data   * Training results
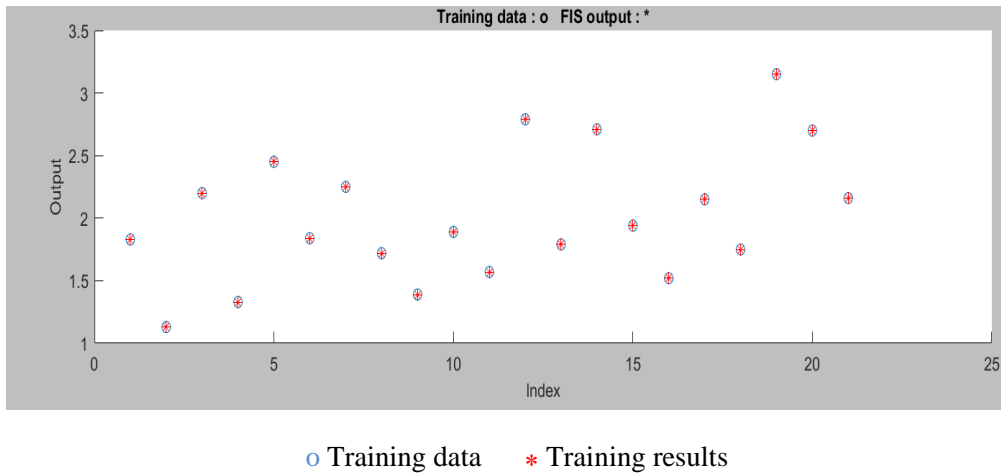
Figure 23. Illustration of testing data vs training data for width of HAZ with the RMSE (0.00000279)

After the training, the validating process was carried out with the remaining six (6) groups of data. The predictive accuracy of the adaptive neuro fuzzy system and the test values in Tables 2,3,4 and 5 (which represent real-life experimental data) are compared to the predicted value of ANFIS. As shown in the tables 2,3,4 and 5, the predicted values are very close to the real-life experimental data with little error.

Table 2.Test data for depth of penetration

S.N	Measured DP (mm)	Predicted DP (mm)	Error	Error^2
2	1.25	1.16	-0.09	0.0081
5	1.39	1.37	-0,02	0,0004
9	1.23	1.31	0.08	0,0064
13	2.06	1.98	-0.08	0,0064
17	1.65	1.66	0.01	0,0001
22	2.23	2.08	-0.15	0,0225
			RMSE	**0.085244**

Table 3.Test data for depth of bead width

Measured BW (mm)	Predicted BW (mm)	Error	Error^2
4.71	4.47	-0.24	0.06
4.93	4.78	-0.15	0.0225
4.55	4.73	0.18	0.0324
6.59	6.45	-0.14	0.0196
5.45	5.77	0.32	0.1024
7.19	6.74	-0.45	0.2025
		RMSE	**0.269877**

Table 4. Test data for depth of depth and width of HAZ

S.N	Measured Depth of HAZ (mm)	Predicted Depth of HAZ (mm)	Error	Error^2
2	1.19	1.28	0.09	0.0081
5	1.33	1.46	0.13	0.0169
9	1.23	1.37	0.14	0.0196
13	2.65	2.34	-0.31	0.0961
17	1.86	1.92	0.06	0.0036
22	3.32	2.71	-0.61	0.3721
			RMSE	**0.293371**

Table 5. Test data for width of HAZ

Measured width of HAZ (mm)	Predicted Width of HAZ (mm)	Error	Error^2
1.35	1.31	-0.04	0.0016
1.63	1.59	-0.04	0.0016
1.46	152	0.06	0.0036
2.41	2.61	0.20	0.04
2.02	2.26	0.24	0.0576
2.89	2.82	-0.07	0.0049
		RMSE	**0,134969**

The graphs of observed data are plotted against the predicted value shown in Figures 24 to Figure 27. It can be deduced from the graph shown in Figure 24 that the predicted value of depth of penetration against the real experimental data are very close to the results of the experimental data. Also, a plot of observed bead width vs. experimental bead width showed little variation when compared to each other as illustrated in Figure 25. Similarly, Figures 26 and 27 illustrate the measured depth of HAZ vs the predicted one and the measured width of HAZ vs the predicted one indicates a close prediction. However, compared to the training RMSEs, the validated RMSE is larger than the real experimental data, therefore more training data will help to improve the accuracy of results of the ANFIS model.
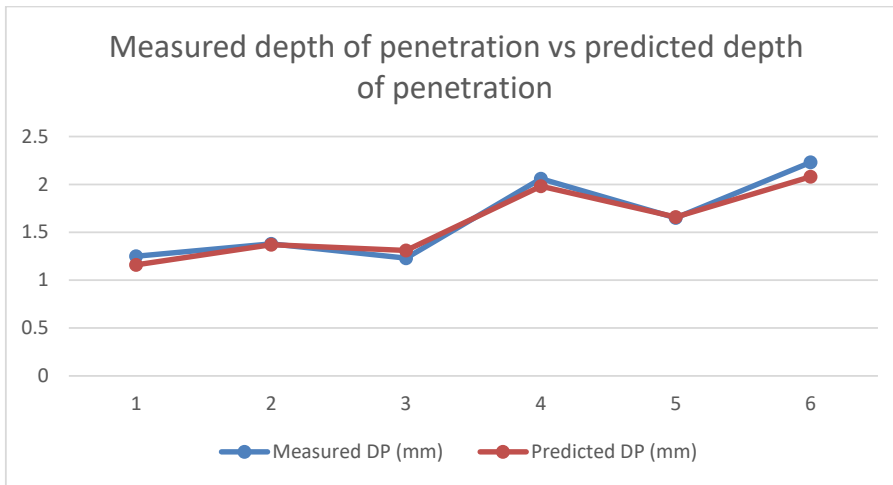
Figure 24. Illustration of observed depth of penetration (DP) vs Predicted depth of depth penetration (mm)
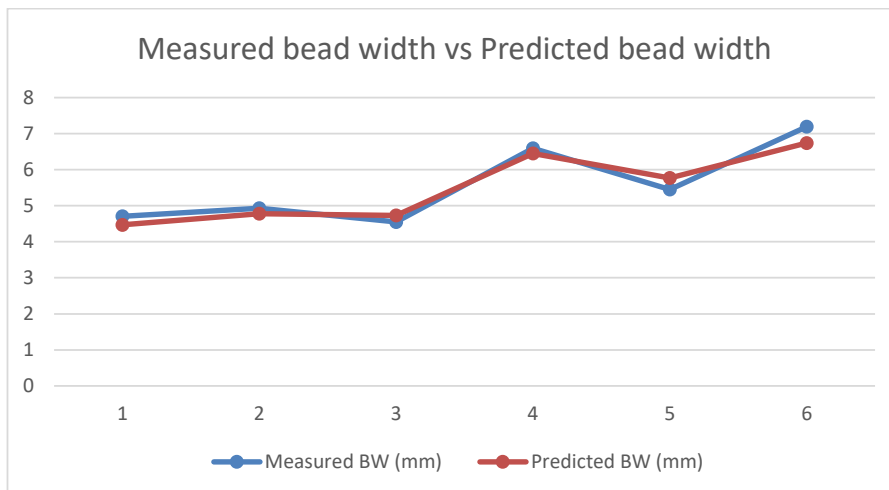
Figure 25. Illustration of observed bead width vs predicted bead width (mm)
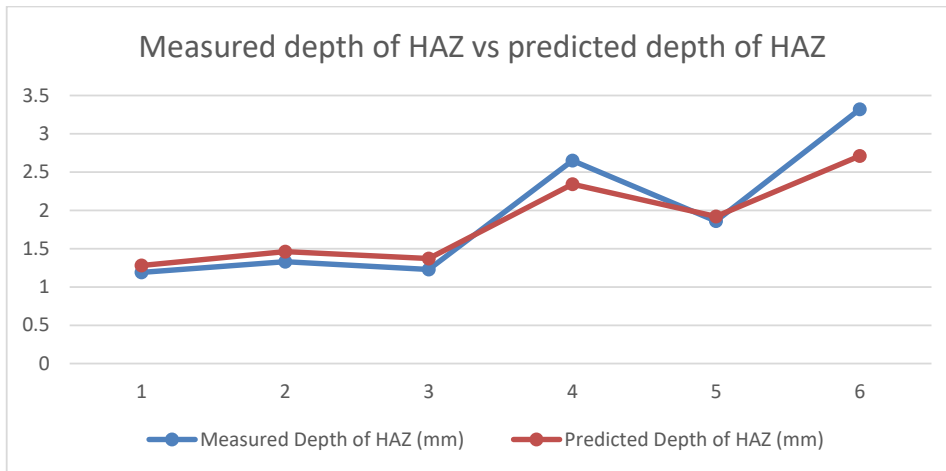
Figure 26. illustration of observed Depth of HAZ vs predicted Depth of HAZ (mm)
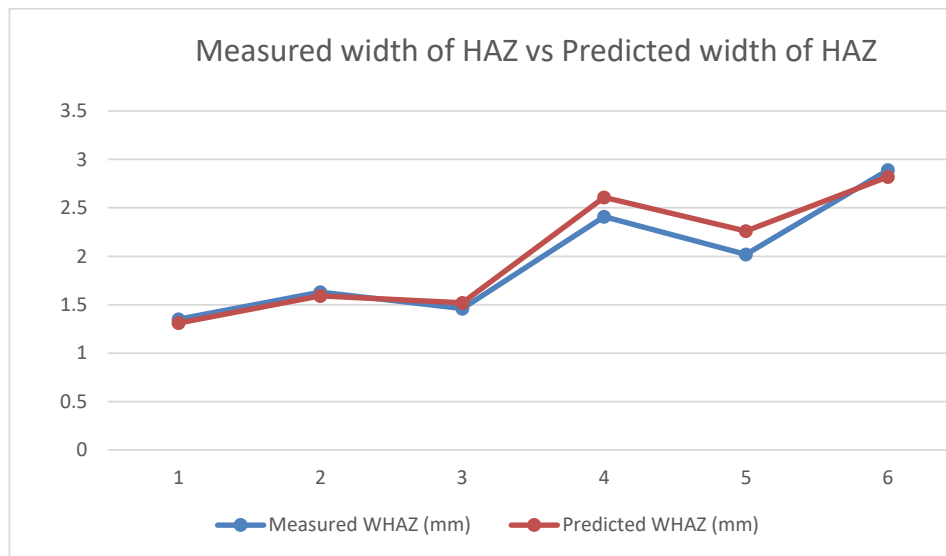
Figure 27. Illustration of observed width of HAZ vs predicted width of HAZ (mm)

3.3   **Reliability analysis of the research method**

Reliability and validity are important concepts used to evaluate the quality of a research method. Together, they can indicate the extent to which a method measures what it purports to measure. The two concepts work hand in hand with reliability dealing with the issue of consistency and validity being about accuracy. In the work of (Stenbacka,

2001), it is stated that "the concept of reliability is even misleading in qualitative research". However, (Patton, 2002) states that validity and reliability are two factors that should be considered by a qualitative researcher when designing a study, assessing its quality, and analysing the results to produce a finding.

Sensitivity is a key concept in reliability and needs to be considered during reliability analysis. Sensitivity analysis determines how ''sensitive'' a model is to changes in the value of the parameters of the model and to changes in the structure of the model. It must be noted that sensitivity coefficients usually describe the changes in the system's outputs due to variations in the parameters that affect the system (Mohammad H. M., 2013). High sensitivity to a parameter indicates that the system's performance can change drastically following small variation in a parameter. Similarly, low sensitivity suggests that small variations in a parameter result in only small changes in the performance of the system.

To ascertain the reliability, validity and sensitivity of the research methodology used in this work, the model was tested and validated with a real-life experiment. Its predictive accuracy was tested to establish how close the values obtained with the model match reality (experimental data). Following test simulation, the simulation results showed a predictive accuracy of 92.59%, which indicates 25 out of 27 experimental data used in predictions by the AI algorithm. After training, the model was applied with a different set of data to test its learning and predictive accuracy. It was found that the model had little sensitivity to changes in the data, which is positive for its reliability.

3.4   Comparison analysis of methodology

This section compares the result obtained from the application of ANN and ANFIS. The results showed a good predictive accuracy. However, it was observed that when less data is used for training of the algorithm overfitting occurs and hence this alters the predictive accuracy. Tables 6, 7,8,9,10 and 11 illustrate the comparative analysis of the ANFIS methodology and the other methods that is regression analysis and ANN applied in predicting the output parameters. To carry out the comparative analysis a real experimental data results used. The data was taken from three journal article that is Application of Artificial Neural Network in Predicting the Weld Quality of a Tungsten Inert Gas Welded Mild Steel Pipe Joint (Abhulimen, 2014), Optimization of Weld Bead Profile Parameters in TIG Welding Process for Inconel 718 Alloy Using RSM and Regression Analysis (Jose, 2016) and Application of artificial neural network for predicting weld quality in laser transmission welding of thermoplastics (Acherjeea, 2011). In the first article artificial neural network was used to predict the welding parameters and compared to real experimental data. In the experiment a mild steel pipe of diameter 50.8mm, thickness of 4 mm was welded with a non -consumable filler material Filler material of mild steel ER70SG/2.4 applying TIG welding process. After the welding, the tensile strength and the yield strength were read directly from the Universal Testing Machine. In the second article optimisation of weld bead profile was

carried out using response surface methodology (RSM) and regression analysis. Finally, in the third article a coherent FAP-diode laser system with a 3-axes CNC worktable, coordinated with the motion system and computer interface was used in the experimental setup. The maximum optical power of the system applied in the experiment was 30W which has an output wavelength of 809.40 nm. The FAPSystem optical radiation is delivered via a SMA 905 connector, which mates to an 800-m diameter transport fiber. The imaging module attached to the digital end of SMA 905 connector consists of two lenses mounted in cylindrical stainless-steel housing. The first lens in the optical assembly collimates the output of the fiber end whereas the second lens re-images the fiber end (Acherjeea, 2011).

To test the suitability of the systema generated regression ANOVA testing methodology was applied. The error from the real experiment value and the predicted value were calculated. The RMSE of the ANOVA (0.009) methodology was as compared to average error of the ANFIS (0.215). It can be concluded that the results of ANFIS methodology showed little variation to that of the ANOVA methodology. Secondly, the article that applied the ANN methodology in predicting weld width, weld depth and depth to width ratio was compared to that of the results obtained by the ANFIS. The average error obtained by the ANFIS (11.798 average error) compared to that of the ANN (15.17 average error) showed a much better predictive accuracy by the ANFIS. In the last article the RMSE of the predicted lap shear strength of the ANN (2.7) and that of the predicted by ANFIS (0.707) which showed a better predictive accuracy than the ANN. On the other handed the prediction made by ANN for the weld seam width (0.138) as compared to (0.078) predicted by the ANFIS.

Table 6. illustrates the result obtained in applying ANN (Abhulimen, 2014) and ANFIS to predict 1) tensile strength and 2) yield strength.
   1) **Tensile strength comparison**

current	Gas flow	voltage	Electrode Diameter	Exp. data	ANN	Error	ANFIS	Error
160	27.5	10.5	1	462.05	456.53	-5.52	463.11	1.06
160	25	13.5	0.5	438.94	455.06	16.12	439.27	0.33
180	30	13.5	0.5	462.046	455	-7.046	462.41	0.364
160	25	10.5	1	462.046	466.33	4.284	462.41	0.364
130	27.5	11.5	1	346.535	401.84	55.305	346.14	-0.125
130	30	10.5	0.5	462.046	411.23	-50.816	463.34	1.294
160	27.5	13.5	1	462.046	460.76	-1.286	463.11	1.064
180	30	11.5	0.5	508.251	509.52	1.269	501.41	-6.841
160	25	10.5	0.5	485.148	482.53	-2.618	476.29	-8.858
160	27.5	13.5	0.5	462.046	455.02	-7.026	462.15	0.104
130	25	13.5	0.5	415.84	443.77	27.93	431.27	15.43
130	25	10.5	1	415.841	422.97	7.129	414.15	-1.691
180	25	13.5	0.5	462.046	456.80	-5.246	462.33	0.284
130	25	13.5	0.5	462.046	443.77	-8.276	431.77	-30,276
160	30	10.5	0.5	438.944	421.20	-17.744	438.17	-0.774
						RMSE 22.45885865		RMSE 2.39257611

2) Yield strength comparison

current	Gas flow	voltage	Electrode Diameter	Exp. data	ANN	Error	ANFIS	Error
160	27.5	10.5	1	352.71	**348.59**	**4.12**	**353.43**	**0.72**
160	25	13.5	0.5	335.07	**347.25**	**-12.18**	**323.12**	**-11.95**
180	30	13.5	0.5	352.71	**347.21**	**5.5**	**353.17**	**0.46**
160	25	10.5	1	352.71	**355.93**	**-3.22**	**351.34**	**-1.37**
130	27.5	11.5	1	264.53	**307.64**	**-43.11**	**265.24**	**0.71**
130	30	10.5	0.5	352.71	**314.67**	**38.04**	**340.11**	**-12.6**
160	27.5	13.5	1	352.71	**351.55**	**1.16**	**335.33**	**-17.38**
180	30	11.5	0.5	387.98	**388.27**	**-0.29**	**388.44**	**0.46**
160	25	10.5	0.5	370.34	**368.06**	**2.28**	**348.15**	**-22.19**
160	27.5	13.5	0.5	352.71	**347.22**	**5.49**	**353.12**	**0.41**
130	25	13.5	0.5	317.44	**338.75**	**-21.31**	**317.24**	**-0.2**
130	25	10.5	1	317.44	**323.46**	**-6.02**	**320.43**	**2.99**
180	25	13.5	0.5	352.71	**348.57**	**4.14**	**353.12**	**0.41**
130	25	13.5	0.5	352.71	**338.75**	**13.96**	**317.32**	**-35.39**
160	30	10.5	0.5	335.07	**322.14**	**0**	**335.11**	**-0.06**
						RMSE 16.83370587		**RMSE 12.54623**

Table 7. Illustrates the result obtained in applying ANOVA (Jose, 2016) and ANFIS to predict tensile strength and yield strength.

Exp. No	Welding current	Welding voltage	Welding speed	Shielding gas	Weld depth (EXP.)	ANOVA	ANFIS
2	8	0.8	3	50	3.111	**3.103**	**2.92**
3	8	0.8	1	50	3.052	**3.058**	**2.87**
7	10	0.6	2	60	3.151	**3.161**	**3.3**
9	10	1	2	40	2.954	**2.944**	**2.79**
20	10	0.8	1	40	3.089	**3.080**	**3**
10	8	0.8	2	40	2.968	**2.978**	**2.58**
						RMSE 0.089	**RMSE 0.215**

Table 8. Illustrates the result obtained in applying ANOVA (Jose, 2016) and ANFIS to predict tensile strength and yield strength.

Exp. No	WELD WIDTH EXP.	ANOVA	ERROR	ANFIS	ERROR
2	6.911	**6.966**	**-0.055**	**7.7**	**-0.789**
3	8.300	**8.321**	**-0.021**	**6.690**	**1.61**
7	8.799	**8.756**	**0.043**	**8.67**	**0.129**
9	6.101	**6.141**	**-0.04**	**6.92**	**-0.819**
20	8.287	**8.281**	**0.006**	**8.44**	**-0.153**
10	6.119	**6.107**	**0.012**	**6.19**	**-0.071**
			RMSE 0.0343875		**RMSE 0.809369**

Table 9. Illustrates the result obtained in applying ANOVA (Jose, 2016) and ANFIS to predict tensile strength and yield strength.

DEPTHOF WIDTH RATIO EXP.	ANOVA	ERROR	ANFIS	ERROR
0.450	**0.450**	**0**	**0.411**	**0.039**
0.368	**0.374**	**-0.006**	**0.372**	**-0.004**
0.358	**0.365**	**-0.007**	**0.373**	**-0.015**
0.484	**0.476**	**0.008**	**0.358**	**0.126**
0.373	**0.377**	**-0.004**	**0.412**	**-0.039**
0.485	**0.483**	**0.002**	**0.387**	**0.098**
		RMSE 0.005307		**RMSE 0.184842**

Table 10. comparison of actual and predicted outputs for lap shear strength by ANN (Acherjeea, 2011)   and ANFIS.

Exp. No	Power (W)	Welding speed (mm/min)	Stand-off distance (mm)	Clamp pressure (MPa)	Actual lap-shear strength (N/mm)	ANN	ANN ERROR	ANFIS	ANFIS ERROR
1	19	420	28	6.3	36.17	36.91	0.74	35.9	0.27
2	25	420	36	6.3	28.63	29.14	0.51	28.6	0.03
3	19	300	28	6.3	35.23	34.91	0.32	36.9	1.67
4	19	300	36	12.3	46.03	43.17	2.86	46	0.03
5	22	360	32	9.3	47.43	47.38	0.05	47.8	0.37
6	25	420	28	12.3	38.11	44.05	5.94	38.1	0.01
							RMSE 2.7196		RMSE 0.7072

Table 11. comparison of actual and predicted outputs for weld seam width by ANN (Acherjeea, 2011) and ANFIS.

S.N	Power (W)	Welding speed (mm/min)	Stand-off distance (mm)	Clamp pressure (MPa)	Actual weld-seam width (mm)	ANN	ANN ERROR	ANFIS	ANFIS ERROR
1	19	420	28	6.3	1.92	1.94	0.02	1.82	0.1
2	25	420	36	6.3	2.43	2.58	0.15	2.43	0
3	19	300	28	6.3	2.25	2.04	0.21	2.35	0.1
4	19	300	36	12.3	2.88	3.03	0.15	2.88	0
5	22	360	32	9.3	2.4	2.51	0.11	2.5	0.1
6	25	420	28	12.3	2.22	2.11	0.11	2.22	0
							RMSE 0.137659		RMSE 0.0577

3.5   Application of the Algorithms

One application is using optimisation of an algorithm to find parameters which can be applied in acquiring desired outputs. The importance of the algorithm demonstrated in this dissertation is to optimize the three (3) welding input parameters in order to obtain the desired four outputs namely bead width, depth of penetration, depth of heat affected zone and width of heat affected zone. These outputs are then used to evaluate the error function. The aim of the method is to help in achieving the desired outputs by using an optimisation algorithm to search through the inputs as illustrated in equation 16:

$$\text{objective function} \qquad \min \quad \sum_{k=1}^{4}(Yd^k - ANFIS(I, D.S)^k)^2 \tag{16}$$

where Yd^k is desired outputs, k =1,2,3,4; ANFIS (I, D, S) is the Fuzzy neural network model of welding, I is current, D is arc length and S is welding speed.

The second application is using the ANFIS model as a digital twin of a welding process. During the welding process, it is difficult to measure the output online. However, after developing the ANFIS it can then be used to simulate and predict the welding outputs of the welding process. The method and the results obtain in this work can be used in predicting the outputs which in turn can be optimised in order to reduce the error significantly.

4 Overview of the publications and Findings

This section presents an overview of the publications used in this dissertation and findings. A more detailed description of the individual work can be found in the articles, Publications I-IV. In Publications I and II, a literature review and the usability of the welding process was investigated. In Publication III the neural network part of architecture model was tested on modelling the structural integrity of the welding process and in publication IV, the hybrid architecture was tested.

This section further summarises the findings of Publications I, II, III and IV.

Publication I: "Investigations into enhanced TIG welding processes"

Article I (see Table 12) is a review article that discusses different variants of the TIG welding process. Existing articles on different variants of the TIG welding process were analysed to lay the foundations for Article II. It highlights the benefits of different variants and its area of applicability.

Table 12. Summary of Article I

Title of article	Investigations into enhanced TIG welding processes
Aims	To conduct a review of articles
Objectives	The purpose of this research is to investigate on the various TIG variants and its applicability. Possible optimization for improving TIG welding productivity is also studied.
Research question (s)	Why is there a need for different variants of the TIG welding process and what are their benefits in the weldability of non-ferrous metals?

Main Findings and conclusions	Research showed that studied variants like TIP TIG and TOPTIG, hybrid laser TIG welding improved the productivity challenges seen in traditional TIG welding processes. This finding provides a foundational understanding for journals 2,3 and 4.
	Additionally, the findings show that TIP TIG efficiently provides TIG welding at MIG welding speeds, which indicates that it is possible to combine the benefits of TIG welding, particularly the cleanliness of the weld, with the capability to weld at higher speeds. TIP TIG welding allows a managed separation of the quantity of arc energy and the quantity of filler material introduced into the welding pool. This gives an advantage in controlling the starting and finishing (down-slope) phases of welding cycle. Furthermore, it was noted that TOPTIG, as a spatter-free welding process, has advantages over MIG welding, whose application is limited because the weld current passes through the weld wire, causing unstable arc transfer. The defining characteristic of the process is the configuration of the torch: the weld wire which is fed directly into the arc zone at higher temperatures which ensures continuous liquid-flow transfer as well as high deposition rate. It also showed that combining the TIG welding process with another process, which creates the hybrid welding process, goes a long way to improve the productivity of the welding process. The novel welding process TIP TIG, which uses a continuously fed and sinusoidal stimulated preheated filler metal, improves the deposition rate very significantly. The findings also showed that TIP TIG technology can reduce costs by more than 60% depending on its application and increases productivity by 400%.
Contribution	This was the first review article to introduce and discuss different variants of TIG welding processes. This contributed by identifying various pitfalls that need to be avoided in order to enhance the welding processes in order to help increase its productivity. Different reasons associated with poor weld quality were ascertained. The various welding parameters were identified. The findings form the basis on which further research work in the study was based.

Publication II: "Usability of Laser-TIG Hybrid Welding Processes"

Article II (see Table 13) deals with the usability Laser-TIG hybrid welding process. The article is based on research gaps concerning how to select proper welding parameters to improve on the weldability of laser-TIG hybrid process. Also, the complexity of the process variables when a hybrid welding process is created were investigated. This article was based on the findings in Article I.

Table 13. Summary of Article II

Title of article	Usability of Laser-TIG Hybrid Welding Process
Aims	Higher TIG weld productive process was to be investigated. Laser- TIG hybrid welding was selected due to availability. the purpose is to investigate the range of application and the weld quality attainable in non - ferrous metals.
Research question (s)	Where can the Laser-TIG hybrid welding process best be used?
Main findings and contribution	Industrial application of the welding process was established, and the limitations were stated: the productivity and weld quality attained were identified. Weld undercut which is a weld defect common to laser hybrid welding of non-ferrous metal was observed in the study. the recommendation based on literature review of multiple scientific articles showed that the defect was controllable by optimizing the weld parameter. For example, weld air gap should not be more than 3% of material thickness for limiting weld undercut. This study provides additional knowledge to the limited available knowledge on the applicability of various hybrid laser - TIG welding systems for welding. Also, it is not possible to give a general rule on how various parameters in laser-TIG hybrid can be optimised due to the complexity of the phenomena involved. Finally, the findings show that there is the need to find other means to optimise welding parameters to improve weld quality. Therefore, the combination of two different processes which form a hybrid process is not the only solution in the enhancement of the various welding processes. Although it helps to overcome some challenges in the single process, it is paramount to investigate other means of optimising the welding processes. This article

	formed the basis and the need to apply AI in welding and the role it can play in welding optimisation.

Publication III: Modelling of an artificial intelligence system to predict structural integrity in robotic GMAW of UHSS fillet welded joints.

In Article III (see Table 14) the purpose is to identify and define the relationships between nonlinear weldability factors to enable the creation of an artificial intelligence model. In addition, the possibility of employing an artificial neural network (ANN) to predict full penetration fillet weld characteristics is examined.

Table 14. Summary of Article III

Title of article	Modelling of an artificial intelligence system to predict structural integrity in robotic GMAW of UHSS fillet welded joints
Aims	To present an understanding on the adoptability of artificial intelligence for welding. Welding involves nonlinear weld parameter that needs to be optimized for attaining acceptable quality welds. Modelling using AI system can help in attaining weld optimizations with limited material waste. The purpose therefore is to present the viability of using AI for optimizing weld parameters.
Research question (s)	How can AI be used in modelling in welding process to predict structural integrity of the welded structure?
Main findings and contribution	The study showed that a mathematical model can be used to predict weld output. Therefore, AI system model can be used to optimize weld process parameters and variables. As a result, better weld structural integrity is attainable. An understanding on the possibility of modelling parameters were established. This study showed that there is a large possibility for the use of AI in weld modelling. This adds to the body of knowledge on the use of AI in welding. This article forms the basis of developing a hybrid deep learning algorithm in predicting welding parameters.

Publication IV: Development of an Artificial Intelligence -Powered TIG Welding Algorithm for the Prediction of Bead Geometry for TIG Welding Processes using Hybrid Deep Learning.

While Article III highlighted the application of ANN possibilities in welding processes, it founded the platform for creating the basis for developing a hybrid deep learning algorithm. Article IV (see Table 15) describes more precisely the role AI plays in predicting weld parameters. The proposed algorithm can assist human welders to select desirable end factors to achieve good weld quality in the welding process. As a result, Article IV addresses this research gap.

Table 15. Summary of Article IV

Title of article	Development of an Artificial Intelligence Powered TIG Welding Algorithm for the Prediction of Bead Geometry for TIG Welding Processes using Hybrid Deep Learning
Aims	AI needs large data for learning and providing accurate prediction. Providing such large data for input into AI models is expensive and sometime not viable. The purpose of this study is to create a model that uses small weld data input to generate large data needed in AI prediction of weld outputs and to develop an AI welding algorithm that can assist human welders to select desirable end factors to achieve good weld quality in the welding process.
Research question (s)	How can an AI model based on hybrid Fuzzy-Deep Neural Network (DNN) architecture help the human welder avoid trial and error during the selection of welding parameters?
Main findings and contribution	24,000 weld parameter inputs were generated by data augmentation from 27 Weld samples of 3 parameters each. these 24,000-input data were used in the AI model for training and verification. The output showed high predictability of weld bead. The novelty therefore is that the model for predicting weld output designed in data size flexible. Both small and large data can be used on the model. The applicability of this work is that welders can also predict or determine weld parameter inputs based on desired output. It is important to state that the model can be further improved to take into consideration more weld parameters. The results show around 92.59 predictive accuracy when compared to the results from an experimental data set. In addition, it creates a platform which helps in data flexibility such that both small and big data can be applied. This is a major challenge in

	welding technology in that it has less data, however, the findings show that small data can be applied in the hybrid fuzzy deep learning algorithms incorporated into the Likert scale.

Remarks on this chapter

In this chapter, the overview of the supporting articles and findings were discussed. This chapter discussed the contribution each article played in achieving the overall objective of the study. In a nutshell, Articles I and II were the main catalysts for the other two articles. It was in Articles I and II that the research gap as to how different methods regarding AI applicability in dealing with nonlinearity in welding processes to improve the welder's performance during welding came to light. The AI hybrid deep learning algorithm framework was tested with a real-life welding data set, which was validated and had a very good predictive accuracy. Also, the applicability of AI and its prospects in the welding industries proved to be a novel approach regarding data argumentation. The contributions in Articles I, II, III and IV demonstrated the theoretical and practical relevance of this study in the field of welding and how this can go a long way to advance the cause of AI in the field of welding. The next section will describe the discussion, conclusions and suggestions for further studies.

5 Discussions

This study investigates the applicability of AI in modern welding technology. The focus is on how an AI framework model can be developed to improve welding performance and remove operator trial and error during welding. Usually, the welding procedure is selected based on experience and sometimes based on a DoE when needed. However, it is practically unfeasible to run a full factorial design to find optimal values, since the number of experiments increases exponentially with the number of welding parameters (Jesus, 2016).

This is composed of how different welding processes can be developed to improve quality and efficiency, and how simulation processes can be applied in welding technology. Recent developments in the quality and efficiency of welding operations have been the main drivers for competitiveness in the welding industry. Applying simulation to welding enables the implementation of AI techniques. The need to get items to the market quickly and the need to "do it right for the first time" are also pushing the industry towards greater use of virtual tools (Lindgren, 2007).

In order to achieve the stated objective of this study, it was important to conduct a background study on the various welding processes to identify areas where AI can be applied. A brief explanation of different variants of TIG welding was provided and investigations examined how TIG welding can be combined with other processes (hybrid welding) to improve on productivity. During this work, it was realised that combining two processes, that is laser and arc welding, to form a single process zone creates numerous process parameters. The process parameters need to be carefully controlled to achieve good-quality welds. The various parameters and interactions that occur when these processes are combined, that is parameters related to the individual processes and those that occur because of the use of two processes, have been examined by various authors (Hyatt, 2001) (Sugino, 2005) (Kim I. S., 2003) (Petring, 2003) (Hayashi, 2004).

To affirm the views of these authors, an investigation was carried out on the combination laser and TIG welding processes which produced some interesting findings. It was observed that laser-TIG hybrid welding can lead to improvements in penetration and generate cost savings for applications where filler wire is not needed. In addition, although the hybrid process can go a long way to help improve weld quality, the complexity of the process variables that arise because of the combination of the welding processes creates a requirement for other improvements. However, the investigations showed that it is not possible to propose an optimum weld process for all materials for different structures because the optimum weld process is case-specific and can be influenced by factors like joint design and joint accessibility.

Study of the TIG welding process and its productivity showed that different variants of the TIG welding process have been developed in recent years in efforts to improve productivity. However, it was found that scientific investigation into the new variants is

minimal, especially with regard to TOPTIG, TIP TIG and TIG-MIG. An exception is the hybrid welding technique of using laser sources combined with a TIG welding process.

Investigation of TIP TIG has shown that it is possible to achieve speeds equivalent to those of MIG welding. The advantages of this novel welding process help to counteract the main drawback of traditional TIG welding with regard to low welding speed. Another TIG variant, TOPTIG, which is a spatter-free welding process, has an advantage over MIG welding because in MIG welding the weld current passes through the weld wire and causes unstable arc transfer. From a welding efficiency perspective, the spatter-free nature of TOPTIG reduces the need for cleaning and polishing of welds and thus saves time and costs. In standard TIG welding, one major drawback is the need to direct the wire at an angle of approximately $90°$ with respect to the electrode and the wire must be parallel to the weld. However, the integrated wire system in TOPTIG, which is fed directly into the arc zone at a higher temperature, ensures continuous liquid flow and higher deposition rate.

In view of the potential benefits, it seems likely that utilization of the different variants of TIG welding in welding of thin sheet metals will increase. The limitation of low productivity in the use of conventional TIG welding processes seems to be being overcome as a result of these novel developments in different variants of TIG welding.

Most researchers are of the view that LTHW is mainly applicable to thin materials that are less than 5mm thick, which can be considered a major drawback for LTHW. However, observations have shown that LTHW is capable of welding plates with thicknesses of 16mm and achieving good welds. In addition, the findings show that when used in welding, LTHW utilises laser energy more efficiently and improves energy coupling between the plasma and molten pool, which is advantageous in welding of thick materials.

The Welding Institute (TWI) carried out an experiment on 304L austenitic stainless steel (10mm, butt welds and 16mm, melt runs) using CO_2 and Yb fibre lasers, and found that it was possible to use LTHW on thick materials. The flexibility in being able to weld either with or without filler wire provides an advantage in terms of cost reduction, especially when the metal to be welded does not need the addition of filler wire.

When examining the benefits of hybridisation in welding, the Institute of Welding and Joining Technology (ISF) at the Rheinisch Westfälische Technische Hochschule (RWTH), Aachen, used a 2 kW Nd: YAG laser combined with TIG welding and reported a price reduction of up to 50%, a reduction in necessary joint edge preparation, and higher efficiency. Undercuts, which have been reported as the most common weld defect with LTHW, could be eliminated by choosing suitable welding parameters. Results obtained from applying LTHW showed an improvement in weld quality and led to a reduction in pores and cracks when compared to using TIG welding.

Hybridisation of the welding process creates numerous process parameters, hence one question that comes to mind is how suitable parameters can be selected during welding

and how this selection can be done such that it eliminates defects and saves time by avoiding the need for trial and error by the human welder. One possible way to address or alleviate weldability challenges associated with nonlinear factors (welding parameters) is by deploying AI systems. Therefore, the AI framework used in this dissertation does not rely solely on human perspectives or theories.

As mentioned earlier, the objective of this study was to apply AI to welding technology to predict weld parameters and avoid trial and error by the human welder. To assess the feasibility of using AI, an AI-powered TIG welding algorithm, based on the architecture of a hybrid fuzzy deep neural network algorithm was developed. The model was tested with experimental data from 27 welds.

Current, arc length and welding speed were applied as control parameters in the test case. Using these control parameters, 24,012 training samples were used to train a fuzzy driven deep neural network implemented using Keras Library with a Google TensorFlow backend. The 24,012 samples were mathematically learnt from expert-level fuzzy rules using one of the subsystems of the proposed system called a Fuzzy Likert System (see methodological section). The system architecture used during the validation is presented in Publication IV. In brief, during the training, the algorithm automatically split the training data sets into training and validation data sets. In this data split, the algorithm used 14,407 training data sets for training and 9,593 for validation. It is important to note that the training and validation data can leak during optimisation and training. In machine learning, testing a data set is a post-validation strategy used to offer an objective evaluation of the algorithm beyond the validation data. Using this post-validation strategy, independent data (out-of-sample test data) of 27 experimental data sets were used to further test the generalisability of the welding algorithm. The model's generalisability is a measure of predictive accuracy. Predictive accuracy defines how closely the model performs to reality. Running the simulation, the results showed a predictive accuracy of 92.59%, which indicates that the AI algorithm made 25 out of 27 correct predictions.

Additionally, the algorithm gives an indication of the maximum and minimum control range in which the human welder can obtain the desired output. The ability to predict the range introduces flexibility and enables the welder to select from a range of parameters while still being able to achieve quality welds. For example, the algorithm suggested that if the current is controlled within 51.00 to 67.00 A, the arc length is selected within 1.70 to 3.00 mm, and the welding speed is set up to a maximum of 17.04 mm/s or less, a moderately high weld bead width of approximately 5.00 to 6.70 can be achieved. This prediction is in line with the real-life case in the experiment, where a weld bead of 5.50 mm was recorded, which is within the predictive range of the algorithm. This performance demonstrates the feasibility of the method for supporting the human welder in automatic selection of control parameters to obtain the desired weld bead without going through a time-consuming trial-and-error approach.

The welding information presented together with the neural network schematic model shows that it is possible to accurately predict welding parameters and process outputs using learning algorithms.

With lots of inspiration been drawn from recent automation system and machine learning it is expected that the welding industry will be able to increase its productivity by integrating its systems which includes monitoring system, the utilisation of advanced welding equipment and software applications. It is expected that adopting these systems will improve on the benefits derived from technological achievements and economic enhancement. The application of big data management in the welding industry will go a long way to improve on welding productivity by reducing the number of errors caused by the human welder. Additionally, rework in welding will reduce tremendously thereby helping to save cost as well increase in weld productivity. One major benefit the welding industry stands to gain by utilising aspects of automation and machine learning is that it gives the entire welding team and not just the welder access to data which enables one to confirm or reject a welded joint based on quality requirements.

In summary, it can be concluded that advances in variants of the TIG welding process that improve its usability for welding of different materials and material thicknesses will lead to greater use of TIG welding throughout the welding industry. The drawback of low productivity due to low speed will become a thing of the past due to the emergence of hybrid welding processes that utilise the advantages of two processes. To ascertain the applicability of AI to welding and the ability of AI to handle the complexity inherent in welding processes, this study utilised a hybrid deep learning algorithm to predict weld bead parameters and observed that the algorithm could predict parameters with high accuracy. The research method was shown to be effective in dealing with the big data requirements when applying advanced AI method to welding technology. The novelty of the work in this study is that the AI approach used overcomes the limitation of the big data requirement. Where big data is not available for the algorithm to learn from, the system can mathematically manipulate the small data using its inference engine and extract its own big data from the available small data using the technique of data augmentation and reach a conclusion about the required range of welding parameters.

6 Conclusions

In recent times, welding has emerged as the most used method to join different metals of varying strength. Welding quality can be achieved when quality requirements are met such as those related to bead geometry and porosity inclusions. During arc welding, the weldment goes through thermal cycles that are usually characterised by very fast heating and cooling. The weldment shape together with the shape of the HAZ are results of the welding process and define the overall integrity of the welded joint. Therefore, accurate prediction of the weld shape together with that of the HAZ can help avoid the need for costly and time-consuming experiments. The ability to control welding parameters using sensing devices either directly or indirectly can advance the cause of achieving quality in welding. Moreover, it also improves the productivity of the welding process. One important task in automation of welding is to understand how welding parameters affect bead geometry so suitable models for predicting the desired outputs can be developed. In recent years, AI methods are being increasingly utilized in welding technology to predict process parameters and improve on the performance of welding process such as TIG, MIG and spot welding.
To explore the feasibility of extending the use of AI in welding further, a comprehensive literature review on variants of TIG welding was carried out and experimental simulation performed AI technique in TIG welding.

The first research question considered the welding process studied and was addressed with a systematic investigation into different variants of TIG and their application areas.

One major characteristic of TIG arc welding is that it is not able to transfer a lot of filler metal when filler wire is used because part of the heat of the arc is used to melt the filler wire. The usage of filler wire in TIG welding is optional, which can bring cost savings. In view of the low productivity of conventional TIG welding, variants have been developed that try to overcome productivity issues, such as hot wire TIG, TIP TIG Hot Wire, Double Shielded TIG, TOPTIG, Laser-TIG hybrid and laser -MAG/MIG hybrid. These TIG welding process variants have helped mitigate problems related to low penetration and control of the starting and finishing phases of the welding cycle. They have further improved the weldability of different range of diameters and have improved stability. In addition, improvements in the weldability of thin sheets, improved metallurgical properties and reduction of weld width have been achieved.

The second research question covered aspects of the usability of LTHW. Laser-TIG can be used to join both ferrous and non-ferrous metals and is suitable for aircraft, aerospace and automotive industry applications. The superior corrosion resistance, light weight and high strength-to-weight ratio of LTHW welds makes the process appropriate for most metals. The combination of a laser and TIG arc creates a complex process with a high number of variables. Consequently, it is a significant challenge to find a general rule for how the various parameters in LTHW can be optimised. Undercuts, which have been

found to be the most common weld defect during welding with LTHW and which occur due to deflection of the arc, can be eliminated by choosing suitable welding parameters.

The third research question investigated how AI can be used in modelling of welding to predict the structural integrity of the welded structure. Structural integrity is a very important property for a welded structure because it determines if the structure is fit for the purpose for which it has been designed and can function under normal conditions. In addition, a safety margin needs to be included so that the structure is safe even beyond its original design purpose its original design purpose. Modelling to guarantee better structural integrity in lightweight-welded materials is particularly relevant in modern welding manufacturing and production because energy efficiency and environmental impact are major concerns. Being able to identify and define proper relationships between nonlinear weldability factors will enable the creation of an artificial intelligence model that can predict full penetration in fillet welded joints. It was noted that nonlinear variables associated with welding processes, such as heat input, CTWD and torch angle, which usually pose weldability difficulties, can be modelled by applying AI systems.

The final research question deals with how an AI model based on HFDNN architecture can help the human welder avoid trial and error during selection of welding parameters.

In view of the ongoing discussions, one of the major conclusions that can be drawn from this study regarding the applicability of AI in welding technology is about its learning capabilities and versatility. The AI method applied in this study was fuzzy deep learning incorporated with Likert scaling. Normally, AI decision-making tools use deep learning techniques, which require big data to learn from. In the field of welding, obtaining this big data is challenging because little experimental data is available. The added value of this work is that the method proposed helps overcome the limitation of a big data requirement. Where big data is not available for the algorithm to learn from, the system can mathematically adjust the small data by using its inference engine and extracting its own big data from the available small data using the technique of data augmentation. The findings of this research suggest that the artificial intelligence system used can effectively help the welder in avoiding trial and error when choosing welding parameters to help improve on weld quality. The results of the study showed that the hybrid fuzzy deep learning-based decision-making system could provide a consistent weld output in varying welding conditions. Even though, the test case carried out in this dissertation is regarding TIG welding process, the effect and the outcome proved that it is likely to have same effect when applied to other welding process such as MIG/MAG, SMAW, friction welding and Laser-arc hybrid welding processes.

7 Suggestions for further studies

In future work, the aim should be to test the developed AI system with more experimental cases and expand its knowledge development to cover penetration depth and width of weld bead, depth and width of HAZ, cross-sectional area of weld bead and HAZ. The model should be tested on best practices in different domains of welding to improve the knowledge base of the proposed system and thus facilitate progress in the field. In the ANFIS methodology, a feed-forward neural network approach was applied and therefore, in the future, a combination of the ANFIS and a DNN model will be applied in order to create a fuzzy logic control system that can help predict a given input if the desired output is known - by applying back-propagation in order to reduce the error significantly. In addition, considering the aspects to increase productivity and quality in welding technology it is expected that more research will be carried out in areas such as big data, autonomous robots and how it can be used in welding technology to increase productivity. Finally, the revolution where robots are developed with humans returning to production process will be of immense benefit to welding industry if proper investigation is carried out in the future for proper integration of these various advancement. The objectives and the contribution should be clearly stated, so that the success of the research work and the acceptability of the work as a dissertation can be measured. However, the Introduction should be concise and not go into too many details.

A common approach for writing the introduction is to start from the background and then gradually introduce the scope and objectives of the work. Another approach is to first determine the objectives and contribution and then explain the background and how the objectives are reached in the work. As an example, this document applies the latter approach (see Introduction): the objective and the contribution were stated in the first sentences followed by short explanations of the background and the contents of the work.

References

Aikenhead, M. M. (2003). A neural network face recognition system. *Engineering Applications of Artificial Intelligence*, 167-176.

Albaum, G. (1997). The Likert scale revisited: An alternate version. *Journal of the Market Research Society, 39*, 331-349.

Anand, K. E. (2018). Modelling and prediction of weld strength in ultrasonic metal welding process using artificial neural network and multiple regression model. *Material Sci & Eng. Int. Journal, 2*(2), 40-47.

Antoniou, A. S. (2017). Data augmentation generative adversarial networks. *arXiv preprint arXiv:1711.04340*.

Arias, J. L. (2005). Laser TIG hybrid welding of very thin austenitic stainless steel sheets. *In Proceedings of the 24th Int. Conf. on Applications of Lasers and Electro Optics*, (ss. 104-107). Miami, USA.

Åstrand, E. Ö. (2013).) Cost affecting factors related to fillet joints. *In: Jármai K, Farkas J (eds) Des. Fabr. Econ. Met. Struct. Springer Berlin Heidelberg, Berlin, Heidelberg,*, pp 431–435.

Bagger, C. O. (2005). Review of laser hybrid welding. *Journal of Laser Applications, 17*(1), 2-14.

Benyounis, K. O. (2008). Optimization of different welding processes using statistical and numerical approaches - A reference guide. *Advances in Engineering Software, 39*(6), 483–496.

Berman, D. B. (2019). A survey of deep learning methods for cyber security. *Information mdpi, 10*, 122.

Bonanno, D. &. (2017). An approach to explainable deep learning using fuzzy inference. *Proc. of SPIE Vol. 10207 102070D-1*. doi:10.1117/12.2268001.

Buah, E. L. (2020). Emotional responses to energy projects: A new method for modeling and prediction beyond self-reported emotion measure. *Energy, 190*, 116-210.

Buncher, C. R. (2006). Statistics in the pharmaceutical industry, Chapman and Hall–CRC. *3rd Ed*.

Chang, L. (1994). A psychometric evaluation of 4-poing and 6-point Likert-typescales in relation to reliability and validity. *Applied Psychological Measurement, 18*, 205–215.

Chen, S. B. (2004). Welding robotic systems with visual sensing and real-time control of dynamic weld pool during pulsed gtaw. *" International Journal of Robotics and Automation, 19*(1), 28-35.

Chen, S. B. (2014). Research evolution on intelligentized technologies for arc welding process. *J Manuf Process*, 16:109–122. doi:https://doi.org/10.1016/j.jmapro.2013.07.002

Chen, S. Z. (2016). Droplet transfer in arcing-wire GTAW. *Journal of Manufacturng Processes*, 149-156.

Cheryl Quing, L. (2010). *A New Liker Scale Based on Fuzy Sets Theory.* United states: UMI dissertation.

Chokkalingham, S. C. (2010). Artificial Neural Network Modeling for Estimating the Depth of Penetration and Weld Bead Width from the Infra Red Thermal Image of the Weld Pool during A-TIG Welding.In: Deb K. et al. (eds) Simulated Evolution and Learning. *Springer, Berlin, Heidelberg.* doi:https://doi.org/10.1007/978-3-642-17298-4_28

Clark, J. (1985). Effect of process parameters on dimensions of weld bead and heat-affected zone. *Materials Science & Technology 1: 1069-1080.* doi:http://dx.doi.org/10.1179/mst.1985.1.12.1069.

Dutta, P. D. (2007). Modeling of TIG welding process using conventional regression analysis and neural network-based approaches. *Journal of Materials Processing Technology, 184*, 56-68.

Eguchi, K. Y. (1999). Application of neural network to arc sensor. *Science and T echnology of Welding and Joining, 4*, 327-334.

Fu, G. L. (2016). Influence of the welding sequence on residual stress and distortion of fillet welded structures. *Marine Structures, 46*, 30–55.

Goodfellow, B. Y. (2016). *Deep Learning.* MIT Press. Noudettu osoitteesta http://www.deeplearningbook.org

Gyasi, E. A. (2017). Modeling of an artificial intelligence system to predict structural integrity in robotic GMAW of UHSS fillet welded joints. *Int J Adv Manuf Technol*, 93:1139–1155. doi: https://doi.org/10.1007/s00170-017-0554-0

Harold, F. G. (2014). *Extrusion: The Definitive Processing Guide, 2nd ed.;.* Wayne, PA, USA: Willian Andrews Publications.

Hayashi, T. K. (2004). High power CO2 laser- MIG hybrid welding for increased gap tolerance. Hybrid weldabilit of thick steel plates with square groove. *Welding International, 18*(9), 692-701.

Henderson, D. E. (1993). Adaptive control of an arc welding process. *IEEE Control Systems, 13*(1), 49-53.

Hinton, G. (20. 05 2020). *Deep Learning in Digital Pathology.* Noudettu osoitteesta http://www.global-engage.com/life-science/deeplearning-in-digital-pathology

Hirai, A. (2001). Sensing and control of weld pool by fuzzy-neural network in robotic. *The 27th annual conference of the IEEE Industrial Electronics*, (ss. 238-242).

Hodge, D. ,. (2003). Phrase completions: An alternative to Likert scales. *Social Work Research, 27*, 45-55.

Holmes, J. S. (AIME 2015). Artificial intelligence in medicine . *Elsevier*, 1-2.

Hon, S. P. (2013). FPGA Based Sun Tracking System Using Fuzzy Logic. *International Journal of Scientific and Technology Research, 2*(9), 217-220.

Hyatt, C. M. (2001). Laser-Assisted Gas Metal Arc Welding of 25-mm-Thick HY-80 Plate. *Welding Journal, 80*(7), 163-172.

Ibrahim, I. A. (2012). The Effect of Gas Metal Arc Welding (GMAW) Processes on Different Welding Parameters. *International Symposium on Robotics and Intelligent Sensors. 41*, ss. 1502-1506. Elsevier.

Inoue, H. (2018). Data augmentation by pairing samples for images classification. *arXiv preprint arXiv :1801.02929* .

Ishide, T. N. (2001). Latest MIG, TIG arc-YAG laser hybrid welding system. *Journal of the Japan Welding Socienty, 72*(1).

Jamieson, S. (2004). Likert scales: How to (ab)use them. *Medical Education, 38*, 1217-1218.

Jeng, J. Y. (2000). Prediction of laser butt joint welding parameters using back-propagation and learning vector quantization networks. *Journal of Materials Process Technology, 99*, 207-208.

Jesus, R. B. (2016). welding sequence optimization using artificial intelligence techniques, an overview. *SSRG International Journal of Computer Science and Engineering (SSRG-IJCSE)*, 90-95.

Joshi, S. R. (2014). Application of statistical and soft computing based modeling and optimization techniques for various welding processes a review. *International Journal of latest trends in Engineering and Technology, 3*(4), 375–384.

Kah, P. S. (2015). Robotic arc welding sensors and programming in industrial applications. *Int J Mech Mater Eng*, 10:13. doi: https://doi.org/10.1186/s40712-015-0042-y

Kiaee, N. A.K. (2014). Optimization of gas tungsten arc welding process by response surface methodology. *Materials & Design, 54*, 25-31.

Kim, I. S. (2003). Prediction of welding parameters for pipeline welding using an intelligent system. *Int J Adv Manuf Technol, 22*, 713–719. doi:https://doi.org/10.1007/s00170-003-1589-y

Kim, I. S. (2004). Optimal design of neural networks for control in robotic arc welding. *Robot Comput Integr Manuf., 20*(1), 57-63.

Kim, J. W. (2008). A control system for uniform bead in fillet arc welding on tack welds. *J Mech Sci Technol*, 22:1520–1526. doi:https://doi.org/10.1007/s12206-008-0433-6

Kumar A., C. V. (2013). Role of artificialRole of artificial neural networks in welding technology : A survey. *International Journal of Computer Application, 67*(1), 32-37.

Laserline. (accessed on 3.8.2020). Noudettu osoitteesta https://www.laserline.com/en-int/laser-hybrid-welding/.

LeCun, Y. B. (2015). Deep learning. Nature. *521*, 436–444. doi:https://doi.org/10.1038/nature14539

Likert, R. (1932). A Technique for the Measurement of Attitudes. *Archives of Psychology, 140*, 1-55.

Lindgren, L.E. (2007). "Computational welding mechanics", in Computational Welding Mechanics ser. Woodhead Publishing Series in Welding and Other Joining Technologies L.,E. Lindgren, Ed. Haettu Available: http://www.sciencedirect.com/science/article/pii/B9781845692216500045

Liu, F.-Q. W.,Y.J. (2015). Tacked weld point recognition from geometrical features. *In: Tarn T-J, Chen S-B, Chen X-Q (eds) Robot. Welding, Intell. Autom. RWIA'2014. Springer International Publishing, Cham*, 47–56. doi: https://doi.org/10.1007

Liu, Y. K. (2013). Control of 3D weld pool surface, Control Engineering Practice. *Control Engineering Practice, 21*, 1469-1480.

Lopez, B. M. (2017). Special section on artificial intelligence for. *Elsevier*, 26-27.

Lucas, W. H. (1996). *Activating flux - increasing the performance and productivity of the TIG and plasma processes' Welding and Metal Fabrication.*

Mahrle A., B. E. (2009). Heat sources of hybrid laser arc welding processes. Woodhead Publishing Limited, Cambridge.

Mahrle, A. B. (2006). Hybrid laserbeam welding-classification , characteristics and appliaction. *Journal of laser Applications, 18*(3), 169-180.

Messler, R. W. (20 (2000). Autom., (s. 118).

Mohammad, A. K. (2012). Handbook of Research on Industrial Informatics and Manufacturing Intelligence: Innovations and Solutions. Teoksessa M. A. Khan. Ministry of Communications and Information Technology., India.

Mohammad, H. M. (2013). Sensitivity Analysis of the Artificial Neural Network Outputs in Friction Stir Lap Joining of Aluminum to Brass. *Advances in Materials Science and Engineering*, 1-7. doi: https://doi.org/10.1155/2013/574914

Nagesh, D. D. (2002). Prediction of Weld Bead Geometry and Penetration in Shielded Metal Arc Welding using Artificial Neural. *Journal of Materials Processing Technology*, 123, 303-312.

Narang, H.;Singh, U.;Mahapatra, M.;& Jha, P. (2011). Prediction of the weld pool geometry of TIG arc welding by using fuzzy logic controller. *International Journal of Engineering, Science and Technology*, 77-85.

Nielsen, S. E. (ei pvm). Hybrid welding of thick section C/Mn steel and aluminium., (s. 15).

Ohlsson, O. (2005). Relationship between complexity and liking as a function of expertise. *Music Perception, 22*, 583.

Parikshik dutta, D. K. (2007). Modelling of TIF welding process using conventional regression analysis and neural network-based approaches. *Journal of Materials Procesing Technology, 184*, 56-68.

Park, Y. W. (2002). Real time estimation of CO2 laser weld quality for automotive industry ,. *Optics & Laser Technology, 34*(2), 135-142.

Pashazadeh, H. G. (2016). Statistical modelling and optimization of resistance sport welding process parameters using neural networks and multi-objective genetic algorithm. *Journal of Intelligence Manufacturing, 27*(13), 549-559.

Patcharaprakiti, N. P. (2005). Maximum Power Point Tracking Maximum Power Point Tracking Maximum Power Point Tracking. *Renewable Energy, 30*(11), 1771-1788.

Patton, M. Q. (2002). Qualitative evaluation and research methods (3rd ed.). Thousand Oaks CA: Sage Publications, Inc.

Paul, A. (2016). Robust product design using sosm for control of shielded metal arc-welding (smaw) process. *IEEE Transactions on Industrial Electronics, 63*(6), 3717–3724.

Petring, D. F. (2003). Investigations and Applications of Laser-Arc Hybrid Welding from Thin Sheets up to Heavy Section Components. *22nd International Congress on Applications of Lasers and Electro Optics ICALEO Congress Proceedings*, (ss. 1-10). October 13-16 Jacksonville(FL), USA, LIA.

Pett, M. (1997). Nonparametric statistics for health care research: Statistics for small samples and unusual distribution. *SAGE Publication*.

Podržaj, P. (2019). An Overview of Arc Welding Control Systems. *Progress of Electrical and Electronic Engineering*.

Qing, L. (2013). A novel Likert scale based on fuzzy sets theory. *Expert Systems with Applications, 40*, 1609-1618.

Ragin, C. C. (2000). Fuzzy-Set Social Science.

Rayes, M. E. (2004). The influence of various hybrid welding parameters on bead geometry. *Welding Journal, 83*(5), 147 -153.

Romero, J. B.-B. (2016). Welding Sequence Optimization Using Artificial Intelligence Techniques, an Overview. *SSRG International Journal of Computer Science and Engineering* .

Ross, T. J. (2003). Fuzzy logic and probability applications: Bridging the gap, society for industrial and applied.

Ross, T. J. (2004). Fuzzy logic with engineering applications. John Wiley.

Schuberth, S. S. (2008). Next generation vehicle engineering guidlines for stainless steel in automotive applications. *Proceedings of the 6th STAINLESS STEEL SCIENCE AND MARKET*. Helsinki, Finland June 10-13.

Sjarif, N. N. (2019). "Endpoint Detection and Response: Why Use Machine Learning?,". *International Conference on Information and Communication Technology*

Convergence (ICTC), (ss. 283-288). Jeju Island, Korea (South). doi:doi: 10.1109/ICTC46691.2019.8939836

Smart, H. B. (1993). Intelligent sensing and control of gas metal arc welding. *CONF-9305134.* Idaho 83415-2210, U.S.A.

Stenbacka, C. (2001). Qualitative research requires quality concepts of its own. Management Decision. *39*(7), 551-555.

Sugino, T. T. (2005). Fundamental Study on Welding Phenomena in Pulsed Laser-GMA Hybrid Welding. *In Proc. of 24th International Congress on Applications of Lasers and Electro-Optics (ICALEO)*, *302th paper*, ss. 108-116. 31th October to 3rd November. Miami, Florida, USA. Laser Institute of America.

Tan, W. B. (2013). Investigation of keyhole plume and molten pool based on a three-dimensional dynamic model with sharp interface formulation. *Journal of Physics D : Applied Physics, 46*(5, 055501).

Taylor, J. L. (2018). Improving deep learning with generic data augmentation. *IEEE Symposium Series on Computational*, (ss. 1542–1547).

Team, D. (2019). *Artificial Neural Networks for Machine Learning – Every aspect you need to know about.* Noudettu osoitteesta https://data-flair.training/blogs/artificial-neural-networks-for-machine-learning/

Touileb, K. O.-S. (2020). Effects of ATIG Welding on Weld Shape, Mechanical Properties, and Corrosion Resistance of 430 Ferritic Stainless Steel Alloy. *Metals, 10*(404). doi: https://doi.org/10.3390/met10030404

Tsai, C. H. (2006). Fuzzy control of pulsed GTA welds by using real-time root bead image feedback. *Journal of Materials of Materials Processing Technology, 176*(1), 158-167.

Tzafestas, S. G. (2009). Expert control systems. Teoksessa: H. D. Unbehauen, toim. Control System, robotics and automation. 196-218.

Uchiumi, A. W. (76-85). Penetration and welding laser MIG hybrid welding of aluminum alloy. *In Proceedings of the 23rd International Congress on Applications of Lasers and Electro Optics.* San Francisco, USA.

Ushio, M. (2009). *Proceedings of the IIW International Conference on Advances in Welding and Allied Technologies.* Singapore.

Wei, J. W. (2019). Eda: Easy data augmentation techniques for boosting performance on text classification tasks. *arXiv preprint arXiv :1901.11196.*

Vemanaboina, H. E. (2018). Simulation of hybrid laser-tig welding process using FEA. *Journal of Engineering Science and Technology, 13*, 1782-1792.

Vendan, S. A. (2018). Interdisciplinary Treatment to Arc Welding Power Sources. *Springer*.

Vitek, J. M. (2001). Weld pool shape prediction in plasma augmented laser welded steel. *Science and T echnology of Welding and Joining, 6*, 305-314.

Vonglao, P. (2017). Application of fuzzy logic to improve the Likert scale to measure latent variables. *Kasetsart Journal of Social Sciences, 38*, 337-344.

Wu, C. P. (2000). Gas metal arc welding process monitoring and quality evaluation using neural networks. *Science and technology of welding and joining, 5*(5), 324–328.

Xu, Y. Y. (2012). Real-time seam tracking control technology during welding robot gtaw process based on passive vision sensor. *Journal of Materials Processing Technology, 212*(8), 1654–1662.

Yadav, N. Y. (2015). An introduction to neural network methods for different equations. *Springer Briefs in applied sciences and technology. Computational intelligence, Springer Science + Business Media B.V, Dordrecht.*

Yen, J. L. (2004). *Proceedings of the Second International Workshop – industrial Fuzzy control and Intelligent Systems* (ss. 1-9). College Station: TX: IEEE Press.

Zadeh, L. (1965). Fuzzy set. Information and Control. *6*, 338-353.

Zadeh, L. (1975). The concept of a linguistic variable and its application to approximate reasoning—II. *Inf. Sci, 8*, 301–357.

Zakariah, A. &. (2005). Medium size dual-axis solar tracking system with sunlight intensity comparison method and fuzzy logic implementation. *Jurnal Teknologi*.

Zhao, D. S. (2001). "Intelligent control for the shape of the weld pool in pulsed gtaw with filler metal. *Welding Journal, 80*(11), 253.

Publication I

Kesse, A. M., Kah, P., and Martikainen, J.
Investigations into enhanced TIG welding processes

`Proceedings of 20th International Conference. Mechanika. 2015*

Investigations into enhanced TIG welding processes

Martin Kesse*, Paul Kah**, Jukka Martikainen***

* *Lappeenranta University of Technology, P. O. Box 20, 53851 Lappeenranta, Finland*, *Email: martin.kesse@lut.fi*
** *Lappeenranta University of Technology, P. O. Box 20, 53851 Lappeenranta, Finland, Email:paul.kah@lut.fi*
***Lappeenranta University of Technology, P. O. Box 20, 53851 Lappeenranta, Finland,Email:jukka.martikainen@lut.fi*

Abstract

Industries like the automobile, aeronautic, construction, shipping, and oil and gas industries are always seeking means to maximize profit in their firms. One way that these industries can reduce costs and improve profitability is through the use of lighter material in their products. Consequently, industrial use of thin sheets (less than 10 mm thick) has increased from 10% to 90% of total production. Recently, interest has grown, particularly in the oil and gas sector, in the prospects of using aluminum in drill pipes, casings, tubing and risers, due to benefits accruing from its advantageous strength–to-weight ratio. However, producing welded constructions from non-ferrous metals like aluminum alloys is challenging compared to steel. This paper presents a literature review of TIPTIG, TOPTIG, Hot wire TIG, Laser-TIG and MIG-TIG hybrid welding by examining their benefits and limitations and how they can effectively be used in the welding of non-ferrous metals. The review shows that TIPTIG efficiently provides TIG welding at MIG welding speeds, which implies that it is possible to combine the benefits of TIG welding, particularly the cleanliness of the weld, with the capability to weld at higher speeds. Furthermore, it is noted that TOPTIG, as a spatter free welding process, has advantages over MIG welding, whose application is limited because the weld current passes through the weld wire, causing unstable arc transfer.
KEY WORDS: *TOPTIG, TIPTIG, activated TIG, TIG arc, pulsed TIG, productivity, weld quality*

1. Introduction

Industries like the automobile, aeronautic, construction, shipping, and oil and gas industries are always seeking means to maximize profit in their firms. One way that these industries can reduce costs and improve profitability is through the use of lighter material in their products. However, the welding of non-ferrous metals over the past years has been very challenging for technologist and designers, since properties such as high thermal conductivity, solidification shrinkage, oxide layer, high solubility of hydrogen make the welding of non-ferrous metals very difficult. Many researchers have reported on further   problems occurring when dealing with heat-treatable alloys, because the heat produced can cause deterioration in the mechanical properties of the metals, which occurs due to phase transformation and the softening in the alloys[1, 2].

TIG arc welding uses a non-consumable tungsten electrode and an inert gas which is used as a shielding gas, to fuse metals together. TIG arc welding is well-known technology and is commonly used for welding of hard-to-weld metals such as stainless steel and Al-Mg-alloys. In TIG arc welding, weld quality is strongly characterized by the weld pool geometry, because of the role it plays in determining the mechanical properties of the weld. It has been reported that during the welding of lighter materials having edge joints and flanges, welders usually exempt from the need to use of filler metals. TIG welding finds its greatest usage in the joining of thin materials in the manufacturing industries and it can augment weld quality. Several authors, for example, Fujii et al.[3] and Huang [4], have noted the limitations of TIG welding such as inferior joint penetration, poor tolerance on many material compositions, including cast-to-cast variations in the composition of certain impurities and its inability to weld thick materials in a single pass. Arias et al.[5] reported that TIG arc cannot transfer filler metal effectively because part of the heat of the arc is used to melt the wire.

Due to the above mention limitations, the TIG welding process has become a subject of research interest, in an effort to make the process more productive, and in recent times various developments have occurred that have enhanced its capabilities. This paper therefore presents a literature review of TIPTIG, TOPTIG, Hot wire TIG, Laser-TIG and MIG-TIG hybrid welding examining their benefits and limitations and how they can effectively be used in the welding of non-ferrous metals.

2. Enhanced TIG welding processes

Different types of TIG welding processes exist namely; alternating current and direct (AC/DC) TIG, dual shielded TIG, TOPTIG, TIPTIG, MIX TIG, Pulsed TIG, micro –TIG, hot wire TIG, Narrow gap TIG and activated TIG . Fig. 1 shows five different TIG welding process combinations. In the pre heated consumable, the filler wire is usually heated before usage whereas in the double shielding two gas mixtures are used. The automatic consumable electrode feeding combined with TIG is usually used in automatic welding process. The laser or pulsed combination can be used in hybrid

laser-TIG welding process. Finally the MIG/MAG welding process combined with TIG welding process will result in TIG-MIG/MAG hybrid welding process which was developed recently.
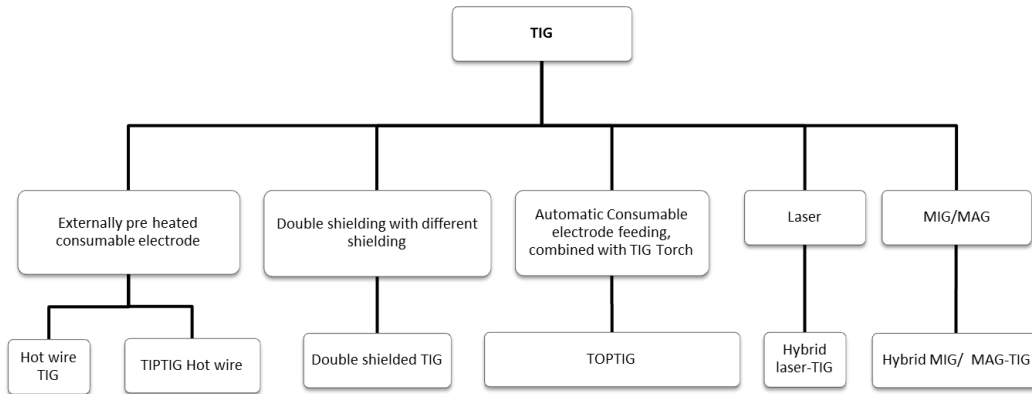

FIG.1 shows different TIG welding process combinations

In the following, different types of enhanced TIG welding processes will be presented. This will include a fundamental principle of dual shielded TIG, TIPTIG, TOPTIG, hot wire TIG, laser TIG hybrid, TIG-MIG hybrid, pulsed laser-TIG and activated TIG. These processes where conceded in the review because of their potential in overcoming the limitation of low productive in the conventional TIG welding process. Finally, a discussion on reported improvements will be presented.

Double-shielded TIG was developed in order to improve on the low penetration which has been a major drawback for the use of conventional TIG welding on thick materials[6, 7]. In double shielded TIG welding process pure inert gas is passed through the inner pipeline to keep the arc stable as well as protecting the tungsten electrode, while a mixed gas which contains an active gas, passes through the outer pipeline to serve as an active element which dissolves in the weld pool so as to change the Marangoni convection and the weld pool shape [8]. Fig.2 illustrates the double-shielded TIG process.
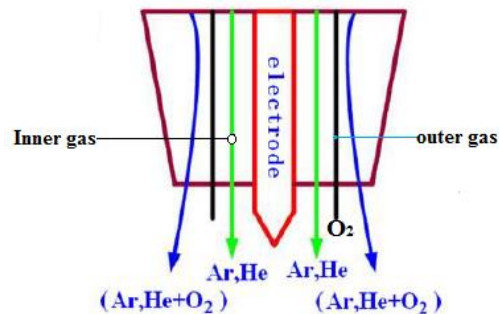

FIG.2 Double shielded TIG process [modified according to [8]

TIPTIG hotwire welding is a rather new process that was invented by Ing.Siegfried Plasch and patented in 1999, after about 1.5 years of development[9]. The main advantage of the TIPTIG hotwire process compared to those using a fusible electrode lies in the fact that TIPTIG welding allows a managed separation of the quantity of arc energy and the quantity of filler material introduced into the welding pool. This gives an advantage in controlling the starting and finishing (down-slope) phases of welding cycle [10]. Consequently, it combines the benefits of TIG welding, particularly the cleanliness of the weld, with the capability to weld at higher speeds comparable to MIG.

TOPTIG is a new TIG robotic welding process that combines the high weld quality of TIG process and the productivity of the MIG welding process. The defining characteristic of the process is the configuration of the torch: the weld wire which is fed directly into the arc zone at higher temperatures which ensures continuous liquid-flow transfer as well as high deposition rate [11, 12]. Fig. 3 illustrates the layout of TOPTIG welding torch. The benefits of TOPTIG can be

summarized as follows: absence of spatter (avoiding cleaning and polishing after welds), low distortion, high quality welds and productivity at reasonable cost. The excellent appearance of weld bead and better accessibility for welding complex structures are further benefits.
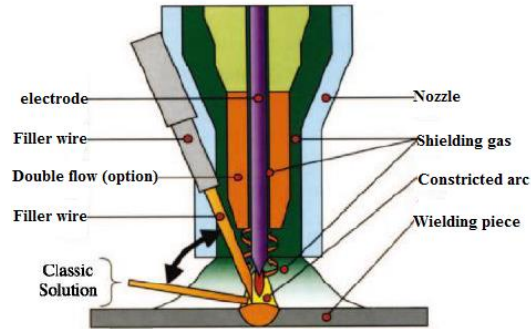

FIG.3 Layout of TOP TIG welding torch [11]

Hot wire TIG welding which has been in existence since 1960s but it has been underutilized. Using hot wire TIG welding, especially in the downward direction, it is possible to weld a larger diameter pipe with good quality. It has been reported that a high deposition rate comparable to that of MIG welding can be achieved with hot wire TIG welding. Fig. 4 shows the layout of hot wire TIG welding principle. Combining the hot wire TIG welding process with a narrow gap preparation makes it possible to make high productive welding without reducing the excellent quality gain from TIG processes [15]. However, hot wire TIG welding has some limitations; it is not normally used for manual welding and an additional equipment costs for the hot wire power supply.
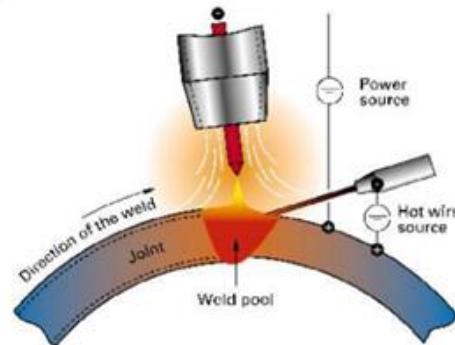

FIG.4 Shows the layout of hot wire TIG welding principle[13]

Laser-TIG hybrid welding is the combination of the laser beam welding and TIG arc welding processes. Many benefits have been realized from combining laser welding with conventional welding methods: improvement in arc stability, because of the absorption of the laser energy by the arc plasma, high efficiency and economy, high gap bridging capacities, increase in permissible tolerances, and greater weld speed [14]. One major advantage is the capability of adding filling material separately to the work piece, which enables independent determination of welding current and filler material feeding rate. As there is no transfer of metal across the arc, there are no molten droplets to contend with [15]. However to achieve the full benefits of laser-TIG it is important to ensure appropriate selection of welding parameters to enable the synergy of the two processes.

TIG-MIG hybrid welding process combines the quality of conventional TIG welding process and the efficiency of MIG welding process. Stability is realized when MIG arc is combined with TIG arc even when pure argon is used as shielding gas, this occurs because the cathode spots of MIG arc do not act unstable in TIG MIG hybrid welding process [16] . Benefits such reduction in welding time for butt joints from about 17-44% compared to conventional TIG welding has been realized using TIG-MIG hybrid welding process [17]

Pulsed Laser-TIG hybrid welding was developed in order to improve on the weldability of thin sheets[18]. The pulsed laser TIG process combines pulsed laser source and a pulsed TIG process in order to improve weld quality. Ben-

efits such as reduction in interaction time, which restrains the growth of plasma, and deeper penetration, have been reported. A major limitation is that more parameters have to be adjusted compared with continuous wave laser-TIG hybrid welding.

Activated TIG welding process applies a thin coating flux on the surface of the material to be welded, a constricted arc is then applied to the material increasing the current density at the anode root and the force acting on the weld pool[19]. Benefits such good metallurgical properties, reduction of the weld width, stabilization and increase of the depth of penetration have been achieved with the use of Activated TIG-welding

3. Current research

This section presents reported improvements on penetration, weld quality and high productivity of enhanced TIG welding processes over conventional TIG welding process.

Various test carried on TIP TIG indicate that, it is possible to achieve over 20 per cent cost savings over pulsed MIG for every meter of weld, which makes adoption of the process cost effective with quick payback, in addition to improved weld quality [9]. Table 1 shows comparison of TIP TIG to other welding processes. As shown TIP TIG cold wire (CW) gives a good depositions rate which is equal to that of MIG pulsed. In addition, TIP TIG hot wire (HW) showed higher deposition rate compared to conventional TIG, MIG pulsed and TIP TIG (CW).

Table 1.Comparison of different welding processes with TIP TIG [18]

Process	MIG PULSED	TIG	TIPTIG CW	TIPTIG HW
Metals	Steel, stainless steel	All weldable metals	All weldable metals	All weldable metals (except Al)
Thickness	> 0,60 mm	> 0,25 mm	> 0,25 mm	> 10,00 mm
Relative Speeds	Fast	Slow	Fast	Fast
Deposition Rates kg/h	1.0-3.6	0.6-0.7	1.0-3.6	1.4-5.4
Relative Operating Cost (time& materials)	Low	High	Low	Low
Weld Dressing needed	High	Low	Low	Low

Lu et al. carried out an experiment on 0Cr13Ni5Mo martensite stainless plate [8] and reported that the weld depth in double-shielded TIG welding increases about two to three times as compared to conventional TIG. Fig. 5 shows the weld shapes under different arc lengths and oxygen content in weld pool. The experiments showed that by adjusting the process parameters, the oxidation of the electrode tip can be completely avoided in the double shielded TIG welding.
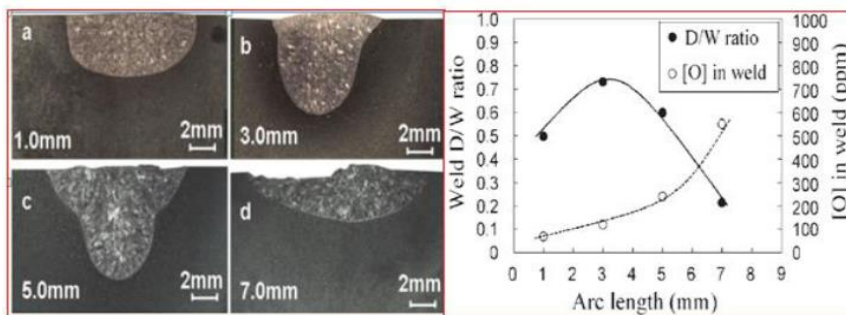

FIG. 5 Weld shapes under different arc lengths and oxygen content in weld pool (D/W ratio under different arc lengths)

V. Birdeanu et al.[18] confirmed the increase in penetration for pulsed laser –TIG in the welding of 1.2 mm thick 304 stainless steel plate and 1.5 mm thick coated unalloyed steel think sheets. In regard to efficiency pulsed laser-TIG

showed increased in penetration as compared to using each of the welding process separately. Fig. 6 shows the obtained penetration depths using each of the process separately.
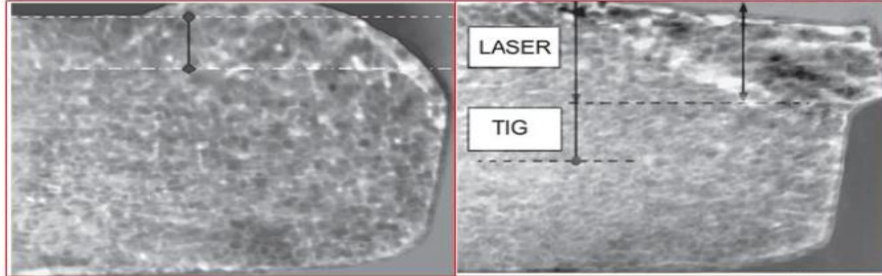

FIG. 6 Maximum penetration depth using pulsed TIG process and pulsed laser process (same joint configuration, same laser process parameters and lower travel speed)[18]

Kulikov F. R. [20] et al reported that during the welding of OT4 titanium alloy with Activated TIG welding process, one is able to produce welds with the same depth of penetration as that of welding without flux; however a reduction in current intensity was realized. On the other hand, Gurevic S. V. et al [21] reported that an increase in weld penetration and half the weld width can be achieved when alkali metals of about 80% are present in the flux used when welding of titanium grade BT alloy as compared with the situation in which flux does not contain those compounds. Fig. 7 shows the shape of butt joint in a 4mm thick titanium plate welded with activated TIG. As shown, the width of the weld heat affected zone (HAZ) is minimal with deep penetration.
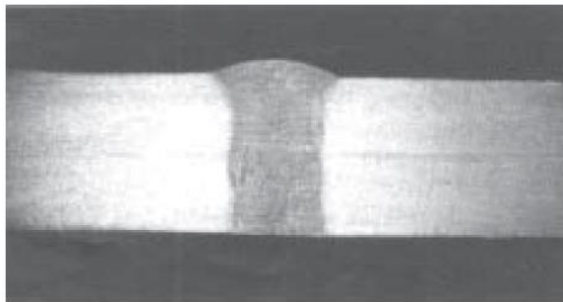

FIG.7 Shape of butt joint in a 4mm thick titanium alloy plate welded with Activated TIG.

4. Conclusion

In conclusion, there have been various developments of TIG arc welding process in recent years. However, scientific investigation on them is minimal, especially as regards TOPTIG, TIPTIG and TIG-MIG. An exception is the hybrid welding technique of using laser sources combined with TIG arc. It has been reported that laser-TIG hybrid can lead to improvements in penetration and cost savings for applications where filler wire is not needed. With regard to TIPTIG, speeds equivalent to those of MIG welding has been realized. Furthermore, it is important to mention that TOPTIG, as a spatter free welding process, has an advantage over MIG welding, whose application is limited because the weld current passes through the weld wire, causing unstable arc transfer. These benefits seem likely to increase the usage of enhanced TIG welding processes in the welding of thin sheet metals. Enhanced TIG welding processes seem to be overcoming the limitation of low productivity found with conventional TIG welding process.

5. References

[1] **Norman, A. F., Brough, I., Prangnell, P.B. ,** 2000, "High resolution EBSD analysis of the grain structure in a AA2024 friction stir weld," Materials Science Forum, vols. 331–337, Trans Tech Publications, pp. 1713–1718.
[2] **Norman, A. F., Drazhner, V., Prangnell, P.B. ,** 1999, "Effect of welding parameters on the solidification microstructure of autogenous TIG welds in an Al–Cu–Mg–Mn alloy," Mater. Sci. Eng. A259, pp. 53–64.

[3] **Fujii, H., Sato, T., Lu, S., P. and Nogi, K.,**2008, "Development of an advanced A-TIG (AA-TIG) welding method by control of Marangoni convection.," Material science Engineering, A4(95), pp. 296–303.

[4] **Huang, H. Y.,** 2009, "Effects of shielding gas composition and activating flux on GTAW weldments," Mater.Des.(30 (7)), pp. 2404-2409.

[5] **Arias, J., L., Romero, P., and Vandewynckele, A.,** 2005, "In: Proc. of ICALEO (Miami, USA)," p. 104.

[6] **Lu, S., P., Fujii,H., Sugiyama,H., Tanaka, M. and Nogi, K.,** "Weld Pool Shape Variations and Electrode Protection in Double Shielded TIG Welding," ISIJ Int., 2003,, 43, pp. 1590-1595.

[7] **Lu, S., P., Fujii, H. and Nogi, K. and Sato T.**, 2007, "Weld Pool Shape Variations and Electrode Protection in Double Shielded TIG welding," Science and Technology of Welding & Joining(12), pp. 689-695.

[8] **Dongjie L .I. A., S. L. B., Dianzhong LI C., Yiyi LI D.,** 2010, "Mechanisms increasing welding efficiency during new development of double shielded TIG process," Science and Technology of Welding & Joining, 15(6), pp. 528-533.

[9] **Mike, W.,** 2007, "TIP TIG: new technology for welding," Industrial Robot: An International Journal, 34(6), pp. 462–466.

[10] **Plasch, J.,** 2010, "TIP TIG -The welding revolution," https://ssl.plasch.at/index.php?option=com_content&view=article&id=32&Itemid=48&lang=en.(Date accessed 12.12.2013)

[11] **Opderbecke, T., and Guiheux, S.,** 2009, "TOPTIG: robotic TIG welding with integrated wire feeder," Welding International, 23(7), pp. 523-529.

[12] **Air liquide, E.,** 2008, "Top TIG," www. airliquide.com.

[13] **Bernard Kopecky, P. N., France,** "with the narrow gap TIG Hot wire welding multiply your productivity by a factor of 9, without sacrificing the quality.," http://www.fpga-faq.org/sb-metal_hold/cd_22/presse%255cpress_release_hot_wire_narrow_gap_welding.pdf, pp. 1-5(Date accessed 14.10.2014)

[14] **Dilthey, U., and Wieschemann, A.,** 2000., "Prospects by combining and coupling laser beam and arc welding processes. Welding in the World," pp. 44(43): 37–46.

[15] **Mahrle, A., Beyer, E., F.O. Olsen.,** 2009, "Heat sources of hybrid laser-arc welding processes," Woodhead Publishing Limited, Cambridge, pp. 47-84.

[16] **Kanomaru S., S. T., Sato T., Tanaka, M.,** 2012, "Basic study of TIG-MIG hybrid welding process," Quarterly Journal of the Japan Welding Society, 30(1), pp. 29-34 (in Japenese).

[17] **Shuhei K., T. S., Toyoyuki S., Hisashi M., Shinichi T., Shinichi T., Manabu T.,** 2013, "Study for TIG-MIG hybrid welding process," International Institute of Welding.

[18] **Birdeanu, V., Dehelean, D., Savu, S.,** 2009, "Laser-TIG hybrid micro-welding process developments," BID-ISIM Welding & Material Testing, 4, pp. 37-42.

[19] **Lucas,W. and Horse, D., S.,** 1996, "Activating flux- increasing the performance and productivity of the TIG and plasma processes," Welding and Metal Fabrication, 64(No.1).

[20] **Kulikov F R et al**: 'The use of fluxes for titanium alloy welding.'Avtomaticheskaya Svarka 1968 (4).

[21] **Gurevic S V et al**: 'Improving properties of titanium alloys in argon- arc welding.' Avtomaticheskaya Svarka 1965 (9) 1–4.

Publication II

Kesse, A. M., Gyasi, A. E., and Kah, P.
Usability of Laser-TIG Hybrid Welding Processes

Usability of Laser-TIG Hybrid Welding Processes

Martin Appiah Kesse, Emmanuel Afrane Gyasi, Paul Kah
Department of Mechanical Engineering, School of Energy Systems
Lappeenranta University of Technology (LUT)
Lappeenranta, Finland

ABSTRACT

Laser-TIG hybrid welding is an important joining technique for ferrous and non-ferrous metals, with the latter finding increasing application in the aerospace, aircraft, automotive, electronics and other industries due to advantageous properties such as superior corrosion resistance, light weight and high strength-to-weight ratio. However, the welding of non-ferrous metals has certain limitations. This paper presents a review of laser-TIG hybrid welding by examining the benefits and limitations of the process, relevant industrial applications, and optimization of parameters. A comprehensive literature review approach is used as a basis for suggestions of possible future areas of improvement. The review shows that laser-TIG hybrid welding has potential to become a versatile welding process and its industrial usage will likely increase due to its numerous benefits, such as porosity reduction, improved arc stability and increased welding speed, and the development of new TIG arcs that enhance the capabilities of the hybrid process. The main limitation found was undercut. However, research shows that this can be eliminated by selecting correct welding parameters. Finally, the paper suggests areas for further studies to improve understanding and utilization of laser-TIG hybrid welding processes. The findings are useful for industries that work with metal welding processes and as an educational tool.

KEY WORDS: Laser-TIG hybrid welding, TIG arc welding, low power laser technology, pulsed –TIG, ferrous and non-ferrous metals

INTRODUCTION

Laser welding technology has become an integral part of modern welding due to the unique fabrication opportunities it offers. Although its invention dates to the 1970s, practical application of the technology is still relatively new and the use of laser welding has only increased significantly following the development of high efficiency lasers. Limitations to the technology, such as the negative effect of high metallic surface reflection, depth penetration restrictions ($\leq$ 25mm) and strict tolerances for groove preparation, have led to the development of modified welding processes, e.g. hybrid laser welding, which aim to combine the benefits of both laser welding and arc welding.

In a hybrid laser welding process the laser beam interacts in the molten pool created by a secondary heat source, i.e., both heat sources are incident on a single weld pool (Mahrle and Beyer, 2006 and Bagger and Olsen, 2005). Hybrid laser-arc welding compensates for the limitations of the individual processes and thus offers advantages such as deeper welding penetration, high welding speed, reduced deformation, the ability to bridge relatively large gaps and a capability to handle highly reflective material (Bagger and Olsen, 2005 and Ishide et al. 2001). These advantages have meant that hybrid laser-arc welding has received significant attention in welding research.

The hybrid laser-arc welding process that is of interest in this work is laser-TIG hybrid welding (LTHW). LTHW was first investigated in the late seventies of the last century by Professor Steen and coworkers at Liverpool University. In their experiments, they combined a CO_2 laser and TIG arc and reported that the electric arc is rooted to the point where the laser interacts (Steen, 1979). In more modern research, benefits such as an improvement in heat efficiency and an increase in penetration and arc stability when welding Al alloys have been reported (Hu et al. 1993 and Diebold, 1998). Additionally, the possibility of determination of penetration sensitivity as a function of laser power using neural network modeling has been reported (Vitek, 1998). In addition to these findings, Gao et al. (2009) proved that a LTHW welding process can be applied effectively in the welding of ultra-fine grained steel and that the process permits the use of higher welding speed while obtaining sound welds with good mechanical performance. In recent times, the development of different laser sources such as disc, fiber and fiber-delivered high-power diode lasers and heat sources has further stimulated interest in hybrid welding and has led investigation of LTHW to become more immediately relevant – particularly since the last decade has seen the development of a variety of different TIG process (TIPTIG, TOPTIG, hot wire TIG). In view of the changed technological context, the importance of welding in industrial processes, and the possible benefits from combining laser and TIG arc heat sources, there is a considerable interest in the prospects of LTHW. However, despite considerable research interest, there is limited information on LTHW that provides in-depth knowledge of the process and surveys the technology from an industrial application viewpoint.

This paper presents an overview of laser-TIG hybrid (LTHW) welding processes by examining the benefits and limitations of the process, relevant industrial applications and optimization of parameters. Suggestions for possible future areas of improvement are made based on analysis of the literature reviewed.

PRINCIPLES OF THE LASER-TIG HYBRID WELDING PROCESS

Two basic configurations are used in LTHW; namely, the laser leading hybrid process (the laser beam precedes the arc) (Rayes et al. 2004 and Uchiumi et al. 2004) and the arc leading hybrid process (the arc precedes the laser beam) (Nielsen et al. 2006), illustrated in Fig. 1. The laser leading position is often used in the welding of aluminum since this arrangement removes the oxide layer prior to arc welding, resulting in a significantly more stable process (Uchiumi et al. 2004)
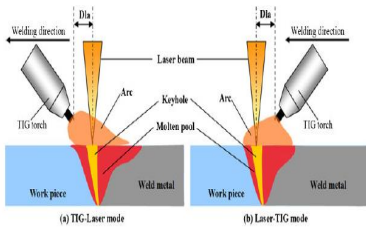

Fig.1.Schematic illustration of hybrid welding with leading arc (left) and leading laser (Uchiumi et al. 2004).

Improvement in the bead appearance and deeper penetration are some of the advantages realized in the use of a laser leading arc configuration (Abe and Hayashi, 2002 and Katayama, 2009). About bead appearance the laser leading process was found to be superior because the assist gas flow does not affect the molten pool created by the arc, however in the leading arc arrangement the shape of the bead surface is disrupted by the assist gas blowing into the molten pool. Contrary, it was reported that the arc leading arrangement gives a more stable arc (Dilthey, 1999). This is achieved within a relatively wide range of process distances. The leading arc process gives deeper penetration, probably due to the fact that the laser beam impinges the hot weld pool with better absorption than a solid surface and the energy losses from laser through heat conduction is reduced (Dilthey and Wieschemann, 2009 and Abe and Hayashi 2002 and Katayama, 2009)

Plasma characteristics (laser beam and arc interaction)

In LTHW, understanding of the physical phenomena is important. As stated previously, the configuration is either laser leading, e.g. hybrid laser-TIG, or arc leading, e.g. TIG –YAG, and the key hole is generally formed in the molten pool. Subsequently, a plume, vapors, fumes and spatters are also formed. A schematic illustration of a LTHW process is given in Fig. 2 (Uchiumi et al. 2004 and Baito et al. 2004). In the example in Fig. 2, the laser beam is focused on the workpiece and the TIG torch is at an angle of 20° and follows the laser beam. A keyhole is formed by the melt flow in the molten pool and the plume moves toward the incident laser beam.
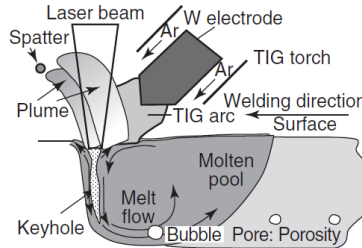

Fig.2 Schematic illustration of laser –TIG hybrid ((Uchiumi et al. 2004)

The arc plasma formed during TIG welding and hybrid TIG-YAG laser welding for a leading TIG torch are shown in Fig. 3 (Naito, 2005 and Naito, 2006). As illustrated in Fig. 3, an increase in arc voltage is released and is directly proportional to the YAG laser power. In addition, the plume affects the arc column making it brighter and longer, leading to an increase in the arc voltage.It has been reported by several authors that the arc is stabilized by the presence of the laser induced plasma (Kutsuna, 2002 and Biffin, 1994) Rooting and narrowing of the arc at the laser-generated hot spot and an increase in electrical conductivity and consequent reduction in the arc gap causes an increase in arc efficiency (Steen, 1981 and Gornyi and Redozobov, 1990). Fig.4 shows how evident this narrowing is when only 200 W of laser irradiation is used (Ireland, 1997). It can be seen in Fig. 3 that the arc is fixed at the beam irradiation spot, perhaps because an anode is generated, or the plume is dissociated by the laser beam.
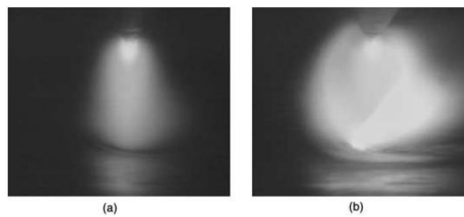

Fig.3.Observation results of arc behavior of Type 304 steel during (a) TIG and (b) hybrid TIG–YAG laser welding (Naito, 2005 and Naito, 2006)

Factors like the arc current, the distance between the electrode and plate, the distance between the laser-irradiation spot and electrode target on the plate, the inclination of the electrode, and the type of laser and shielding gas affect the interaction between the arc and the laser-induced plume.
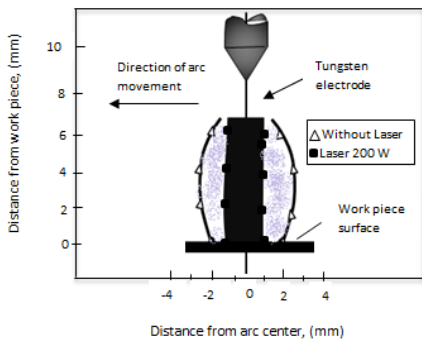
FIG.4. Shape of TIG arc with laser impinging in dark shading and without laser in gray shading (Ireland, 1997).

It has been reported that absorption of the laser light does not occur in Nd:YAG/TIG hybrid welding with a 10 kW laser (Ishide et al. 2002). However, it is unclear whether this is true of all metals. During Nd: YAG/TIG welding, the TIG arc voltage has been found to drop due to shortening of the arc, possibly as a result of the arc flowing along the laser plume. In a study of Nd: YAG/TIG hybrid welding using high speed photography (40 500 f/s), it has been observed that the arc moves more dynamically and rapidly around the outlet of the keyhole than in TIG arc welding alone. This behavior can be attributed to the instability in the direction of the ejected plume (Kutsuna, 2002).

During LTHW welding, the electric arc dilutes the electron density of the laser plasma, which weakens the ability of the laser plasma to absorb and reflect the laser energy and therefore improves the heat efficiency of the laser beam (Hu et al. 1993). In investigation of the stabilizing effect of the laser beam arc, which is an important factor in LTHW, it was found that an increase of about 300% in welding speed can be obtained when the laser and TIG arc are on opposite sides of the workpiece. When the laser and TIG arc were on the same side of the workpiece, 100% increase in welding speed was achieved during welding of 0.8 mm thick titanium and 2 mm thick mild steel (Steen et al.1979).

Dynamic behavior

The arc and laser-induced plume exhibits dynamic behavior during LTHW. This behavior has been observed by high-speed video cameras in hybrid TIG-YAG laser welding and it was reported that the arc sometimes concentrates around the keyhole inlet near the TIG electrode (Naito, 2005 and Katayama, 2007 and Naito, 2006), from which evaporation occurs in addition to the laser-induced plume, as seen in Fig. 5. The images in Fig. 5 suggest that the arc barely enters the keyhole, although it is also possible that the arc enters the inside of the keyhole and thus improves melting efficiency (Beyer et al. 1994). This phenomenon explains why the generation of spatter is suppressed by a laser-induced plume, which leads to the formation of a molten pool that is wide enough to accommodate keyhole expansion (Olsen, 2009).
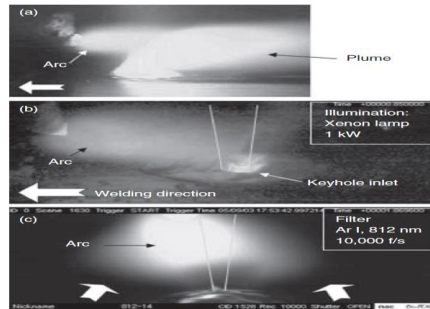

FIG.5. Observation results of CCD and high-speed video of arc and plume behavior during hybrid TIG–YAG laser welding. In a, b, and c it can be seen that the arc is concentrated in the keyhole (Petring and Poprawe, 2003)

Melt Dynamics

The melt dynamics helps to determine the keyhole stability and melt flows in the molten pool during hybrid welding. Experimental investigation of the melt dynamics of hybrid TIG–YAG laser welding of Type 304 steel used a ZrO_2 particle tracer and high speed video camera to study melt flows around the molten pool surface, as illustrated in Fig.6. At a current of 100A, the ZrO_2 particles were first seen to move towards the keyhole, like the findings presented in Fig.5; however, the arc then immediately moved away from the keyhole inlet, probably due to the stream shear stress caused by the laser-induced plume ejected from the inlet. It must be noted that at a current of 200A a concave shape was formed on the surface of the molten pool due to high arc pressure. The arc pressure caused ZrO_2 to move towards the keyhole inlet but it immediately moved away as also seen with the 100A current (Naito, 2005 and Naito, 2006).
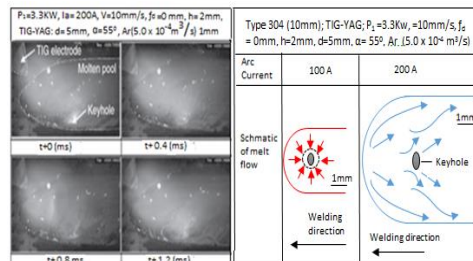

FIG.6. Observation results of molten pool surface and ZrO_2 particle tracer during hybrid TIG–YAG laser welding at 200 A in Ar gas and schematic melt flow patterns on the molten pool surface during hybrid TIG–YAG laser welding at 100 A and 200 A (Naito, 2005 and Naito, 2006).

LASER-TIG HYBRID PARAMETERS

Process variables in LTHW have a similar effect on welding performance as in autogenous laser welding. However, the increase in the number of variables as compared to the single process is a disadvantage because it adds additional complications. Despite the

increase in the number of variables, LTHW offers a lot of flexibility in parameter selection, which therefore widens the possible areas of application. The following parameters have been found to affect the quality of welds when laser welding is combined with TIG: type of secondary heat source, electrode, order of configuration – laser or secondary heat source (arc) first, distance between laser beam focal plane and workpiece (defocusing value), and arc travel speed.

Selection of secondary energy source for laser-TIG hybrid

The LTHW process is mostly used for thin gauge materials (Beyer, 1994). In selection of the secondary source, it is important that attention is paid to proper integration of the laser and secondary energy source. Graf and Staufer, 2003 has developed an integrated – head that finds usage in the automobile industry. In addition, an advanced optical system with split lenses, which helps with proper control during hybrid welding, is also available. It has been reported that other integrated heads exist; however, they require retrofitting with a CNC controller. In this regard, the TIG power supply has to be isolated and placed in such a way that it does not create disturbing electromagnetic fields for the CNC controller during arc ignition; if not, the CNC control system may break down (Bagger, 2003). Table 1 presents the main process characteristics of LTHW.

Table 1. Characteristics of Laser-TIG hybrid welding process

Process characteristics	LASER-TIG HYBRID WELDING
Ideal thickness of material	Few mm
Process stability	
	High RF ignition but process is stable
Ability to close gap	Useful
Change in ductility	Can improve

Travel Speed

Travel speed has influence on both weld width and penetration, but its effect on weld width is more significant. With an increase in the welding speed there is a decrease in both width and penetration, because the thermal input to the base metal decreases as the welding speed increases. However, it has been reported that in welding of magnesium alloys using low-power laser-TIG hybrid welding, the welding arc is stable even at high welding speeds in the range of 150-200 mm/min (Song et al. 2006). FIG. 7 shows the arc stability at various speeds. As presented in Fig. 7, instability occurred during TIG arc welding for TIG current of 40- 60A. However, the arc is more stable when combined with a laser, possibility because the laser generated plasma, having greater electron density, leads to a reduction in arc resistance, causing the arc to root to the laser action point. Information on the formation of pores and the melt pool dynamics, which are also influenced by welding speed, has been reported by Jasnau et al. (2003)
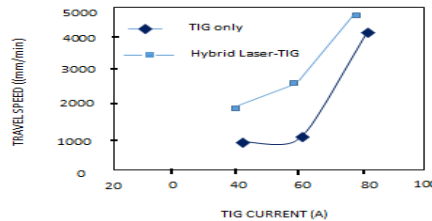

Fig.7.Stability of laser-TIG welding and TIG arc at various travel speed as a function of TIG current (Liming et al. 2004).

Distance between laser beam and arc

The distance between the laser beam and tungsten electrode (D_{LA}) can be considered one of the most important control parameters in laser-TIG hybrid welding. D_{LA} influences the weld seam and the penetration. D_{LA} depends on the energy supplied from the source as well as the secondary energy. Most researchers are of the view that a range of 1-3mm is an ideal distance between the laser and the arc. It has been reported that weld penetration increases significantly with decrease in D_{LA}. However, penetration decreases when D_{LA} is set at 0.5 mm. The effect of electrode to laser beam distance has been investigated using a 1.8 kW Nd: YAG laser coupled to a TIG torch (Kah et al. 2010) and the results are illustrated in Fig.8 For a laser-leading configuration with TIG arc (YAG/TIG) the penetration is deepest at 1 mm and is shallower at distances of 5- 9 mm. However, for leading TIG arc (TIG/YAG), the penetration is deeper and the bead width narrower at distances up to 5 mm (Petring et al. 2003).
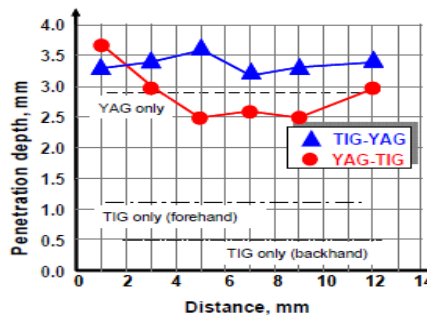

Fig.8.Effect of distance between the laser beam axis and TIG electrode on penetration depth in Nd: YAG laser-TIG hybrid welding (Kah et al. 2010)

Liu et al. 2012 carried out an experiment to investigate the effect on melting efficiency and penetration depth of the relative location of the laser beam and TIG arc (DL_A) in different hybrid modes in the welding of magnesium alloy. They reached the following conclusions; the penetration depth decreases with increase in DL_A in the laser-TIG mode; however, in the laser mode, penetration depth first increases and then decreases. In addition, they noted that the penetration depth can attain a maximum value of 4.1 mm at DL_A of 4 mm in TIG-laser mode and a penetration depth of 2.5 mm was obtained at DL_A of 1 mm. On the other hand, the penetration drops to <1 mm when DL_A reaches 5 mm, which is like that of a single TIG welding process.

Defocus value

The defocus value characterizes the position of the laser focal plane in relation to the surface of the workpiece. In hybrid welding, the weld pool surface is concave, because of arc dynamic pressure, and the optimal focal plane position is thus shifted deeper into the material. As illustrated in Fig.9, welding penetration is deepest and the formation of the weld seam is best when the defocusing value is within the range - 0.8 mm ~ 0.8 mm (Naito, 2006). Contrary to this, Investigations also show that no change in focal point position is needed for Nd:YAG/TIG hybrid welding compared to pure laser welding (Petring et al. 2007)
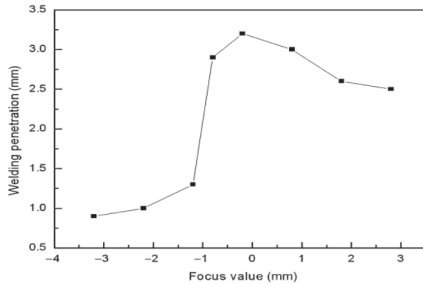

Fig 9. Influence of focus value on the welding penetration (P = 400 W, fd = −0.8 mm, I = 100 A, h = 2 mm, DLA = 2.0 mm, V = 1200 mm/ min, argon 10 L / min) (Song et al. 2006)

Shielding Gas

Shielding gas is commonly used to stabilize the welding process, to improve the welded joint characteristics and to protect the welded seam from oxidation (Ready ,2001). Plasma absorption occurs when using CO_2 lasers and consequently special measures must be adopted to mitigate this problem. Plasma reduction nozzles are used in order to obtain deep penetration welds at high power (Miyamoto, 1984), combined with low ionization gases such as helium or nitrogen. However, when solid-state lasers are used in hybrid welding, pure argon produces a stable synergistic effect between the laser and the arc, because solid-state lasers are not sensitive to the laser-induced plasma (Liming et al. 2004). Fujinaga et al. 2003 carried out experiments combining a YAG laser and TIG arc in welding of aluminum using pure argon as a shielding gas and found that the penetration depth of the hybrid weld (10 mm) was nearly twice that of the single laser weld, indicating an obvious enhanced laser–arc synergy effect. However, in pure argon shielded YAG laser–TIG hybrid welding of 304 stainless steel carried out by Natio et al. 2006 the penetration depth of the hybrid weld was only 0.5 mm deeper than that of the single laser weld, 5 mm, as noted earlier. The study also demonstrated that an increase in the gas ratio of O_2 to argon shielding gas had an influence on the weld bead shape, especially at an arc current of 100 A.

Hybrid YAG laser and double flux TIG welding with Ar+H_2 center gas and Ar environmental shielding gas has been developed in recent years, to produce deeper penetration. Consequently, an experiment carried out with YAG–TIG hybrid welding using double flux TIG arc has been applied to cover plate welding for a superconductive coil of stainless steel (Asai et al. 2005 and Shiihara et al. 2007) and the result showed improvement in weld joint.

In addition, investigation carried out on hybrid welding with a 5 kW CO_2 laser and 300 A TIG on 3 mm thick 316L stainless steel plate, proved the importance of a stable process and efficient synergistic effects. Except for some CO_2 laser–TIG hybrid welding where pure helium shielding gas has been applied, hybrid CO_2 laser– arc welding usually employs a He–Ar binary mixed shielding gas (Uchiumi et al. 2004 and Kutsuna, 2002)

Bagger et al.2005 used pure N as a shielding gas in hybrid CO_2 laser–TIG welding of 4 mm X6Cr17 steel to 2 mm 316L austenitic stainless steel and obtained good results which fulfilled product demands. Apart from this, nitrogen and hydrogen are not often used in laser-arc hybrid welding.

Workpiece parameters

Workpiece parameters also play an important role in achieving quality welds in the LTHW process. Fig.10 shows workpiece parameters in LTHW. In LTHW, the use of filler material is optional, hence during LTHW of butt-joint configurations a square groove edge and zero air gap between the joint faces is preferred (Ready, 2001 and Steen, 2003). However, if the air gap exceeds 3 % of the material thickness of the thinner joint member, there is a possibility of under fill.
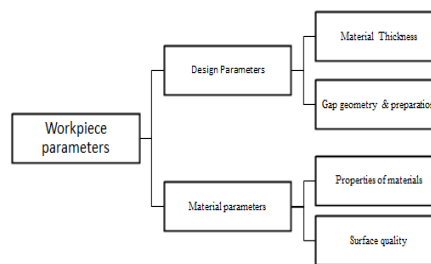

Fig.10 Workpiece parameters in laser-TIG hybrid welding

LASER TYPES USED IN LASER-TIG HYBRID WELDING

A variety of different lasers are used in materials processing. The most common laser types used in welding are Nd: YAG, solid-state and CO_2 gaseous state lasers. Recently, Yb:YAG , disc and fiber lasers, which have high output power as well as high beam quality, are increasingly being used(Boisselier et al. 1998)

WELD QUALITY IN LASER-TIG HYBRID WELDING

Several improvements in weld quality have been realized by combining laser and TIG arc welding. These improvements consist primarily of improvements in ductility, pore reduction and susceptibility to cracking.

Weld penetration

Due to the higher amount of energy delivered to the workpiece during LTHW, there is deeper penetration as well as the possibility of increasing the welding speed compared to TIG arc welding.

It has been reported that during LTHW, penetration increases and arc stability improves when welding an Al alloy, particularly using high rates of travel and low TIG current levels (Ueyama et al. 2004). Secondly, the heat efficiency of the laser is improved since the electric arc dilutes the electron density of the laser plasma, which weakens the ability of the laser plasma to absorb and reflect the laser energy (Niato et al. 2006). Coaxial gas shielding of the laser, which restrains growth of plasma, leads to increasing penetration (Ueyama et al 2005). Matsuda et al. 2006 reported on an increase in weld penetration of 1.3-2 times for LTHW of 12 mm mild steel with a 5-kW laser and TIG arc welding. However, other authors have reported no improvements

(Nielsen et al and Nilsson and Kaplan, 2002). Fig.11 shows the overall performance of the Nd: YAG/TIG hybrid welding process at different welding speeds. For welding speed in the range 6 to 12 mm/min, the penetration of hybrid welds is deeper than that of YAG welds and TIG welds. As the speed increases, the difference in penetration between hybrid and laser welds becomes smaller (Naito and Matsunawa, 2002). An increase of welding speed from 5 to 8 m/min has been reported using YAG laser and TIG arc in the welding of 2 mm AlMg3 with 1.9 k W laser power.
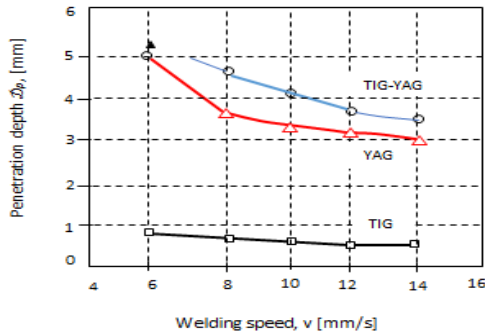

FIG.11 Overall performance of the Nd:YAG/TIG hybrid welding

process at different welding speeds (Naito et al. 2002).

Liming et al. 2004, who conducted experiments on the welding of AZ31B, reported that the penetration of LTHW is double that of TIG arc welding and four times that of laser beam welding (LBW), and that this improvement is achieved due to the synergistic effects of the laser beam and TIG arc during the welding process.

Weld stability

To determine the weld stability, analysis is usually carried out on the welded structure after welding. The welding arc has a direct influence on the weld stability. It is reported that in LTHW welding, the arc stability is greater than when using TIG arc alone, especially at high welding speed. This stability is characterized by a linear bead with uniformity throughout the entire weld length, like the welding process using laser alone. Fig. 12 shows weld surfaces welded by laser beam welding, TIG arc welding and LTHW (Liming et al. 2004)
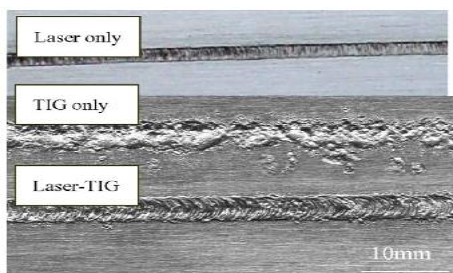

Fig.12. Comparison of weld surface for three welding methods: P_{laser}= 400 W; I_{arc} = 70 A; and v = 1100 mm/ min (Liming et al. 2004)

It is reported that in laser-TIG double side welding (LTDSW) at low current (I= 40A) and 1 m/min welding speed, the anode spot is unstable, as illustrated in Fig 13a. However, when the laser beam acts on the opposite side to the TIG arc, a hot spot is generated on the workpiece and the arc burning becomes stable due to stabilization of the anode region of the thermal action caused by the hot spot, as shown in Fig.13b.
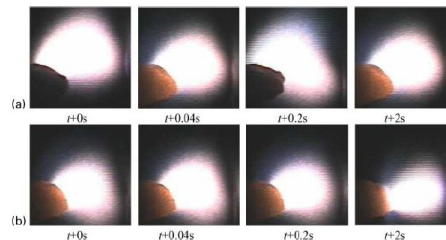

Fig.13. Arc stability of TIG welding and LTDSW process (a.

TIG welding and b. LTDSW) (Chen et al. 2008)

Cracks and reduction

During the welding of non-ferrous metals at high speed, porosity usually occurs, which results in a deterioration in mechanical properties. Two types of porosity are commonly found: pores with diameters larger than 0.2 mm, which can be observed by radiography and are known as macro pores; and pores with diameters of several micrometers, which can only be observed by optical microscopy and are known as micro pores (Liu et al. 2005). It has been reported that lack of shielding gas is the leading cause of macro porosity. Gao et al. (2009) reported on obtaining lower micro hardness, which resulted in higher toughness, in the welding of ultra-fine grained steel using laser-TIG hybrid welding. In addition, with a low laser-to-arc energy ratio, it was found out that laser-TIG hybrid welding of ultra-fine grained steel had a softening zone in the heat affected zone (HAZ). On the other hand, with a high-energy ratio, the softening zone in the HAZ disappeared, probably due to the reduced heat input and narrow HAZ.

Complete elimination of cracks has been reported in LTHW (3.5 kW YAG laser as the energy source) of an aluminum alloy (A6061) of 10 mm thickness, with an effective penetration of 6–8 mm being realized (Fujinaga et al. 2003).

On the other hand, it has been reported that when welding stainless steel AISI 304 with Nd: YAG lasers of 1.3 kW and 1.7 kW coupled to TIG arc sources, the use of an argon shield resulted in either a complete elimination or clear reduction in the number of pores (Ishide et al. 2002 and Naito and Matsunawa, 2002 and Dilthey and Wieschemann, 2002)

INDUSTRIAL APPLICATIONS

The industrial application of laser hybrid welding usually depends on the arc process used. Hence the combination of a TIG arc with lasers such as CO_2, Nd: YAG and fiber lasers usually find use in thin sheet applications. In recent years, however, research has been carried out on laser-TIG hybrid welding of thick materials. Zhang et al. 2013, investigated the use of laser-TIG hybrid welding in the welding of high strength low alloy structural steel (10CrNiMnMoV) of 16 mm thickness. This type of steel is widely used in the nuclear power, electric power equipment and shipbuilding industries. Improved mechanical properties were noted. As part of efforts to improve fuel efficiency, the automobile industry has focused on weight reduction

using lighter materials such as aluminum and magnesium alloys. LTHW has good potential to weld these lighter materials with excellent results. In current weight reduction measures, parts like the engine hood, trunk cover, body panels and suspension components are often manufactured with aluminum (Funatani, 2000). In summary, it is evident that laser-TIG hybrid can find usage in manufacturing for road transport, shipbuilding, rail transport, oil and gas.

SUGGESTIONS FOR FUTURE STUDIES

Presently, the most proven laser systems for LTHW technology are CO_2 and Nd: YAG lasers. Resent developments and improved commercial availability of fiber and disc laser systems mean that such systems should be considered as an attractive alternative to conventional laser beam source. It is an anticipated that the improved properties of these new laser beam source will lead to further development and improvement of LTHW. Another interesting area is investigation of LTHW with different shielding gas mixtures i.e. mixtures with active gas content.

CONCLUSIONS

This paper presented an overview of LTHW welding of ferrous and non-ferrous metals by examining the benefits, limitations, industrial applications and optimization possibilities, and suggested possible future areas of improvement.

The combination of a laser and TIG arc creates a complex process with a high number of variables. It is not possible to give a general rule on how various parameters in laser-TIG hybrid can be optimized due to the complexity of the phenomena involved. The findings presented in the literature should be considered as evidence for specific applications only.

Most researchers are of the view that LTHW welding is mainly applicable to thin gauge materials (< 5mm). However, investigations have also been carried out using LTHW on thick plate (16mm) of high strength lower alloy structural steel 10CrNiMnMoV with quality results. In addition, it has been reported that LTHW makes use of the laser energy more efficiently and improves energy coupling between the plasma and molten pool in welding of thick materials. To complement its capability of welding thick plates which has been a major drawback of LTHW, the Welding Institute (TWI) carried out and experiment on 304L austenitic stainless steel (10mm, butt welds) and (16mm, melt runs) using CO2 and Yb fiber lasers and found that it was possible to use LTHW on thick materials.

The flexibility in either welding with filler wire or without filler wire gives an advantage in terms of cost reduction, especially when the metal to be welded does not need the addition of filler wire. The Institute of Welding and Joining Technology (ISF), Rheinisch-Westfälische Technische Hochschule (RWTH), Aachen, reported a price reduction of up to 50 %, higher efficiency and a reduction in necessary joint edge preparation with the use of 2 kW Nd: YAG laser combined with 2 kW TIG.

Undercut is the most common weld defect identified during welding with LTHW. Undercut occurs due to the direction of the arc, which is usually deflected aside. However, it can be eliminated by choosing suitable welding parameters. Various experiments have showed that smaller process separation would make it possible to increase the penetration. Based on various results obtained using LTHW it can be ascertained that LTHW improves weld quality and gives fewer pore and crack defects compared to using TIG arc welding alone.

In conclusion, while LTHW finds usage mainly in the welding of thin gauge materials (<5mm), the excellent quality welds obtained in welding of thick plates (> 10mm) prove that LTHW has the capability of welding thicker materials. Although less experiments have been carried out to that effect it can be said that various synergies indicate that LTHW has good prospects for quality welding of thick materials.

REFERENCES

Abe, N, Hayashi, M (2002). "Trends in laser arc combination welding methods," *Welding International*, 16(2), pp.94-98.

Arias, JL, Romero, P, Bandewynckele, A, Vazquez J (2005). "Laser-TIG hybrid welding of very thin austenitic stainless steel sheets." *In Proceedings of the 24th Int. Conf. on Applications of Lasers and Electro- Optics, Miami, USA*, pp.10-107.

Asai, SMK, Shiihara, K, Makino, Y, Kanehara, T and Shibui, M (2005). "YAG–TIG hybrid welding process for coil cover plate of stainless steel," *58th Annual Assembly of IIW, Prague, IIW Doc. No. XII-1855-05,* pp. 376–382.

Bagger, C and Olsen, FO (2005). "Review of laser hybrid welding. *Journal of Laser Applications* ", pp. 17(11): 12–14.

Bagger, C (2003)."Comparison of plasma, metal inactive gas (MIG) and tungsten inactive gas (TIG) processes for laser hybrid welding," *Proceedings of ICALEO 2003, LMP*, paper 302.

Baito, YM, Katayama, S and Bang, HS (2004). "Hybrid laser welding (CD: 207)," *Proc. of the 23rd ICALEO '04, San Francisco, LIA*

Beyer, EDU, Imhoff, R, Majer, C, Neuenhahn, J and Behler, K (1994). "New aspects in laser welding with an increased efficiency," *Proc. of Int. Congress on Applications of Lasers & Electro-Optics (ICALEO) '94 Orlando, LIA*, pp. 183–192.

Biffin, JRR, Walduck, P (1994). "Plasma arc augmented laser welding (PALW)," *Proceedings EUROJOIN, 2nd European Conference on Joining Technology, Firenze, Italy,* pp. 295-304.

Boisselier, D, Gaufillet, J, Hamy, D and Marchand (1998). "Le soudage Laser," p. 88.

Chen, B, Miao Y, Li L and Wu, L (2008). "Arc characteristics of laser-TIG double-side welding," *Science and Technology of Welding and Joining,* 13(5), pp. 438-444.

Diebold, TP, Albright, CE (1998). *Weld., Join,* 6(5), pp. 18-24.

Dilthey, U, Lueder, F, Wieschemann, A. Expanded capabilities in welding of aluminum alloys with laser-MIG hybrid process. - Aluminum 75, 1999, 1(2), p.64-75.

Dilthey, U and Wieschemann, A (2002). "Prospective offered by combining a laser Beam with arc welding procedures," *Welding International, 16(9), pp. 711-719.*

Fujinaga, S, Katayam, S and Matsunawa, A (2003)."Improvements of welding characteristics of aluminum alloys with YAG laser and TIG arc hybrid system," *Proceedings of SPIE, 4831*, pp. 301–306.

Funatani, K (2000). "ICMCTF 2000 B4-7, and Surface and Coatings Technology," 133, 134, p. 264.

Gao, M, Zeng, X, Hu, Q and Yan J (2009). "Laser-TIG hybrid welding of ultra-fine grained steel." *Materials Processing Technology*, 209, pp. 785-791

Gornyi, L and Redozobov (1990). "Examination of the electrical characteristics of the arc in laser-arc welding," *Welding Int*.

Graf, T, Staufer, H (2003). "Laser-hybrid welding drivers VW improvements," *Welding Journal*, 17(1), pp. 42-48.

Hu, SS, Zhao JR and Chin, Trans (1993). *Weld., Inst.*, 3(159).

Ireland, CLM (1997). "Dual-technology Welding-will it come of age," *Industrial Laser Review* 12, pp. 11-15.

Ishide, T, Nayama, M, Watanabe, M and Nagashima, T (2001). "Coaxial

TIG-YAG & MIG-YAG welding methods." *Welding International*, 15(12), pp. 940-94

Ishide, T, Tsubota, S and Watanabe, M (2002). "Latest MIG, TIG arc-YAG laser hybrid welding systems for various welding products," *First International Symposium on High-Power Laser Macroprocessing, edited by I. Miyamoto (Proc. SPIE 4831)*, pp. 347–352.

Jasnau UH and Seyffarth (2003)."Nd:YAG-Laser MSGHybridschweißen von Aluminiumlegierungen im Schiffbau', in Schweißen und Schneiden " *DVS– Berichte 225, Düsseldorf, DVS Verlag*, pp. 181-186.

Kah, P (2011)."Current trends in welding processes and materials: Improve in effectiveness," *Lappeenranta University of Technology*

Kah, P, Salminen, A, Martikainen, J (2010). "The effect of the relative location of laser beam with arc in different hybrid welding processes," *MECHANIKA,* 3(83).

Katayama, S (2007). "Plume behavior and melt flows during laser and hybrid welding," *Proc. of 4th Int. WLT-Conf. on Lasers in Manufacturing*, pp. 265–271

Katayama, S (2009). "Fundamentals of hybrid laser-arc welding. *In Hybrid Laser-Arc Welding. Edited by Flemming Olsen*," pp. 28-43.

Kutsuna, MAC (2002). "Interaction of both plasma in CO2 laser-MAG hybrid welding of carbon steel," *International Institute of Welding, IIW document*, XII 1708-02.

Liming, L, Jifeng, W and Gang, S (2004). "Hybrid laser–TIG welding, laser beam welding and gas tungsten arc welding of AZ31B magnesium alloy," *Materials Science and Engineering: A,* 381(1–2), pp. 129-133.

Liu, LM, Yuan, ST and Li, CB (2012). "Effect of relative location of laser beam and TIG arc in different hybrid welding modes," *Science and Technology of Welding & Joining,* 17(6), pp. 441-446.

Liu, L., Song, G., Liang, G., and Wang, J (2005). "Pore formation during hybrid laser-tungsten inert gas arc welding of magnesium alloy AZ31B—mechanism and remedy," *Materials Science and Engineering: A,* 390(1-2), pp. 76-80.

Mahrle, A and Beyer, E (2006). "Hybrid laser beam welding - Classification, characteristics, and applications. *Journal of Laser Applications*," pp. 18(13): 169–180.

Miyamoto, I (1984). "The role of assist gas in CO2 laser welding," *Proceedings of ICALEO, Department of Welding Engineering and Welding Research Institute, Osaka, japan,* Vol. 44, pp. 68-75.

Naito, Y (2005). "Fundamental study of hybrid welding phenomena with YAG laser and TIG arc," *Doctor Thesis, Osaka University, Japan, (in Japanese).*

Naito, Y (2006). "Electrical measurement of arc during hybrid welding – welding phenomena in hybrid welding using YAG laser and TIG arc (Third report)," *Quarterly Journal of the Japan Welding Society (JWS), (24(1)), pp. 45–51(in Japanese).*

Naito, Y (2006). "Elucidation of penetration characteristics, porosity prevention mechanisms and flows in molten pool during laser–arc hybrid welding – welding phenomena in hybrid welding using YAG laser and TIG arc (Fourth report)," *Quarterly Journal of the Japan Welding Society* (24(2)), pp. 149–161 (in Japanese).

Naito, Y, Mizutani, M, Katayama, S (2006). "Penetration characteristics in YAG laser and TIG arc hybrid welding, and arc and plasma /plume behavior during welding. Welding phenomena in hybrid welding using YAG laser and TIG arc (First Report)," *Welding International*, 20(10), pp.777-784.

Naito, YKS and Matsunawa, A (2002). "Keyhole behavior and liquid flow in molten pool during laser-arc hybrid welding," LAMP 2002 Proceedings, Volume 4831, p.357.

Natio, Y, Mizutani, M and Katayama, S (2006). "Effect of oxygen in ambient atmosphere on penetration characteristics in single yttrium–aluminum–garnet laser and hybrid welding," *Journal of Laser Applications,* 18, pp. 21–27.

Nielsen, SE, Andersen, MM, Kristensen, JK, Jensen, TA (2002). "Hybrid welding of thick section C/Mn steel and aluminum." p.15.

Nilsson, HE and Kaplan, A (2002). "Influence of butt- and T-joint preparation in laser arc hybrid welding."

Olsen, FO, 2009. "Hybrid Laser-arc welding". *Woodhead Publishing Limited Oxford, Cambridge, New Delhi.*

Petring, D, Wolf, N, Poprawe, R (2003). "Investigation and applications of laser–arc hybrid welding from thin sheets up to heavy section components," *Proc. of the 22nd ICALEO '03, Jacksonville, LIA*, Section a, 1–10 (CD: 301)

Rayes, ME, Walz, C and Sepold, G (2004). "The influence of various hybrid welding parameters on bead geometry," *Welding Journal,* 83(5), pp. 147-153.

Ready, JF (2001). "LIA Handbook of Laser Materials Processing," *1st edition. Orlando: Laser Institute of America/Magnolia Publishing*, p. 715.

Shiihara, KMY, Ogawa, T, Asai, S, Kanahara, T, Senda, I, Okuno, K and Koizumi, K (2007). "Laser–arc hybrid welding for the cover plate of ITER TF coil ICALEO 2007 "*Congress Proc., Laser Materials Processing Conf., LIA, Florida*, pp. 316–324.

Song, G, Liu, L and Wang, M (2006). "Overlap welding of magnesium AZ31B sheets using laser–arc hybrid welding process," *Mater. Sci. Eng. A*, 429 pp. 312– 319.

Steen, EM (1979). "Metal Construction," 11(7), pp. 332-335.

Steen, WM, Eboo, M, 1979, "Arc augmented laser welding," *Metal Construction,* 2(17), pp. 332-335

Steen, WM (2003). "Laser Material Processing. 3rd ed," *London: Springer-Verlag London Limited.*

Steen, WJ (1981). "Arc augmented laser welding," *Joining of Metals, Proceedings Spring Residential Conference, Coventry, England.*

Uchiumi, S, Wang, J, Katayama, S, Mizutani, M, Hongu, T and Fuji, K (2004). "Penetration and welding laser MIG hybrid welding of aluminum alloy," *In Proceedings of the 23rd International Congress on Applications of Lasers and Electro-Optics, San Francisco, USA*, pp. 76-85.

Ueyama, T, Tong H, Yazawa I, Hirami M, Kihara, T, Nakata K and Ushio, M (2004). "Aluminum alloy sheet welding by the laser AC pulsed MIG hybrid process," *Welding International,* 18(5), pp. 345-350.

Vitek, JM, David, SA et al. (1998). *Science and Technology of Welding & Joining, 6(5),* pp. 305-314.

Wang, J, Takenaka, Y, Hongu, T, Fujii, K and Katayama, S (2007). "Laser-MIG arc hybrid welding of aluminum alloy - Comparison of melting characteristics between YAG laser and diode laser," *Welding International, 21(1),* pp. 32-38.

Zhang, S, Qiu, H (2013)."The technology and welding joint properties of hybrid laser-TIG welding on thick plate," *Optics & Laser Technology* (48), pp. 381–388.

Publication III

Gyasi, A. E., Kah, P., Wu, H., and Kesse, A. M.
Modeling of an artificial intelligence system to predict structural integrity in robotic GMAW of UHSS fillet welded joints

CrossMark

ORIGINAL ARTICLE

Modeling of an artificial intelligence system to predict structural integrity in robotic GMAW of UHSS fillet welded joints

Emmanuel Afrane Gyasi[1] · Paul Kah[1] · Huapeng Wu[1] · Martin Appiah Kesse[1]

Abstract The use of welded lightweight steels in structural applications is increasing due to the greater design possibilities offered by such materials and the lower costs compared to conventional steels. Ultra-high-strength steels (UHSS) having tensile strength of up to 1700 MPa with a high strength-to-weight ratio offer a unique combination of qualities for diverse industrial applications. For productivity and quality reasons, gas metal arc welding (GMAW) is usually utilized for welding of UHSS. However, for full penetration fillet welded joints, the need for high heat input to gain acceptable weld penetration is problematic when welding UHSS. This is due to UHSS sensitivity to heat input and possible heat-affected zone (HAZ) softening. In this paper, an attempt is made, on the basis of analysis of experimental reviews, to identify and define relationships between nonlinear weldability factors to enable creation of an artificial intelligence model to predict full penetration in robotic GMAW fillet welded joints of UHSS S960QC. Welding variables and parameters associated with GMAW are first evaluated by reviewing scientific literature. The possibility of employing an artificial neural network (ANN) to predict full penetration fillet weld characteristics is then examined. It is noted that nonlinear variables associated with the GMAW process, such as heat input, contact tip to work distance (CTWD), and torch angle, and their related parameters, which pose weldability challenges, can be modeled by applying artificial intelligence systems. Ensuring full penetration in fillet welded joints of UHSS using artificial intelligence is thus feasible. Further, an optimized control system could potentially be developed by incorporating adaptive robotic GMAW with an artificial intelligence-based system to guarantee sound structural integrity that conforms to EN ISO 5817. The paper increases awareness of welding aspects of UHSS S960QC and presents an approach for overcoming existing limits to GMAW via adaptive robotic welding and artificial intelligence systems.

Keywords Ultra-high-strength steel (UHSS) · Robotic GMAW · Artificial intelligence · Structural integrity · Artificial neural network · Full penetration · Weld quality

1 Introduction

Nowadays, manufacturing industries are increasingly employing lightweight steels of high tensile strength in welded structural applications as a response to the need to reduce structural weight and attain cost reductions in welding manufacturing and production. These needs stem from demands for increased energy efficiency, which has become critical from the environmental point of view. Ultra-high-strength steel (UHSS) is one material choice for lightweight manufacturing. UHSS has superior strength-to-weight ratio and excellent physical, mechanical, and low-temperature properties, which enable lower fuel consumption and lower carbon emissions [1–4] than when using conventional steels. Industries that produce and operate mobile structures such as offshore platforms, floating production, storage, and offloading (FPSO) units, heavy-duty vehicles for mining or lifting purposes, and alternative energy industries operating in the fields of solar power, wind power, and liquefied natural gas (LNG) production stand to benefit from increased use of UHSS.

✉ Emmanuel Afrane Gyasi
  emmanuelgyasi.giw@gmail.com; emmanuel.gyasi@student.lut.fi

[1] School of Energy Systems, Mechanical Engineering Department, Laboratory of Welding Technology, Lappeenranta University of Technology, P.O. Box 20, 53851 Lappeenranta, Finland

✎ Springer

A major challenge facing manufacturing industries is to guarantee that full penetration is achieved in fillet welded joints of structural applications. Increased heat input is generally utilized to ensure acceptable full weld penetration in fillet joints.

As a result of the alloying elements and production process used in its manufacture, UHSS possesses a dual-phase microstructure consisting of bainite and martensite [1]. Its microstructure, similar to advanced high-strength steels (AHSS), is sensitive to high heat input, and exposure to elevated temperature can change its mechanical properties. More critical effects of heat input are heat-affected zone (HAZ) softening and an increased propensity to fatigue failure, which affect the toughness and strength of welded joints of UHSS [2, 3].

For productivity and quality reasons, fusion welding processes, especially gas metal arc welding (GMAW), have been favored for joining lightweight high tensile strength steels. A number of studies have been presented where GMAW has been employed for welding of UHSS S960QC [1–3]. Successful implementation of robotic GMAW in UHSS welding would have a significant effect on the profitability of manufacturing industry, where repeatability, precision, cost, time, and quality are key drivers in manufacturing and production. However, utilizing robotic GMAW in an uncontrolled manner poses weldability challenges for the structural integrity of UHSS fillet welded joints. The outcome of the GMAW process is dependent on a number of nonlinear variables, such as heat input, contact tip to work distance (CTWD), and torch angle, and their related parameters, e.g., arc current, arc voltage, welding speed, gas flow rate, arc efficiency, electrode stick out, wire feed speed, electrode diameter, torch position, and torch travel angle.

Development in artificial intelligent system for robotic welding shows that adaptive features such as sophisticly sensory, monitoring, and control systems could be incorporated in the entire robotic artificial intelligent welding system to help the robot to adjust to its operating environment to enable monitoring, detection, measurement, inspection, and recording welding process parameters, and other features such as joint geometry and weld pool geometry. A typical example like infrared thermography-based sensors could be used in adaptive robotic artificial intelligent system to measure thermal profiles during welding to check susceptibility to heat inputs and temperature variations to assure weld integrity. However, for the robot to be capable to self-adjust to its functions and operations, artificial intelligent systems such as artificial neural network (ANN), fuzzy logic system, neural-fuzzy network (NFN), adaptive neuro-fuzzy inference system (ANFIS), genetic algorithm (GA), or swam particle optimization (SPO) need to be used as a data modeling tool. These artificial intelligent systems not only adapt, aid prediction of desired outcomes, and operate real time but are also capable to learn new input and output relationships and previously unknown situations and environments.

Therefore, development of a system able to account for and control the nonlinear factors associated with GMAW would alleviate weldability problems and guarantee sound structural integrity and full penetration in fillet welded joints of UHSS, enabling the joints to conform to the EN ISO 5817 standard, and would be a valuable scientific contribution to welding science, and manufacturing and production industries.

In this paper, an attempt is made, on the basis of analysis of experimental reviews, to identify and define relationships between nonlinear weldability factors to enable creation of an artificial intelligence (AI) model to predict full penetration in robotic GMAW fillet welded joints of UHSS S960QC. Figure 1 illustrates the concept of modeling an AI system for robotic welding of UHSS. It is assumed that all required inputs and the relationship between the inputs and the corresponding output requirements must be identified and considered. In addition, it is anticipated that the AI system should be able to predict desirable weld characteristics, such as weld bead penetration depth and weld geometry, based on the input data and expected outcomes.

A further requirement for the system is the ability to predict, during the welding process, possible weld flaws or errors in data modeling, as outputs, on receiving input requirements like welding parameters. In situations where undesirable outcomes and defects are likely to occur, the intelligent system should be able to capture, control, and correct the errors. This important adaptive function requires an optimized control system, whose discussion is beyond the scope of this work.

2 Material and welding considerations for welding of UHSS S960QC

Experimental studies have shown that welding of UHSS is challenging due to several nonlinear factors that affect weldability [1]. For example, weldability problems can occur as a result of inappropriate heat input and choice of filler materials [2], and problems can arise from fatigue effects related to weld geometry/profiles [3]. Figure 2 presents and
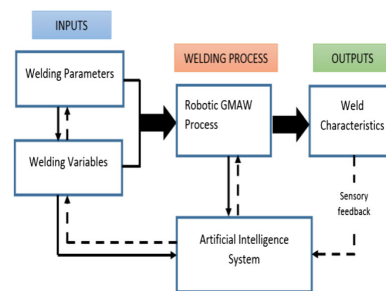

Fig. 1 Schematic diagram of modeling of an artificial intelligence system for a robotic GMAW process
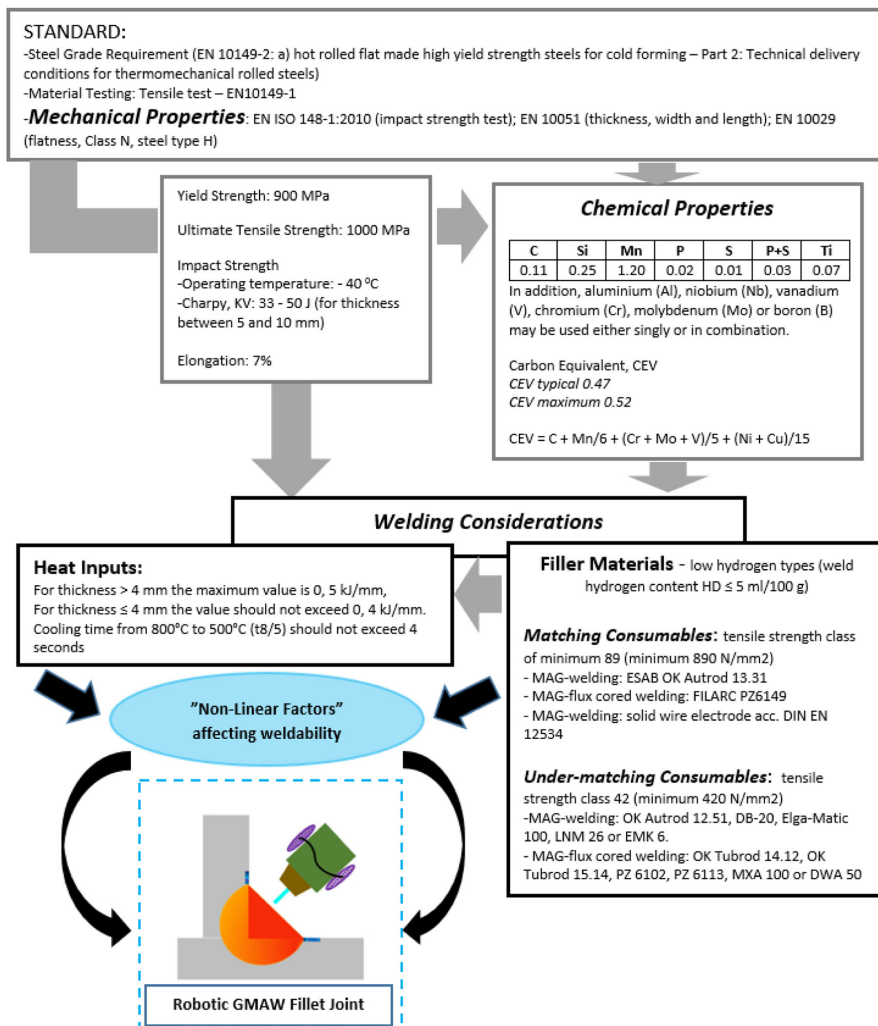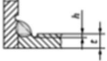
STANDARD:
-Steel Grade Requirement (EN 10149-2: a) hot rolled flat made high yield strength steels for cold forming – Part 2: Technical delivery conditions for thermomechanical rolled steels)
-Material Testing: Tensile test – EN10149-1
-*Mechanical Properties*: EN ISO 148-1:2010 (impact strength test); EN 10051 (thickness, width and length); EN 10029 (flatness, Class N, steel type H)

Yield Strength: 900 MPa

Ultimate Tensile Strength: 1000 MPa

Impact Strength
-Operating temperature: - 40 ºC
-Charpy, KV: 33 - 50 J (for thickness between 5 and 10 mm)

Elongation: 7%

Chemical Properties

C	Si	Mn	P	S	P+S	Ti
0.11	0.25	1.20	0.02	0.01	0.03	0.07

In addition, aluminium (Al), niobium (Nb), vanadium (V), chromium (Cr), molybdenum (Mo) or boron (B) may be used either singly or in combination.

Carbon Equivalent, CEV
CEV typical 0.47
CEV maximum 0.52

CEV = C + Mn/6 + (Cr + Mo + V)/5 + (Ni + Cu)/15

Welding Considerations

Heat Inputs:
For thickness > 4 mm the maximum value is 0, 5 kJ/mm,
For thickness ≤ 4 mm the value should not exceed 0, 4 kJ/mm.
Cooling time from 800°C to 500°C (t8/5) should not exceed 4 seconds

"Non-Linear Factors" affecting weldability

Filler Materials - low hydrogen types (weld hydrogen content HD ≤ 5 ml/100 g)

Matching Consumables: tensile strength class of minimum 89 (minimum 890 N/mm2)
- MAG-welding: ESAB OK Autrod 13.31
- MAG-flux cored welding: FILARC PZ6149
- MAG-welding: solid wire electrode acc. DIN EN 12534

Under-matching Consumables: tensile strength class 42 (minimum 420 N/mm2)
-MAG-welding: OK Autrod 12.51, DB-20, Elga-Matic 100, LNM 26 or EMK 6.
- MAG-flux cored welding: OK Tubrod 14.12, OK Tubrod 15.14, PZ 6102, PZ 6113, MXA 100 or DWA 50
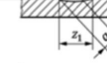
Robotic GMAW Fillet Joint

Fig. 2 Schematic representation of UHSS S960QC material data and robotic GMAW process fillet joint

summarizes information regarding standard requirements, material properties, and welding of UHSS S960QC. The schematic data representation does not provide a complete welding procedure specification (WPS) since items such as welding position, type of polarity, size of filler material, need for pre-heating or post-heating, and procedure sequence are missing. Such information is case-specific to the particular structure being welded, and it thus cannot be generalized but must be validated for the specific welding procedure. Nevertheless, the schematic data serves as relevant technical information when considering UHSS S960QC for experimental study.

For fillet welded joints, higher levels of structural integrity cannot be guaranteed due to susceptibility to a lack of full penetration [5]. In most cases, extra material preparations such as beveling have to be done, especially on the upright member of the fillet joint profile. This requirement increases material preparation costs and such pre-welding preparation cannot be utilized in many applications. Tables 1 and 2 show quality levels and critical imperfections in fillet welded joints according to EN ISO 5817. The quality levels are designated by symbols B, C, and D, where B corresponds to the highest requirement on the finished weld. The load types evaluated

Table 1 Surface imperfections in fillet welded joints [6]

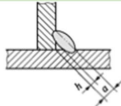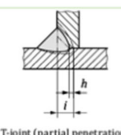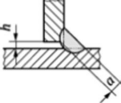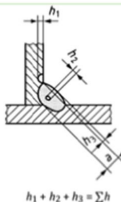| No.	Reference to ISO 6520-1	Imperfection designation	Drawings and Remarks	t, mm	Limits of imperfections for quality levels		
					D	**C**	**B**
1.	**Surface imperfections**						
1.7	5011	Continuous undercut		0,5 to 3	Short imperfections: $h \leq 0,2$ t	Short imperfections: $h \leq 0,1$ t	Not permitted
	5012	Intermittent undercut	Smooth transition is required. This is not regarded as a systematic imperfection	> 3	$h \leq 0,2$ t, but max. 1 mm	$h \leq 0,1$t, but max. 0,5 mm	$h \leq 0,05$ t, but max. 0,5 mm
1.10	503	Excessive convexity		$\geq 0,5$	$h \leq 1$ mm + 0,25 b, but max. 5 mm	$h \leq 1$ mm + 0,15 b, but max. 4 mm	$h \leq 1$ mm + 0,1b, but max. 3 mm
1.12	505	Incorrect weld toe	$\alpha_1 \geq \alpha$ and $\alpha_2 \geq \alpha$	$\geq 0,5$	$\alpha \geq 90°$	$\alpha \geq 100°$	$\alpha \geq 110°$
1.16	512	Excessive asymmetry of fillet weld (excessive unequal leg length)	In cases where an asymmetric fillet weld has not been prescribed	$\geq 0,5$	$h \leq 2$ mm + 0,2 a	$h \leq 2$ mm + 0,15 a	$h \leq 1,5$ mm + 0,15 a
1.20	5213	Insufficient throat thickness		0,5 to 3	Short imperfections: $h \leq 0,2$ mm + 0,1 a	Short imperfections: $h \leq 0,2$ mm	Not permitted
			Not applicable to processes with proof of greater depth of penetration	> 3	Short imperfections: $h \leq 0,3$ mm + 0,1 a, but max. 2 mm	Short imperfections: $h \leq 0,3$ mm + 0,1 a, but max. 1 mm	Not permitted
1.21	5214	Excessive throat thickness	The actual throat thickness of the fillet weld is too large	$\geq 0,5$	Permitted	$h \leq 1$ mm + 0,2 a, but max. 4 mm	$h \leq 1$ mm + 0,15 a, but max. 3 mm

in definition of these quality levels include static load, thermal load, corrosion load, and pressure load [6].

Tables 1 and 2 serve as a guide for the objective of creating an AI model to predict full penetration in robotic GMAW fillet welded joints of UHSS S960QC. Surface imperfections such as excessive convexity, incorrect weld toe, excessive asymmetry of the fillet weld, insufficient throat thickness, and excessive throat thickness must fall within the acceptable quality level range in accordance with the EN ISO 5817 standard for material thickness greater than or equal to 0, 5, to 3 mm. Similarly, in Table 2, the quality level range in accordance with EN ISO 5817 standard for material thickness greater than or equal to 0, 5, to 3 mm must be observed for internal, joint geometry, and multi-imperfections.

2.1 Case study 1

Hemmilä et al. [1] investigated the weldability of Optim 960QC, which is the same as UHSS S960QC, for 3- and 6-mm-thick plates. In order to establish a basis for comparison of the effects of heat input, 3-mm-thick plates were prepared for laser welding and MAG welding, and 6-mm-thick plates were prepared for hybrid laser welding (CO_2 laser and MAG welding using shielding gas: 50% He + 45% Ar + 5% CO_2) and MAG welding using shielding gas: 80% Ar + 20% CO_2. Experimental data from the study is shown in Table 3. The MAG welding equipment employed was ESAB LAH 630 from Ruukki Productions, nowaday a division of SSAB. The laser and laser-hybrid welding equipment used were,

Table 2 Surface imperfections in fillet welded joints [6]

No.	Reference to ISO 6520-1	Imperfection designation	Drawings and Remarks	t, mm	Limits of imperfections for quality levels		
					D	C	B
2.	**Internal imperfections**						
2.13	402	Lack of penetration		> 0,5	Short imperfection: $h \leq 0, 2a$, but max. 2 mm	Not permitted	Not permitted
			T-joint (partial penetration)	≥ 0,5	Short imperfections: butt joint: $h \leq 0,2\ s$ or i, but max. 2 mm T-joint: $h \leq 0,2\ a$, but max. 2 mm	Short imperfections: butt joint: $h \leq 0,1\ s$ or i, but max. 1,5 mm fillet joint: $h \leq 0,1\ a$, but max. 1,5 mm	Not permitted
3.	**Imperfections in joint geometry**						
3.2	617	Incorrect root gap for fillet welds	Gap between the parts to be joined. Gaps exceeding the appropriate limit may, in certain cases, be compensated for, by a corresponding increase in the throat thickness.	0,5 to 3	$h \leq 0,5$ mm + 0,1 a	$h \leq 0,3$ mm + 0,1 a	$h \leq 0,2$ mm + 0,1 a
				> 3	$h \leq 1$ mm + 0,3 a, but max. 4 mm	$h \leq 0,5$ mm + 0,2 a, but max. 3 mm	$h \leq 0,5$ mm + 0,1 a, but max. 2 mm
4.	**Multiple imperfections**						
4.1	None	Multiple imperfections in any cross section	$h_1 + h_2 + h_3 = \sum h$	0,5 to 3	Not permitted	Not permitted	Not permitted
				> 3	Maximum total height of imperfections: $\sum h \leq 0,4\ t$ or $\leq 0,25\ a$	Maximum total height of imperfections: $\sum h \leq 0,3\ t$ or $\leq 0,2\ a$	Maximum total height of imperfections: $\sum h \leq 0,2\ t$ or $\leq 0,15\ a$

respectively, a Rofin-Sinar 6000 and ESAB ARISTO 2000 welding system.

In the laser-hybrid welding, the joints were tack welded using the MAG process and the distance between tacks was approximately 100 mm. In the other MAG welding, the 6 mm plate was milled and a V-groove cut. The welding was carried out without preheating using interpass temperatures of 25 °C and arc energies of 0.5 and 0.8 kJ/mm.

Non-destructive visual and X-ray examination conforming to EN ISO 15614-1 showed that class B (stringent) was generally achieved in the MAG-welded joints, but class C dominated in the laser and laser-hybrid welded joints. The lower quality class of the laser and laser-based methods was due to higher porosity, incomplete filling of grooves and roots, and local lack of fusion. Figures 3 and 4 show Vickers hardness profiles across the welds.

It was concluded that the HAZ showed a significant drop in hardness below that of the base plate in the MAG welding of the 3-mm plate, as can be seen in Fig. 3. The narrow, shallow soft HAZ in the autogenous laser weld of the 3-mm plate did not lower the tensile strength of the joint compared to that of the base plate. The use of laser or laser-hybrid welding could therefore help to reduce the width and depth of the HAZ softened zone.

Weld metal was even-matching in the case of the laser-based methods, but slightly under-matching in the MAG weld of the 3-mm plate. However, in both the 3- and 6-mm plates, the MAG welds demonstrated cross-weld tensile strength that was lower than that of the base plate. For a constant heat input (0.5 kJ/mm), the reduction in tensile strength increased as the plate thickness decreased from 6 to 3 mm, as can be seen by comparison of Figs. 3 and 4.

A similar effect was obtained when increasing the arc energy in the case of the 6-mm-thick MAG-welded butt joints: higher arc energy (0.8 kJ/mm) produced greater under-matching. Cross-weld tensile strength decreased as arc energy and cooling time increased.

Table 3 Experimental data for different plate thicknesses and welding processes

Plate thickness	Dimension	Laser welding	Hybrid laser welding	MAG welding
3 mm	500 × 150 mm	Laser type: CO_2 laser		Heat input—0.5 kJ/mm
		Laser power—6 kW		Wire type: matching
		Shielding gas: helium		Wire grade: PZ6149
		Gas flow rate—25 l/min		Shielding gas: 80% Ar + 20% CO_2
		Air gap—0 mm		Root gap—1.5–2 mm
6 mm	500 × 150 mm		Laser type: CO_2 laser	Heat input—0.5 kJ/mm
			Laser power—6 kW	Electrode type: matching
			Shielding gas: 50% He + 45% Ar + 5% CO_2	Electrode grade: OK Autod 13.31
			Gas flow rate—30 l/min	Shielding gas: 80% Ar + 20% CO_2
			Electrode grade: OK Autrod 13.31	Root gap—1.5–2 mm
			Electrode stick out—15 mm	Electrode stick out—15 mm
			Electrode diameter—1.0 mm	Electrode diameter—1.0 mm
			Air gap—0.25 mm	

Laser-based welding processes gave the best combinations of strength and toughness. The impact toughness of the HAZ was better in the laser-hybrid welded joint than in the MAG-welded joint. This improved impact toughness is a result of the finer lath martensitic-bainitic microstructure found in the HAZ of the laser-hybrid joint as a resultant effect of the higher cooling rate. With the MAG weld, the toughness of the fusion line (FL/HAZ) is the limiting factor, whereas in the laser-hybrid weld, the weld metal toughness is the limiting factor.

The susceptibility to HAZ softening of S960QC when MAG welded is a challenge. Although it has been stated that welding of S960QC should be done with as low an arc energy as possible, and that high hydrogen content filler materials should be avoided to prevent hydrogen-induced cracking in the weld metal [2], the precise factors involved and the relationships between the welding variables and parameters have not been clearly established. Therefore, predicting and ensuring toughness and hardness properties in the HAZ similar to those of the base material and achieving even-matching properties of the weld metal to the base material when using GMAW need further research. Welding variables and parameters pertaining to GMAW are discussed more thoroughly in Section 3.

2.2 Case study 2

In another study, Björk, Toivonen, and Nykänen [3] investigated the ultimate load-bearing capacity of typical fillet welded joints made of UHSS S960. Validations of current design rules (Eurocode 3 Parts 1–12) covering steel grades up to S700 were done for fillet welded joints fabricated from direct quenched (un-tempered) UHSS S960. Throat thickness and other dimensions for the fillet welds were validated through experimental testing and nonlinear finite element analysis (FEA). The studied joints were load-carrying (denoted by L-, T-, LT, and X-series) and non-load-carrying (X0 series) joints. Several parameters were considered for each joint type, such as filler metal, and
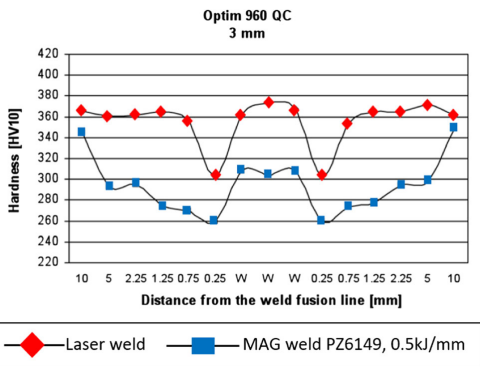

Fig. 3 Hardness profiles across 3-mm-thick laser and MAG-welded butt joints in Optim 960 QC (note that the distance scale is nonlinear) [1]
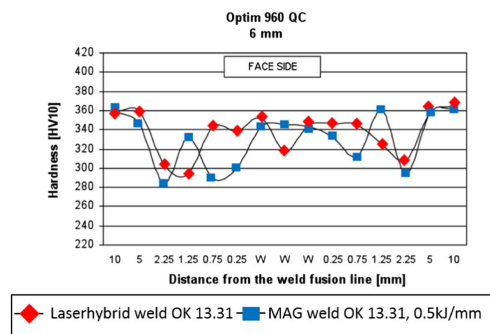

Fig. 4 Hardness profiles across 6-mm-thick laser and MAG-welded butt joints in Optim 960 QC (note that the distance scale is nonlinear) [1]

length and throat thickness of the welds. A fully mechanized GMAW process (MAG) was used for joining the plates of 8 mm thicknesses. The test results showed that ductile rupture occurred in all the joints when tested at room temperature. Additionally, the optimal cooling rate was difficult to reach; low heat input increased the risk of incomplete fusion. In the X0 series, however, the failure and capacity of the non-load-carrying joints seemed to depend on the heat input due to welding. When heat input was low, the softening was local, and it had no effect on the load-bearing capacity of the joint, and the failure occurred outside the joint (typically at an angle of 30°) as shown in Fig. 5. When heat input was increased, the softened width/plate thickness ratio increased and the critical ratio, experimentally about 0.2, was exceeded. Consequently, the failures occurred in the HAZ next to the weld.

It can be seen from Fig. 5 that heat input of 0.61 kJ/mm generated low throat size of 4.5 mm and smaller HAZ than with heat inputs of 0.77 and 0.94 kJ/mm. Based on measured ultimate strength of the base material, strain hardening seems not to compensate the softening effect. Therefore, in addition to ensuring that the load-carrying capacity of the fillet weld agrees with the design rules (Eurocode 3 Parts 1–12), heat input must be considered due to the softening effect on the HAZ. S960 tolerates very high cooling rates and strength properties for the welded joint are reached if the $t8/5$-time is less than 10 s. Consequently, the strength properties of the HAZ will drop by more than 10% of the strength of the base material when the optimal cooling rate is not reached. In addition, for matched filler materials, the weakest strength appears in the HAZ, but for under-matched electrodes, the weakest strength appears in the weld itself. However, utilizing under-matched filler materials can improve the deformation capacity of fillet welds if critical heat input limits are observed.

3 Robotic GMAW process parameters and variables

Development in industrial robotics has had a profound effect on modern welding, and industrial welding geared towards
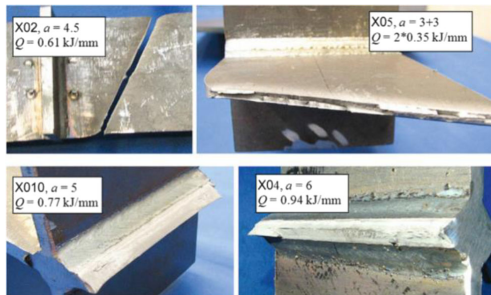

Fig. 5 Failure modes in non-load-carrying joints of UHSS S960 [3]

high quality and high productivity is nowadays often carried out using state-of-the-art robots. The GMAW process is most often used as the joining technique for robotic welding, mainly because of its flexibility and adaptability. Industrial GMAW is commonly a semi-automatic welding process since it utilizes an inert or active gas to shield a consumable and continuously fed filler material.

The GMAW process is defined by the shielding gases used, that is, metal inert gases in MIG welding, which are argon and helium gases, and metal-active gases in MAG welding, generally argon and carbon dioxide.

A large number of welding experiments have been conducted with the GMAW process. Table 4 presents key welding variables and parameters and indicates studies in which they were investigated. The defining welding parameters are heat input, contact tip to work distance, and torch angle. The studies listed in the right-hand column of Table 4 are utilized for the purposes of this work. In the studies, some welding parameters were assumed to be constants, for example arc length. The listed welding variables and parameters affect the weld geometry characteristics and properties of the weld and are considered in more detail in the following sections.

3.1 Heat input

Heat input influences the way molten filler material is transferred to the workpiece, arc stability, generation of spatter, weld bead profile formation, and weld quality. Most importantly, the terminology heat input is used because only part of the welding energy as established from these welding parameters enters the workpiece [17]. The expression for heat input is presented in Eq. (1) [18].

$$\text{Heat input (kJ/mm)}$$
$$= \frac{\text{Arc voltage } (E) \times \text{Arc current } (I) \times 60 \times \text{Arc efficiency } (\eta)}{\text{Welding speed } (V) \times 1000}$$

$$(1)$$

As can be seen from Eq. (1), the relationship between current and voltage greatly influences the heat input value. Arc characteristics under conditions of stable arc and uniform arc length give synergetic control of voltage and current. Ohm's law therefore does not satisfy the current and voltage relationship in welding, where increase in current results in voltage increase [19].

In GMAW, it has been observed that the arc mode, and thus the weld quality, is greatly influenced by the arc current [20] as a heat input parameter. The depth of penetration is significantly influenced by the arc current; depth of penetration increases with increase in current [21]. However, increased joint penetration also increases the possibility of burn-through and solidification cracking. Experiments have shown that a higher

Table 4 GMAW welding variables and parameters used in reviewed experiments	Welding variables	Welding parameters	References
	Heat input	Arc current	[7–15]
		Arc voltage	[7–16]
		Welding speed	[7–16]
		Gas flow rate	[7, 8, 11, 13, 15, 16]
	Contact tip to work distance (CTWD)	Electrode extension	[11, 15]
		Arc length	[7–15]
		Wire feed speed	[11, 15]
		Wire diameter	[7, 8, 10, 11, 13–16]
	Torch angle	Torch position	[8]
		Torch travel angle	[11]

current leads to a higher electromagnetic force, which causes the droplet to detach from the electrode and transfer to the weld pool. Furthermore, with a higher current, the size of the molten droplet is smaller and there is a higher droplet frequency.

Arc penetration depends also on electrode polarity. The penetration characteristic of GMAW with direct current electrode positive (DCEP), i.e., reverse polarity, and direct current electrode negative (DCEN), i.e., straight polarity, are depicted in Fig. 6. DCEP is mostly utilized because it produces good weld bead geometry and depth of weld penetration, and generates only low levels of spatter [20].

The current for a given GMAW solid or metal-cored electrode will reach a maximum density level and once this level is attained, no additional current can be carried by the electrode; thus, the electrode has reached its maximum current density [22]. Notably for a given heat source, the extent to which energy is absorbed by the workpiece depends on the rate of heat absorption of the material, the type of heat source, and the parameters of the welding process (voltage, current, and welding speed) [17]. Thus, from the arc efficiency expression shown in Eq. (2), it is imperative to determine the rate

of heat absorption of the material when considering the relation between the current and voltage values.

$$\eta = 1 - \frac{(1-n)q_{p+}mq_w}{EI} \qquad (2)$$

where

η arc efficiency, expressed as a fraction, %
n proportion of the energy radiated and convected from the arc column per unit of time and transferred to the workpiece, expressed as a fraction, %
q_P energy radiated and convected from the arc column per unit of time, Btu/min (cal/s)
m proportion of heat radiated away from the workpiece, expressed as a fraction, %
q_w rate of heat absorbed by the workpiece, Btu/min (cal/s)
E voltage, V
I welding current, A

Experiments reveal that arc efficiency is higher for consumable electrode processes than for non-consumable electrode processes due to heat losses from the arc to the surroundings. With consumable electrodes, heat loss from the electrode can often be ignored as the energy transferred to the electrode

Fig. 6 Arc penetration characteristics of GMAW with **a** DCEN and **b** DCEP electrode polarity
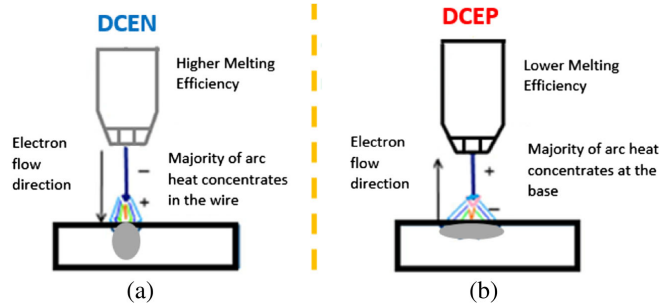
is eventually absorbed by the workpiece. Arc efficiency in GMAW falls within the range 66–85% [17, 23]. It has been observed that gas tungsten arc welding (GTAW) loses substantially more heat from the arc to the surrounding environment than GMAW, shielded metal arc welding (SMAW), and submerged arc welding (SAW). It must be noted that this generalization can result in supplying too high or too low heat input since specifications of material grade and strength are not given [17]. This observation, though, gives an indication of how to determine the rate of heat absorption of a material when establishing welding heat inputs, as in the case of UHSS. It should however be noted that the higher the heat conductivity of a material, the lower the penetration [21].

For the GMAW process, arc voltage is proportional to arc length. Welding with a high voltage produces a wide and flat weld bead with possible undercuts, and welding with too low voltage produces a low-quality weld bead with high concave reinforcement [24, 25] and decreased depth of penetration [21]. Arc voltage can be controlled by altering the arc length [26]. Too small arc length may give rise to poor penetration if the arc power is very low [21].

Gas flow rate and welding speed play major roles in determining heat input. The electric arc is stabilized by the arc plasma as a result of ionization of the shielding gas. In addition, the mode of metal transfer from the consumable electrode is determined by the arc type and also depends on the gas flow rate. In GMAW, binary shielding gas blends (argon + helium, argon + CO_2, or argon + oxygen) or ternary shielding gas blends (helium + argon + CO_2, or argon + CO_2 + oxygen) are mostly utilized [22, 27]. Table 5 shows GMAW arc types, descriptions, and material application.

The extent of convective loss depends on the nature of the shielding gas, its flow rate, and its configuration system [17]. It must be noted that the percentage mixture of CO_2 in both binary and ternary blends has an effect on heat input, and defining the relationship between CO_2 percentage and control of current and voltage values is imperative. Extensive research on arc types has shown that in many applications, greater benefit accrues from spray and pulsed arcs than short and globular arc modes [27]. Moreover, enhanced arc processes such as controlled short arc, heavy deposition rate arc, and controlled spray arc offer significant improvements in efficiency and usability [27].

Welding speed contributes to determining the cooling rate during and after welding. The variation of temperature with time as a function of the cooling rate, often referred to as the *thermal cycle*, affects microstructures, residual stresses, and the extent of distortions in weldments. On the surface of the weld pool, the temperature distribution affects the loss of alloying elements by evaporation as well as absorption and desorption of hydrogen and other gases. The chemical composition of the weldment is affected correspondingly.

The cooling rate of a weldment is a function of the rate of energy dissipation. Fast welding speed generates fast cooling and vice versa. As weld penetration increases with decreasing

Table 5 GMAW arc descriptions and material applications

Type of arc	Shielding gas	Metal transfer	Material application	Material thickness
Short arc	100% CO_2 or a mixture of 75–80% argon, plus 25–20% CO_2	Short-circuiting	Ferrous	0.5–2.6 mm
Globular arc	100% CO_2, and argon/CO_2 blends	Globular	Ferrous	3 mm and beyond
Axial spay arc	Argon + 1–5% oxygen or argon + CO_2, where the CO_2 levels are 18% or less	Axial spray	Ferrous and non-ferrous	5 mm and above
Pulse spray arc	Argon + 18% CO_2	Pulse spray	Ferrous, non-ferrous, and dissimilar	0.3 mm and beyond
Controlled short circuiting arc	Argon and CO_2 based	Short-circuiting	Ferrous, non-ferrous, and dissimilar	0.3 mm and beyond
Controlled globular arc	Argon and CO_2 based	Globular with short arc length (buried arc)	Ferrous	3 mm and beyond
Controlled spray arc	Argon and CO_2 based	Spray	Ferrous, non-ferrous, and dissimilar	1.5 mm and above
High-power arc	Argon and CO_2 based	Stream and rotating	Ferrous, non-ferrous, and dissimilar	3 mm and beyond

welding speed, the final metallurgical structure of the weld zone can be determined by the cooling rate from the maximum, or peak temperature achieved during the weld cycle. The average cooling rate from 1472 to 932 °F (800 to 500 °C, $t_{8/5}$) is particularly significant when welding heat treatable steels, and especially in the case of UHSS. The critical cooling rate for the formation of martensite in these steels is often commensurate with $t_{8/5}$ [17].

The boundary conditions derived from heat transfer equations, which are governed primarily by the time-dependent transport of heat by conduction and convection, may specify the temperature at various locations on the surface of the workpiece. For a large workpiece, the surface temperatures distant from the heat source can be taken as room temperature. However, near the heat source, the surface temperatures are much higher and are unknown in most situations [17].

Monitoring temperature variations across the weldment is important in the welding of UHSS due to its susceptibility to elevated temperatures.

Welding dilution plays a major role when considering heat input and its resultant effect on depth of penetration of the weld metal through the melting and fusion of the filler material with the base material. The selected filler material must be compatible with the base material such that four major areas of requirements are met by welds produced within a range of acceptable dilution rates: metallurgy compatibility, mechanical properties, physical properties, and corrosion properties. The percentage of dilution can be determined by the expression in Eq. (3).

$$\% \text{ of dilution} = \frac{\text{Area of penetration}}{\text{Area of reinforcement} + \text{Area of penetration}} \times 100 \tag{3}$$

Figure 7 illustrates a fillet weld bead geometry with HAZ traces. In Fig. 7, (a_1) is area of reinforcement, ($a_2 + a_3$) is area of penetration, and (a) is the throat thickness. Based on EN
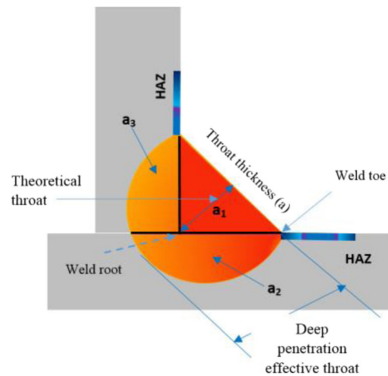

Fig. 7 Fillet weld bead geometry

ISO 15609-1, throat thickness (a) is expressed as $0.5 * t - 0.7 * t$, where t is the thickness of the base material.

In order to predict weld penetration, several factors must be considered and related. The relationship between weld penetration, arc voltage, arc current, and welding speed using a welding technique performance factor (WTPF) is expressed in Eq. (4) as follows:

$$\text{WTPF} = \left(I_S^4 / F_1 \times V_S\right)^{1/3} \tag{4}$$

where I_s is arc-current in amperes, F_1 is the arc-travel rate in centimeters per minute, and V_s is the arc-voltage in volts [28]. Knowledge of the relationship between these and other variables and parameters such as contact tip to work distance and the torch angle could lead to better prediction of depth of penetration.

3.2 Contact tip to work distance

In GMAW, the output characteristics of the arc are controlled by two main power sources: the constant current (CC) power source and the constant voltage (CV) power source. Considering these power sources, the CTWD greatly influences the arc length during welding. With constant current, the CTWD determines the arc length. As the CTWD increases, the arc length increases, and as the CTWD decreases, the arc length decreases. The problem of maintaining a constant arc length when using CC has been resolved by incorporating wire feed speed control. Thus, as the CTWD decreases, the wire feed speed increases, and as the CTWD increases, the wire feed speed decreases. The arc voltage is proportional to the arc length. The arc voltage can therefore be controlled by changing the arc length [22]. Hence, an increase in arc length will generate an increase in arc voltage [29].

With CV power source, however, the CTWD controls the welding current as a function of the arc length. As the CTWD increases, the welding current decreases, and as the CTWD decreases, the welding current increases. Moreover, in the CV scenario, the arc becomes a series circuit, and the CTWD provides resistance to current. Therefore, voltage remains unchanged and the arc length is unchanged despite changes to wire extension dimensions, as shown in Fig. 8. Furthermore, the relationship between CTWD and current, voltage, welding speed, and gas flow rate influences arc penetration. From Fig. 8, the arc penetration can be determined by identifying the arc position, which is the sum of wire extension and arc length [22].

Electrode extension ranges from 5 to 15 mm for dip transfer and up to 25 mm in other transfer modes [24, 25]. Weld properties and geometry can be predicted based on relationships between welding current, arc voltage, gas flow rate, wire feed speed, and CTWD. Electrode diameter varying from 0.8 to

(a)   (b)
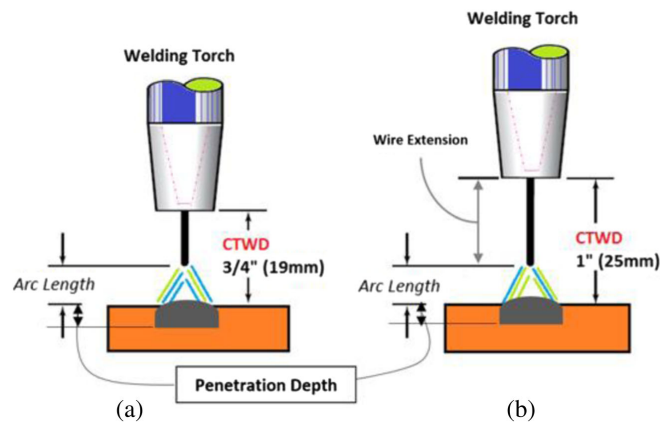
1.6 mm has effects on melting depending on heat input relationships. As smaller diameter electrodes are used for thin materials and vice versa, operational difficulties arise when electrodes are selected wrongly, thus affecting weld joint quality [24, 25].

3.3 Torch angle

The torch angle has an influence on the quality of the weld bead and the weld geometry. The torch angle is characterized by its orientation (torch travel angle) and its linearity (torch position). The deposition rate is lower when the torch angle is off-set or not in correct alignment with the cross-section of a groove. Generally, in fillet weld welding positions such as horizontal down-hand (PB or 2F), it has been estimated that the torch angle with respect to torch position should be 45–50° and the torch travel angle should be 10–15° in the welding direction as illustrated in Fig. 9.

Torch angle discrepancies result in undercut and insufficient fusion, mostly in the upright member of the fillet weld. This phenomenon leads to quality problems and lack of penetration between the upright member and the base member. Investigation of the effect of torch position and torch angle on
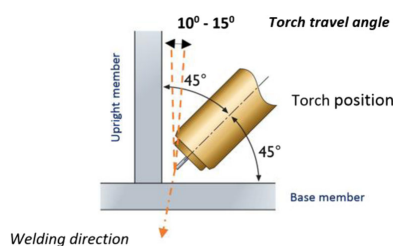

Fig. 9 GMAW torch angle (torch travel angle and torch position) representation

welding quality and welding process stability in pulse-on-pulse MIG welding–brazing of an aluminum alloy to stainless steel in a lap configuration reaches a similar conclusion [30]. In the experiment, direct current with a positively charged electrode (DCEP) was used to weld 6061 aluminum alloy (200 × 60 × 3 mm) and 304 stainless steel (200 × 60 × 2 mm). Images of the arc, electrical signals of the welding current, and welding voltage were acquired in synchronous modes by a high-speed camera and electrical signal acquisition system, respectively. It was concluded that arc shape, macrostructure, microstructure, and mechanical properties are sensitive to torch travel angle and torch position (work angle) for settings of 20° and 0°, respectively. A fracture occurred in the HAZ as a result of the effect of uneven heat distribution. However, when torch travel angle was 20° and work angle was 20°, the effects of torch position with respect to heat distribution were insignificant.

In robotic GMAW, the torch travel angle and torch position can be altered by manually controlling the manipulator and the end effector attached to the welding torch. Incorporation of adaptive features such as sophisticated sensory and monitoring systems make robots adaptive to their operating environment and enable monitoring, detection, measurement, inspection, and recording of welding process parameters and other features such as joint geometry and weld pool geometry [31]. The ability to maintain torch linearity and orientation, follow the desired trajectory, as well as the ability to perform seam tracking, which emulates the behavior of manual welders, is achievable in robotic welding systems [32]. However, an ideal sensor that combines all the aforementioned functionalities with respect to seam finding, seam tracking, quality monitoring, through-arc sensing, and control of welding parameters does not yet exist [33].

Artificial intelligent systems provide possible alternative solutions for adaptive robotic welding. For example, infrared

thermography-based sensors could be used in adaptive robotic GMAW and incorporated with an artificial intelligent system to measure thermal profiles when welding UHSS S960QC to check heat input and temperature variations and assure full penetration welds. In addition, motion control also creates a need to incorporate artificial intelligent systems in adaptive robotic welding for accurate trajectory planning as "teach and play" technique used in robotic programming today has repeatability and precision errors.

Figure 10 shows arc shape and arc characteristic based on torch angle, work angle, and arc length. The arc characteristic in Fig. 10 (y) indicates that adequate fusion and low susceptibility to HAZ are achieved. The dumbbell shape of the arc in Fig. 10 (y) indicates good arc characteristics in terms of its stability. In contrast, Fig. 10 (x) suggests that uneven heat distribution is likely to occur and thus high HAZ susceptibilities in one sample than another.

4 Artificial intelligence system application in welding

Modeling of an artificial intelligence system for robotic GMAW can be done usually by mathematical approaches. AI systems such as artificial neural networks (ANN), fuzzy logic systems, neural-fuzzy networks, adaptive neuro-fuzzy inference systems (ANFIS), genetic algorithms, and swam particle optimization (SPO) systems, which are mathematically based, can be used as data modeling tools to predict desired outcomes. These mathematically based and well-known algorithmic systems are gaining significance in the welding manufacturing industries. In the field of welding, for example, research work has considered the use of one or more artificial intelligence systems to predict weld characteristics such as weld bead strength, weld surface weld surface quality, weld penetration, and weld size for GMAW [34–36]. Different types of artificial intelligence systems to control arc welding processes have been investigated in a recent study on adaptive gas metal arc welding control and optimization of welding parameter output [37]. The study identified the effects and benefits of AI system predictions on metallurgical and geometric qualities in T-joint welds. It was concluded that the quality and properties of welded joints, weld deposition rate, microstructure, and weld geometry can be improved since welding parameters can be predicted by AI systems like ANN [37]. Table 6, supported by references [37–39], provides a comparison between frequently used AI systems in modeling and simulation of welding.

The computational abilities of AI systems, as shown in Table 6, comprise decision-making and/or linguistic performance. Depending on the type of AI system adopted and the output requirement expected, modeling a robust artificial intelligent system for weld characteristic predictions in robotic GMAW process should have enough input data. It should be noted that the output requirement can be limited but the input must have enough data to enable accuracy in predictions. Figure 11 illustrates a framework of a schematic model of an AI system for robotic GMAW. The model considers nonlinear weldability factors associated with robotic GMAW in the welding of UHSS S960QC. Welding variables and parameters are denoted as the input requirements and the corresponding desired output requirements are mapped to various AI systems.

In addressing UHSS S960QC weldability challenges, it is assumed that the output requirements given in Fig. 11 should conform to EN ISO 5817 for fillet weld quality levels as described in Table 1 and Table 2. The HAZ is expected to demonstrate consistent microstructural properties equal to the base material. If softening in the HAZ does occur, hardness should not drop considerably below the hardness value of the base material, and, additionally, toughness, ductility, and tensile strength should not deteriorate. As moderate strength properties for welded joints are reached if the cooling rate ($t_{8/5}$) is less than 10%, then the strength properties of the HAZ should not drop by more than 10% relative to the nominal strength properties of the base material [3]. Monitoring thermal cycles with a thermal profile senor/scanner while welding the UHSS S960QC material would be beneficial for cooling rate evaluation.

It is claimed that an optimal cooling rate is difficult to achieve when using GMAW (MAG) to weld 8-mm-thick

Fig. 10 Arc shape with different torch positions: In image (x), the torch angle is 20° and work angle is 0° and the lengths are
(a) = −2 mm, (b) = −1 mm,
(c) = 0, (d) = 1 mm, and
(e) = 2 mm; In image (y), the torch angle is 20° and the work angle is 20° and the lengths are
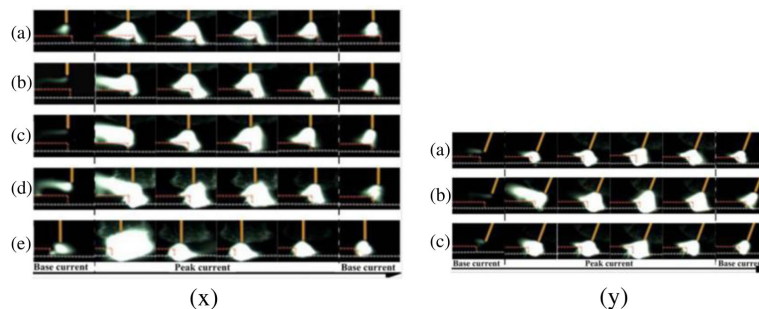(a) = 0 mm, (b) = 1 mm, and
(c) = 2 mm [30]

Table 6 Artificial intelligent systems for arc welding

Artificial intelligence systems	Principles	Advantages	Limitations
Artificial neural network systems	- Operates on feed forward back propagation system - Represents interconnected groups of artificial visible and hidden neurons - Develops models that depict interrelation characteristics between input data and desired output data	- Has learning and training capabilities for nonlinear system modeling - Has pattern recognition, signal processing, data prediction and control, and time series analysis capabilities - Has adaptability abilities where free parameters can be adapted to changes in surrounding environment - Has knowledge discovery and data mining abilities - Has uncertainty tolerance and imprecision abilities	- Lack of linguistic/explanatory ability - Lack of knowledge representation abilities
Fuzzy logic systems	- Operates on a set of linguistic fuzzy rules - Relies on rule-based systems	- Has linguistic/explanatory abilities - Has good knowledge representation abilities, good uncertainty tolerance abilities, and good imprecision tolerance	Lack of self-learning abilities; lack of adaptive and pattern recognition abilities, and rather bad knowledge discovery and data mining abilities
Neuro-fuzzy systems	- Operates by hybridizing fuzzy logic qualitative approach and adaptive neural network system capabilities	- Combines the advantages of both paradigms and conquer their own shortcomings concurrently to produce improved intelligence system	- It is typical for Mamdani fuzzy inference system with a single output defuzzification
Adaptive neuro-fuzzy inference systems	- Uses a hybrid learning algorithm by combining least squares estimators and the gradient descent method	- Both antecedent and consequent parameters are optimized, has the ability to generalize and converge rapidly particularly in online learning, and applicable in adaptive control	- It is typical for Sugeno systems, i.e., for constant and linear output membership functions and single output defuzzification

plates of UHSS S960QC. Moreover, a high risk of incomplete fusion is bound to occur when small heat input is employed [3]. To alleviate HAZ softening and susceptibility to a lack of fusion when welding UHSS S960QC, adaptive robotic GMAW incorporating AI systems for real-time modeling provides an alternative and holistic approach.

Due to its operational functionalities and benefits, an ANN system is selected as a case schematic model (Fig. 11). The schematic model represents an ideal situation to serve as a practical step to design a neural network system modeling input/output data for a given set of parameters from input and output requirements. It is assumed that the neural network model when validated by comparing the predicted results with actual practical results should agree with the results obtained through real-time experiments on UHSS S960QC with a robotic GMAW process.

4.1 Artificial neural network

Considering the schematic model for ANN modeling, the input and output requirements can be represented as data functions in the neural network system. In the model, there are multiple input requirements and multiple output requirements which are mapped in a multilayer perceptron (MLP) neural network architecture as shown in Fig. 12.

The MLP neural network requires supervised learning. Weight adjustments are made based on comparison with some target output. A teaching signal feeds into the neural network for the weight adjustments. These teaching signals are also termed the training sample [40]. The MLP neural network architecture is composed of many simple perceptrons in a hierarchical structure forming a feed forward topology with one or more hidden layers between the input and output layers.

4.2 Multilayer perceptron learning algorithms

In determining an optimized set of weights, the MLP neural network system uses learning algorithms such as back propagation (BP), resilient propagation (RPROP), the Levenberg–Marquardt algorithm, genetic algorithm (GA), or particle swarm optimization (PSO) [40]. Generally, input data are weighted through sum biasing and are then processed through an activation function to produce the output. After each process, the calculated output is matched to the desired output, and the difference between the two gives an error signal. The weight is adjusted by presenting the error back to the neural network system in a manner that will decrease the error for every iteration. The process aims to reduce the error value and drive the neural network system model towards the desired target. The learning algorithm adjusts the weights as the iteration increases, thereby reducing the error and getting closer to the desired target [41, 42].

Fig. 11 A schematic model of artificial intelligence system for robotic GMAW process
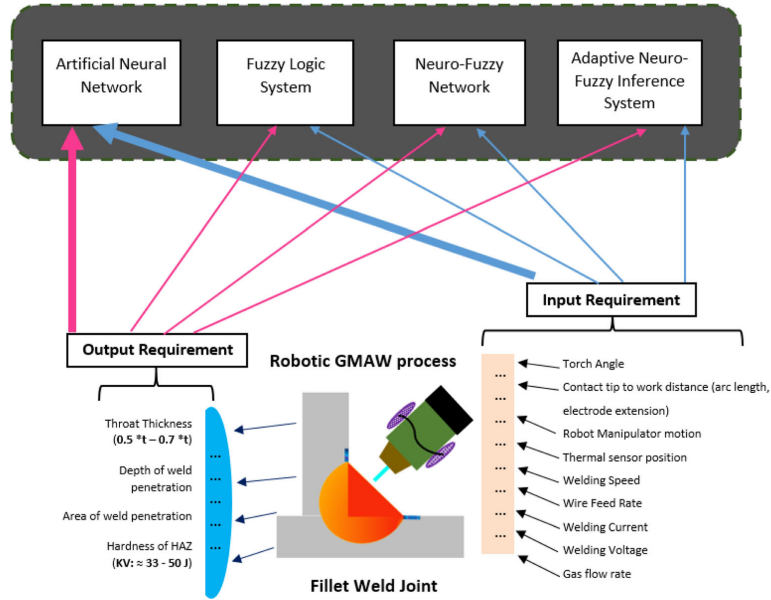
In an ANN system development study [34], weld bead width characteristics were predicted as a function of key process parameters in robotic GMAW. The accuracy of the neural network model was verified by comparing the simulated data obtained from the neural network model with values obtained from actual robotic welding experiments. In the study, BV-AH32 steel of 12 mm thickness was multi-pass welded with GMAW.

The process parameters were the following: number of passes—3; welding current—170, 220, and 270 A; arc voltage—23, 26, and 28 V; and welding speed—12–50 cm/min. All other parameters were fixed. These process parameters were considered as input data and the required weld bead width was the output for the neural network system [34].

A back propagation learning algorithm and Levenberg–Marquardt learning algorithm were employed to train the

neural network based on both the input and output data. A training set of 500 cycles was employed for the training of the network with an initial error of 1.0×10^6 [34].

The training was carried out using MATLAB. It was observed that the Levenberg–Marquardt algorithm gave the lowest root mean square (RMS) error of about 0.0000845 with four neurons in hidden layers in 500 training cycles [34]. Figure 13 illustrates the performance of the back propagation algorithm and the Levenberg–Marquardt approximation algorithm for prediction of bead width [34]. From Fig. 13, it can be seen that the points obtained from the Levenberg–Marquardt predictions correlate with those of the actual experiment.

With back propagation, although the plotted points were not that far from values from the actual experiment, the predictions were not as exact as those of the Levenberg–Marquardt algorithm.

The Levenberg–Marquardt learning algorithm, also known as the damped least squares method, provides numerical solutions by reducing error when solving complicated boundary value problems. In the ANN system study [34], adjustment of the weights and biases was done according to the transfer function expressed in Eq. (5):

$$\Delta W = \left(J^T J + \mu I \right)^{-1} J^T e \qquad (5)$$

where J is the Jacobian matrix of derivation of each error, μ is a scalar, and e is the error function. In other expressions, the Levenberg–Marquardt algorithm could be derived by
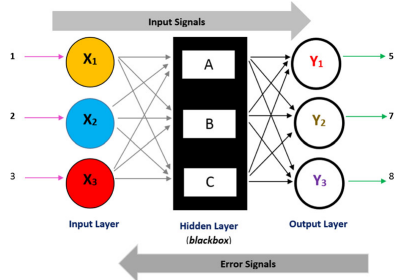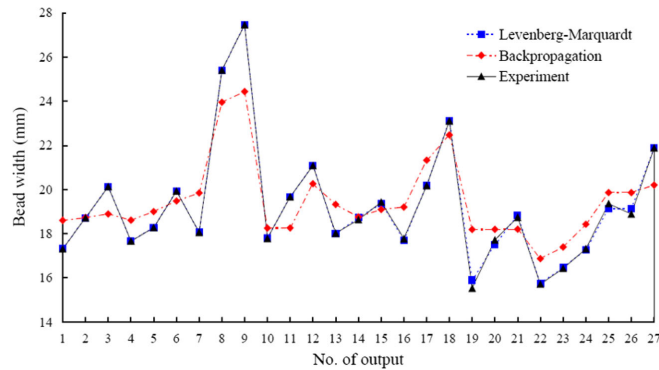

Fig. 12 A 3-3-3 multilayer perceptron neural network architecture

Fig. 13 Performance of learning algorithm prediction data against actual weld bead width data [34]

considering the error E after a differential change in the neural network weights from u_0 to u according to the second-order Taylor series expansion as shown in Eq. (6). Additionally, the Jacobian matrix is used to define the Hessian for special case of sum of squared error as expressed in Eq. (7) [40].

$$E(u) = E(u_0) + f^T(u-u_0) + \frac{1}{2}(u-u_0)^T H(u-u_0) + \dots \quad (6)$$

$$H = 2\,J^T J + 2\frac{\partial J^T}{\partial u}F \quad (7)$$

Levenberg–Marquardt algorithm improved the overall accuracy of the neural network systems since it could provide a faster convergence. Therefore, for welding, where accurate setting of welding variables and parameters are imperative, the use of the Levenberg–Marquardt learning algorithm in ANN systems could guarantee accurate predictions.

5 Discussions

UHSS is becoming more usable for structural applications especially in mobile equipment industries. However, in applications where there is high fatigue loading on the structural welded load-carrying member, UHSS may not satisfy service performance requirements due to weldability challenges that arise from welding heat input, causing HAZ softening effects, lack of fusion, and susceptibility to cracking and fatigue failure. Previous study of structural integrity and the usability of high-strength steels (HSS) has emphasized the need for risk assessment when considering HSS and its variants such as UHSS and AHSS, especially as regards weldability and service performance following high heat input [43].

In this paper, UHSS S960QC material data presented in Fig. 2 shows welding considerations that require risk assessment. Adhering to heat input values and filler material recommendations can ensure sound welded joint characteristics. Nevertheless, weldability challenges clearly exist when manufacturing full penetration fillet welded joints of UHSS S960QC. Weldability challenges are increased where the UHSS S960QC weldments need to conform to ISO 5817.

Previous studies of online welding process monitoring [43] have shown the necessity of using sensing systems like infrared thermography in pre-process monitoring, in situ monitoring, and post-process monitoring for adaptive robotic GMAW. This sensory system will allow temperature differences to be measured and enable the required amount of heat needed for full penetration to be monitored. Despite the ability to acquire this data, such sensory systems are unable to control temperature variations dynamically in tandem with robotic GMAW process variables and parameters. Thus, an AI system for data modeling and process control should be embraced.

The AI model discussed and the welding information presented can provide a useful basis for real-time experimentation on UHSS S960QC. Actual experimentation data can then be compared with data values predicted from different learning algorithms like back propagation (BP), resilient propagation (RPROP), Levenberg–Marquardt, genetic algorithm (GA), and particle swarm optimization (PSO) to ascertain the accuracy of predicted AI values against actual experimental values. As neural network systems can learn new associations, new functional dependencies, and new patterns based on teaching and learning via input data and expected output, accurate prediction of desired outcomes is feasible [44].

6 Conclusion

Modeling of welding systems to guarantee sound structural integrity in lightweight-welded materials is relevant to modern welding manufacturing and production. In the current economic environment, structural weight must be reduced, stability of the welded structure must be assured, manufacturing

must be cost effective, and overall production must be profitable. Lightweight materials of high yield strength like UHSS S960QC are a possible material choice for lightweight manufacturing. UHSS S960QC has a superior strength-to-weight ratio, and excellent physical, mechanical, and low-temperature properties. From the environmental viewpoint, welding usability of UHSS translates into improved energy efficiency through low fuel consumption and low carbon emissions, especially in welded mobile equipment and structures.

In this paper, a schematic model of an AI system has been created by considering identified nonlinear factors associated with UHSS S960QC weldability and robotic GMAW. High heat input, which can result in HAZ softening and greater propensity to fatigue failure, thus affecting toughness and strength properties, is the most critical weldability issue with UHSS-welded joints. The multiple welding variables associated with robotic GMAW, such as heat input, CTWD, and torch angle, and related parameters like arc current, arc voltage, welding speed, gas flow rate, arc efficiency; electrode stick out, wire feed speed, electrode diameter, and torch position and torch travel angle, make accurate prediction of weld characteristics very challenging. Other nonlinear factors connected with the robot manipulator and end effector trajectory bring repeatability and precision errors, which further complicates prediction of the outcome of robotic GMAW.

One possible way to address or alleviate weldability challenges associated with nonlinear factors is by deploying AI systems. The welding information presented together with the neural network schematic model show that it is possible to accurately predict welding parameters and process outputs using learning algorithms. The schematic case model can provide a basis for future experimental study of UHSS S960QC welding in conformance with ISO 5817. Additionally, an optimized control system using infrared thermography-based sensors can be developed, which would enable an adaptive approach in robotic GMAW to be incorporated into the neural network modeling and control system. This paper increases awareness of the potential of UHSS S960QC and presents a scenario for using an AI system to overcome current limits on adaptive robotic GMAW.

References

1. Hemmilä M, Laitinen R, Liimatainen T, Porter D (2010) Mechanical and technological properties of ultra high strength Optim steels. Rautaruukki Oyj, Ruukki Production, Helsinki. http://www.oxycoupage.com/FichiersPDF/Ruukki_Pdf/English/Ruukki-Technical-article-Mechanical-and-technological-properties-of-ultra-high-strength-Optim-steels.pdf. Accessed 20 April 2016

2. Kah P, Pirinen M, Suoranta R, Martikainen J (2014) Welding of ultra high strength steels. Adv Mater Res 849:357–365

3. Björk T, Toivonen J, Nykänen T (2012) Capacity of fillet welded joints made of ultra-high strength steel. Weld World 57:71–84

4. Laitinen R, Valkonen I, Kömi J (2013) Influence of the base material strength and edge preparation on the fatigue strength of the structures made by high and ultra-high strength steels, 5th Fatigue Design Conference, Fatigue Design. Science Direct. Procedia Eng 66:282–291

5. Hicks J (2001) Welded design—theory and practice, Woodhead Publishing Ltd, Cambridge. Elsevier. Chapter 4, p 36–41

6. Finnish Standards Association (SFS): welding—fusion-welded joints in steel, nickel, titanium and their alloys (beam welding excluded)—quality levels for imperfections (ISO 5817:2014)

7. Hemmilä M, Laitinen R, Liimatainen T, Porter D (2005) Mechanical and technological properties of ultra high strength Optim steels. Rautaruukki Corporation, Helsinki

8. Jae-Woong K, Jun-Young L (2008) A control system for uniform bead in fillet arc welding on tack welds. J Mech Sci Technol 22:1520–1526

9. Shi L, Tian X, Zhang C (2015) Automatic programming for industrial robot to weld intersecting pipes. Int J Adv Manuf Technol 81:2099–2107

10. Ahiale GK, Oh Y-J, Choi W-D, Lee K-B, Jung J-G, Nam SW (2013) Microstructure and fatigue resistance of high strength dual phase steel welded with gas metal arc welding and plasma arc welding processes. Met Mater Int 19:933–939

11. Nele L, Sarno E, Keshari A (2013) Modeling of multiple characteristics of an arc weld joint. Int J Adv Manuf Technol 69:1331–1341

12. Jaime A-V F, Reyes R-C, Ismael L-J (2016) On-line learning of welding bead geometry in industrial robots. Int J Adv Manuf Technol 83:217–231

13. Moon H-S, Na S-J (1997) Optimum design based on mathematical model and neural network to predict weld parameters for fillet joints. J Manuf Syst 16:13–23

14. Son JS, Kim IS, Kim HH, Kim IJ, Kang BY, Kim HJ (2007) A study on the prediction of bead geometry in the robotic welding system. J Mech Sci Technol 21:1726–1731

15. Xiong J, Zhang G, Hu J, Wu L (2014) Bead geometry prediction for robotic GMAW-based rapid manufacturing through a neural network and a second-order regression analysis. J Intell Manuf 25:157–163

16. Lin H-L, Yan J-C (2014) Optimization of weld bead geometry in the activated GMA welding process via a grey-based Taguchi method. J Mech Sci Technol 28:3249–3254

17. DebRoy T, Kou S, Tsai C (2001) Heat flow in welding: welding handbook chapter committee. Chapter 3, American Welding Society (AWS)

18. Gunaraj V, Murugan N (2002) Prediction of heat-affected zone characteristics in submerged arc welding of structural steel pipes. Weld J 81:94–98

19. Ibrahim Khan M (2007) Welding science and technology. New Age International Publishers, New Delhi

20. Howard BC, Scott CH (2005) Modern welding technology, 6th edn. Pretice Hall, United States of America

21. Nagesh DS, Datta GL (2002) Prediction of weld bead geometry and penetration in shielded metal arc welding using artificial neural networks. J Mater Process Technol 123:303–312

22. Nadzam J (2014) Gas metal arc welding: production and procedure selection—The Lincoln Electric Company. http://www.lincolnelectric.com/assets/global/products/consumable_miggmawwires-superarc-superarcl-56/c4200.pdf. Accessed 20 April 2016

23. Robert Messler Jr W (2004) Principles of welding: processes, physics, chemistry and metallurgy. WILEY-VCH Verlag GmbH & Co. KGaA, Weinheim

24. Weman K, Gunnar L (2006) MIG welding guide. Woodhead Publishing and Maney Publishing, Cambridge

25. Weman K (2003) Welding process handbook. Woodhead Publishing Limited, Cambridge

26. Naidu DS, Ozcelik S, Moore K (2003) Modeling, sensing and control of gas metal arc welding, 1st edn. Elsevier, Kidlington

27. Kah P, Latifi H, Suoranta R, Martikainen J, Pirinen M (2014) Usability of arc types in industrial welding. Int J Mech Mater Eng 9(15):1–12

28. Jackson CE, Shrubsall AE (1953) Control of penetration and melting ratio with welding technique. Weld J 32(4):172–178

29. Kovacevic R, Zhang YM, Li L (1996) Monitoring of weld joint penetration based on weld pool geometrical appearance. Welding Research Supplement 317-s, University of Kentucky, Lexington, KY

30. Li J, Li H, Wei H, Gao Y (2016) Effect of torch position and angle on welding quality and welding process stability in pulse on pulse MIG welding–brazing of aluminum alloy to stainless steel. Int J Adv Manuf Technol 84:705–716

31. Pires JN, Loureiro A, Bölmsjo G (2006) Welding robots: technology, systems issues and applications. Springer-Verlag, London Limited, p74

32. Kah P, Shrestha M, Martikainen J (2015) Robotic arc welding sensors and programming in industrial applications. Mater Eng 10:13

33. Bolmsjö G, Olsson M (2005) Sensors in robotic arc welding to support small series production. Ind Robot Int J 32(4):341–345

34. Kim I-S, Son J-S, Lee S-H, Yarlagadda PKDV (2004) Optimal design of neural networks for control in robotic arc welding. Robot Comput Integr Manuf 20(1):57–63

35. Chan B, Pacey J, Bibby M (1999) Modelling gas metal arc weld geometry using artificial neural network technology. Can Metall Q 38(1):43–51

36. Sreeraj P, Kannan T (2012) Modelling and prediction of stainless steel clad bead geometry deposited by GMAW using regression and artificial neural network models. Adv Mech Eng. doi:10.1155/2012/237379

37. Mvola B (2016) Adaptive gas metal arc welding control and optimization of welding parameters output: influence of welded joints. Int Rev Mech Eng 20:67–72

38. S-R JJ (1993) ANFIS: adaptive network-based fuzzy inference systems. IEEE Trans Syst Man Cybern 23:665–685

39. Negnevitsky M (2002) Artificial intelligence: a guide to intelligent systems. Addison-Wesley, Pearson Education Limited

40. Yadav N, Yadav A, Kumar M (2015) An introduction to neural network methods for different equations. Springer Briefs in Applied Sciences and Technology. Computational Intelligence. Springer Science + Business Media B.V, Dordrecht

41. Al-Faruk A, Md AH, Ahmed N, Kumar Das U (2010) Prediction of weld bead geometry and penetration in electric arc welding using artificial neural networks. Int J Mech Mechatron Eng 10:19–24

42. Juang SC, Tarng YS, Lii HR (1998) A comparison between the back-propagation and counter-propagation networks in the modeling of TIG welding process. J Mater Process Technol 75:54–62

43. Gyasi EA, Kah P (2016) Structural integrity analysis of the usability of high strength steels. Rev Adv Mater Sci 46:39–52

44. Fuller R (2000) Introduction to neuro-fuzzy systems: advances in soft computing. Physica-Verlag, New York, Heidelberg

Publication IV

Kesse A. M., Buah, E., Handroos, H., and Ayetor, K. G.
Development of an Artificial Intelligence Powered TIG Welding Algorithm for the Prediction of Bead Geometry for TIG Welding Processes using Hybrid Deep Learning

Development of an Artificial Intelligence Powered TIG Welding Algorithm for the Prediction of Bead Geometry for TIG Welding Processes using Hybrid Deep Learning

Martin A. Kesse [1],*, Eric Buah [2], Heikki Handroos [1] and Godwin K. Ayetor [3,4]

[1] School of Energy Systems, Mechanical Engineering Department, LUT University, 53850 Lappeenranta, Finland; heikki.handroos@lut.fi

[2] School of Energy Systems, Sustainability Science Department, LUT University, 53850 Lappeenranta, Finland; Eric.Buah@gmail.com

[3] Department of Mechanical Engineering, Kwame Nkrumah University of Science and Technology (KNUST), Kumasi AK-039-5028, Ghana; kafuiayetor@yahoo.co.uk

[4] The Brew-Hammond Energy Centre, Kwame Nkrumah University of Science and Technology (KNUST), Kumasi AK-039-5028, Ghana

* Correspondence: martin.kesse@lut.fi or martin.a.kesse@gmail.com; Tel.: +358-442795156

Abstract: Recent developments in artificial intelligence (AI) modeling tools allows for envisaging that AI will remove elements of human mechanical effort from welding operations. This paper contributes to this development by proposing an AI tungsten inert gas (TIG) welding algorithm that can assist human welders to select desirable end factors to achieve good weld quality in the welding process. To demonstrate its feasibility, the proposed model has been tested with data from 27 experiments using current, arc length and welding speed as control parameters to predict weld bead width. A fuzzy deep neural network, which is a combination of fuzzy logic and deep neural network approaches, is applied in the algorithm. Simulations were carried out on an experimental test dataset with the AI TIG welding algorithm. The results showed 92.59% predictive accuracy (25 out of 27 correct answers) as compared to the results from the experiment. The performance of the algorithm at this nascent stage demonstrates the feasibility of the proposed method. This performance shows that in future work, if its predictive accuracy is improved with human input and more data, it could achieve the level of accuracy that could support the human welder in the field to enhance efficiency in the welding process. The findings are useful for industries that are in the welding trade and serve as an educational tool.

Keywords: TIG welding; artificial intelligence; deep neural network; automation

1. Introduction

Welding processes and procedures need to follow trends and adapt to changes in industry such as increased usage of robots and mega structural construction. In addition, the application of new materials in modern industries has increased the need for new developments in welding processes. Thick and thin metal plates of increasingly diverse materials are used throughout industry and effective and efficient joining technology is in urgent demand. During welding, problems are usually encountered due to improper control of various parameters associated with the welding process. Normally, a welder, based on experience gained over several years of welding, selects a set of parameters that could produce fairly good results. The trial-and-error inherent in this approach can

be averted if an appropriate automation tool can be created that can predict the output from a set of defined parameters. Such a tool can help improve weld quality by improving the prediction of weld outcome and limiting defects in welded joints.

To address this need, various methods have recently been applied to attain good mechanical properties. These include designs of experiment (DoE) techniques and algorithms, and computational networks including a neural network and fuzzy logic. Design of Experiments is a technique that is used to generate the information required with the minimum amount of experimentation by applying the following conditions: Experimental limits and specific experimental conditions [1]. It also uses mathematical investigation to predict the response at any point within the experimental limits. In welding research, the aim of these methods is the optimization of the different parameters used in welding [2], for example, Parikshit [3], who carried out modeling of a tungsten inert gas (TIG) welding process applying conventional regression analysis and neural network-based approaches and found that the neural network approach is much better than conventional regression analysis. In the paper, it was claimed that the neural network-based approach is better than conventional regression methods since the neural network-based approach can carry out interpolation within a certain range.

However, a limitation of neural networks is that it is a blackbox. This makes it difficult to explain how the algorithm reaches a decision, which is important for a human welder. This problem can be overcome using fuzzy deep learning. Fuzzy deep learning, which is also called a fuzzy deep neural network, is a hybridization of fuzzy logic and deep neural network. In fuzzy deep learning, fuzzy logic is incorporated into the learning process of multiple neural networks algorithms as a deep neural network (DNN) [4]. Figure 1 shows an example of a DNN algorithm, which uses multiple layers unlike a shallow neural network, which uses a few hidden layers to construct its hypothesis. A DNN constructs its hypothesis by building it out of artificial neurons to form a graph. A graph of these hierarchies is many artificial neurons, which are connected layers as illustrated in Figure 1. In this connection, an output of one artificial neuron automatically becomes a piece of input information to another [4–8].
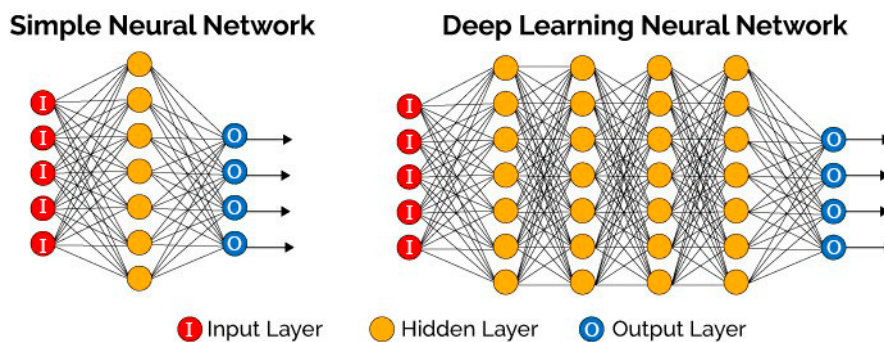
Figure 1. Illustration of a conventional neural network and deep neural network (DNN) [9].

Combining fuzzy logic and DNN allows for the development of an AI model that is not only accurate in prediction but inherently interpretable and understandable to humans. Drawing inspiration from this AI technique, this work presents the development of an AI TIG welding algorithm for selecting control parameters to predict a desired weld bead width using fuzzy deep learning. The paper is divided into four sections. In Section 2, a brief description of the TIG welding process is presented. This is followed by a description of a simulation experiment in Section 3 where the development process of the AI TIG Welding algorithm is explained. The result emerging from this experiment is discussed in Section 4 followed by some concluding remarks.

2. TIG Welding Process

The tungsten inert gas (TIG) welding process produces welds with a non-consumable tungsten electrode. During direct current (DC) welding, the electrodes used are usually made of pure tungsten. Thoriated tungsten which contains thorium oxide in the range of 1% to 4% is used to improve arc ignition. Other additives such as lanthanum oxide and cerium oxide have been identified as giving improved performance in terms of arc starting and lower electrode consumption. Because the welding current has a relation with the electrode diameter and the tip angle, it is important to select this parameter in relation to current and tip angle. Therefore, the lower the current, the smaller the electrode diameter and tip angle. In alternating current (AC) welding, since the electrode operates at a much higher temperature, tungsten with zirconia is added to reduce electrode erosion.

In the TIG welding process, the arc is formed between a pointed tungsten electrode and the workpiece in an inert atmosphere of argon (Ar), helium (He) or an Ar–He mixture. The process uses a power source, a shielding gas and a TIG torch. [10]. It is important to note, however, that although the electrode, in theory, is not consumed, control must consider the deterioration of the sharpened tip that occurs due to contamination when the tip comes into contact with the material during the arc ignition. Additionally, small projections of the melted material impact on the tip, contaminating it and influencing the weld quality. This process leads to consumption of the electrode, especially in the case of welding of carbon steels. It is thus important to sharpen the electrode in this situation.

Depending on the required weld preparation and the workpiece thickness, it is possible to work with or without filler. The filler can be introduced manually or automatically depending on the type of process selected. The process itself can be manual, partly mechanized, fully mechanized or automatic.

Filler is used when welding together metals with high melting points to prevent cracking. In addition, highly corrosive resistant alloys when welded to thicker wall material require a filler wire. Finally, when dissimilar alloys are being joined a filler wire is needed. Metals with a thickness of more than 6 mm require the use of filler wire during welding with TIG welding process.

The power is fed from the power source, down the contact tube and is delivered to a tungsten electrode and an electric arc is then created between the tungsten electrode and the workpiece. The tungsten and the welding zone are protected from the surrounding air by a shielding gas to prevent oxidation or contamination from the atmosphere. The electric arc can produce temperatures up to 19,400 °C and this heat can be a much-focused local heat in the TIG welding process. The weld pool can be used to join the base metal with or without filler material [11,12]. Figure 2 shows a schematic diagram of the TIG welding process incorporated with the filler rod.

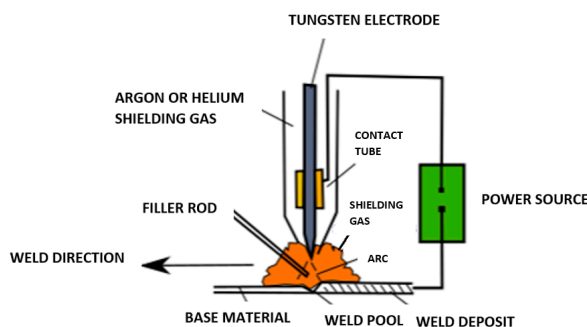**Figure 2.** Schematic diagram of tungsten inert gas (TIG) welding incorporated with a filler rod.

Characteristics of Weld Bead Geometry

Quality is very vital in the welding process and it is important to note that the weld bead plays a major role in achieving the desired quality. The quality of the weld bead geometry and configuration are controlled by various welding process input parameters such as current, voltage and welding

speed [13]. Liquid weld metal solidification during welding results in interfacial tensions that usually determine the final bead geometry [14]. The mechanical properties of the weld, which are an important factor in all welded structures, are also influenced by the weld bead geometry [15].

The main defects that occur in the bead geometry during welding are high heat-affected zone (HAZ) width, high fusion width, excess bead height and lack of penetration. Lack of penetration directly affects the strength and load-bearing capacity of the welded joint. Additionally, lack of penetration increases the stress in the weld joint, thereby resulting in crack propagation which affects the fatigue life of the weld joint [16].

Weld bead geometry is illustrated in Figure 3 showing the depth of fusion, which is the distance that fusion extends into the base material and the bead width, which is the maximum width of the deposited weld metal. Bead height or reinforcement height is the bead height above the surface of the plate. The heat-affected zone is the non-melted area that experiences changes in material properties due to exposure to the welding heat.
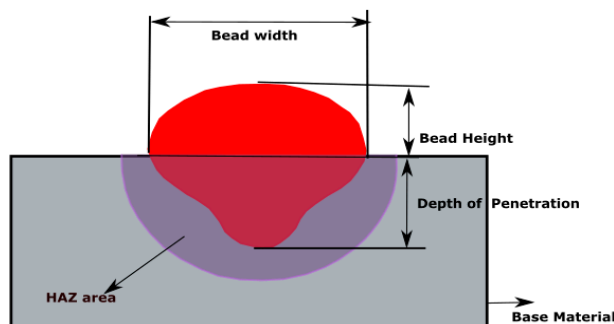

Figure 3. Schematic illustration of bead geometry and heat-affected zone (HAZ) area [13].

3. Simulation Experiments

This section presents the process for simulation experiments using 27 sets of experimental data. Hybrid fuzzy deep neural learning is applied in the simulation process. The section is divided into two main subsections with further subsections. Section 3.1 presents the system modeling, its mathematical logic and how the control variables and the expected output were measured using fuzzy mathematics. Fuzzy mathematics is the area of mathematics that relates to fuzzy sets and fuzzy logic. Section 3.2 presents the objective evaluation of the proposed system using 27 experiments.

3.1. Building the AI TIG Welding Control Algorithm and Datasets

3.1.1. Feature Selection and Measurement using a Fuzzy Mathematical Technique

Methodologically, the proposed AI TIG welding algorithm is a hybrid deep learning AI technique. It is based on a hybridization of the mathematics of fuzzy logic and the learning capability of deep neural networks (DNN). In the pioneering work of Zadeh [17], fuzzy logic was introduced as an attempt to overcome weaknesses in Boolean logical thinking. It provides a mathematical framework to compute with words based on "degrees of truth" rather than the usual "true or false" (1 or 0) Boolean logic on which the modern computer is based. Fuzzy logic includes 0 and 1 as extreme cases of truth but it also includes the various states of truth in between so that, for example, the result of a comparison between two things could not be "tall" or "short" but "somehow tall" and the height can be quantified using a mathematical curve called a membership function (MF). Therefore, the fuzzy inference processes allow the modeling engineer to generate rule-based control structures as illustrated in Figure 4.
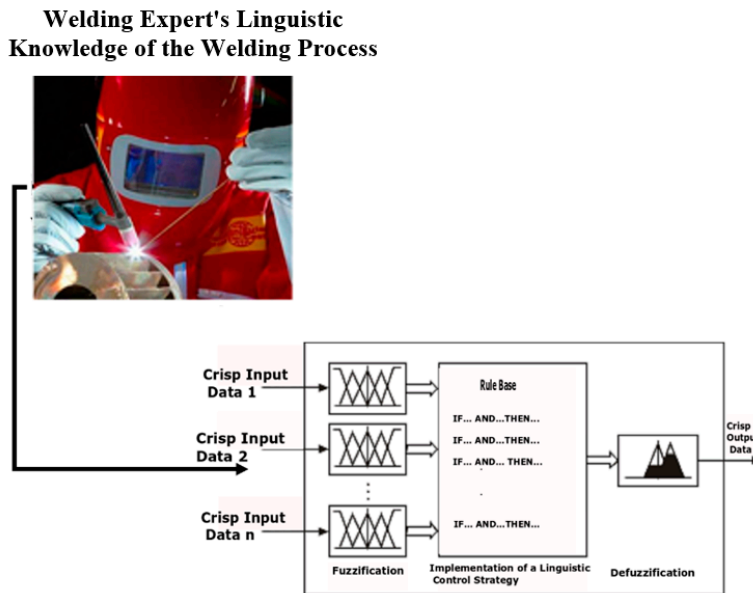
**Welding Expert's Linguistic
Knowledge of the Welding Process**

Figure 4. Illustration of the inference engine of a fuzzy controller.

Using the welding process as a case, as shown in Figure 4, the fuzzy inference system consists of three subsystems: the fuzzifier, the rule inference engine and the defuzzifier. The task of the Fuzzifier is to take the expert natural language about the welding process and transform it into fuzzy values using an MF mathematical curve.

Let us assume the following responses: "when the welding speed is very high . . . ," "when the welding speed is very low . . . .," "the bead width is narrow." For us to know what degree is the bead width narrow or the welding speed very low or very high, it is at the fuzzification process where the system assigns these quantitative weights to incoming data to determine its degree of truth within a universe of discourse (e.g., 0 to 100 mm/s) speed range) on a fuzzy scale using the mathematical curves as depicted in the illustration with "Data 1, Data 2 and Data n passing through the membership function curves.

The task of the rule inference engine is to map a response argument to its expected reality (consequence) using IF...THEN logic. When a condition, for example, is met, the inference engine produces a result sent to the defuzzifier as an input. It is then transformed back to the human language which was initially taken into the system. In this way, both the welder and non-welders can understand the system behavior to influence the environment it observes.

In summary, fuzzy logic is essentially a means to develop human-like capabilities for an AI algorithm that are closer to the way the human brain works. It provides a mathematical framework to model with words and sentences as humans do. In doing so, it helps humans to aggregate data and forms several partial truths which can be aggregated further into higher truths, which, in turn, when certain thresholds or conditions are exceeded, cause certain further results such as motor reaction. By incorporating this knowledge-based AI technique into DNN models, an explainable rule-based structure can be realized in DNN algorithms to alleviate the problems of strictly trading off interpretability for accuracy during the system modeling [18].

In this work, the hybrid fuzzy-DNN technique is necessary for AI TIG Welding system modeling for two reasons. Firstly, because the goal of this work is to develop a system where a human welder can interpret the algorithm decision to make further decisions, and secondly, DNN is a deterministic algorithm that does not account for uncertainties, imprecision, vagueness and ambiguities in the data.

The data we have at hand in modeling the system is human data (i.e., data extracted from a welder). This human data has inherent imprecisions, ambiguities and vagueness. The advantage of fuzzy logic is that it has the capability to model this kind of data. Therefore, incorporating fuzzy logic into the system modeling of a neural deep neural network algorithm helps to manage these imprecisions, ambiguities, vagueness and fuzziness [18].

Buah, Linnanen and Wu [4] showed that when DNN, fuzzy logic and Likert scale measurement techniques are combined, it can lead to an architecture called a fuzzy logic-based Likert Inference engine that can create a high dimensional data space for big augmented data to be extracted to augment small human linguistic statements. This data can be used to train a fuzzy-driven DNN algorithm to achieve results closer to the state-of-the-accuracy in DNN. Building on this prior work, this hybrid fuzzy-DNN architecture combined with Likert capability is the main technique that informed the proposed AI TIG Welding algorithm as illustrated in the process model in Figure 5.
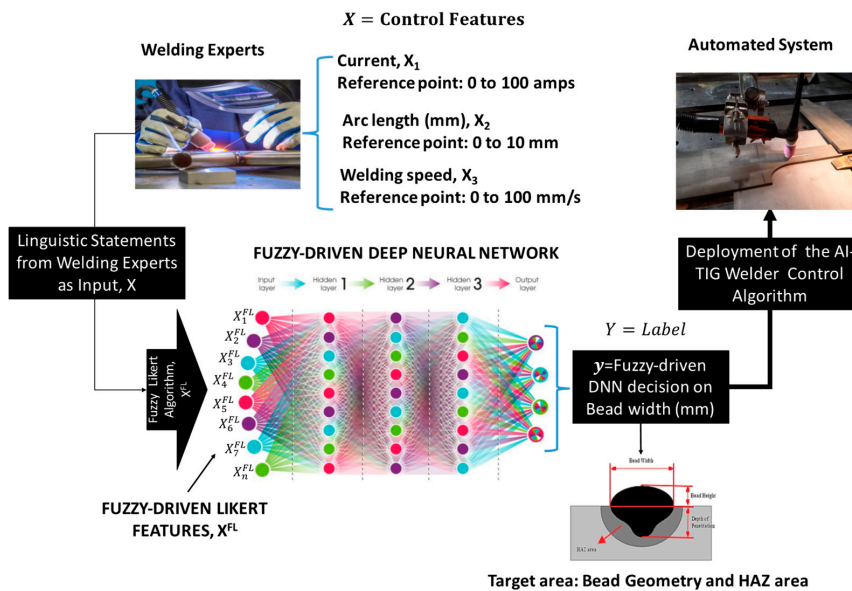
Figure 5. Process model of the artificial intelligence (AI) TIG Welding algorithm modeling steps.

Figure 5 illustrates the AI TIG welding algorithm that was built using three control features: X_1 as current (I), X_2 as arc length and X_3 as welding speed. The control parameters are used to predict weld bead width. Table 1 shows the scale ranges used in the system modeling for each parameter.

Table 1. Psychometric and fuzzy scaling for the parameters.

Control Parameters	Scale Range of Controlled Parameters, X on Psychometric Scale (Likert)	Corresponding Fuzzy Scale Range
Current	0 to 100 amps	0 to 1
Arc length	0 to 10 mm	0 to 1
Speed	0 to 100 mm/s	0 to 1
Bead width	0 to 10 mm	0 to 1

As illustrated in Figure 5, after defining the parameter ranges, the next step is learning about the control parameters and their theoretical association with the expected output from welding "experts". To accomplish this, literature was reviewed, and 13 expert-level rules were extracted. The rules are presented in Table 2.

Table 2. Linguistic rules used in designing the fuzzy logic-based Likert algorithm.

Rules and Variables	IF ... (Premise)			THEN (Conclusion)
Parameters	Current	Arc Length	Speed	Bead Width
Rule: 1	Low	Decrease	Very High	Narrow
Rule: 2	Very High	Decrease greatly	Very High	Wilder
Rule: 3	Low	Increase greatly	Very High	Fairly Wide
Rule: 4	Medium High	Decrease greatly	Very High	Narrow
Rule: 5	Very Low	Decrease greatly	Very High	Narrower
Rule: 6	Very Low	Increase greatly	Very High	Fairly Wide
Rule: 7	Very High	Decrease greatly	Very Low	Fairly Wider
Rule: 8	Very High	Increase greatly	Very Low	Wider
Rule: 9	Low	Decrease	Very High	Fairly Wide
Rule: 10	Low	Increase greatly	Very High	Fairly Wide
Rule: 11	Very High	Increase greatly	Low	Wider
Rule: 12	Very High	Decrease greatly	Low	Moderately Wide
Rule: 13	Low	Decrease	High	Narrower

The model architecture is a hybrid fuzzy–DNN model, hence big data is needed to build the model. The 13 expert-level rules are inadequate to train the deep neural network in the architecture. To manage this problem, we built on the work of Buah et al. [4]. and the X values were passed through a classifier called a fuzzy logic-based Likert algorithm as illustrated in Figure 6.
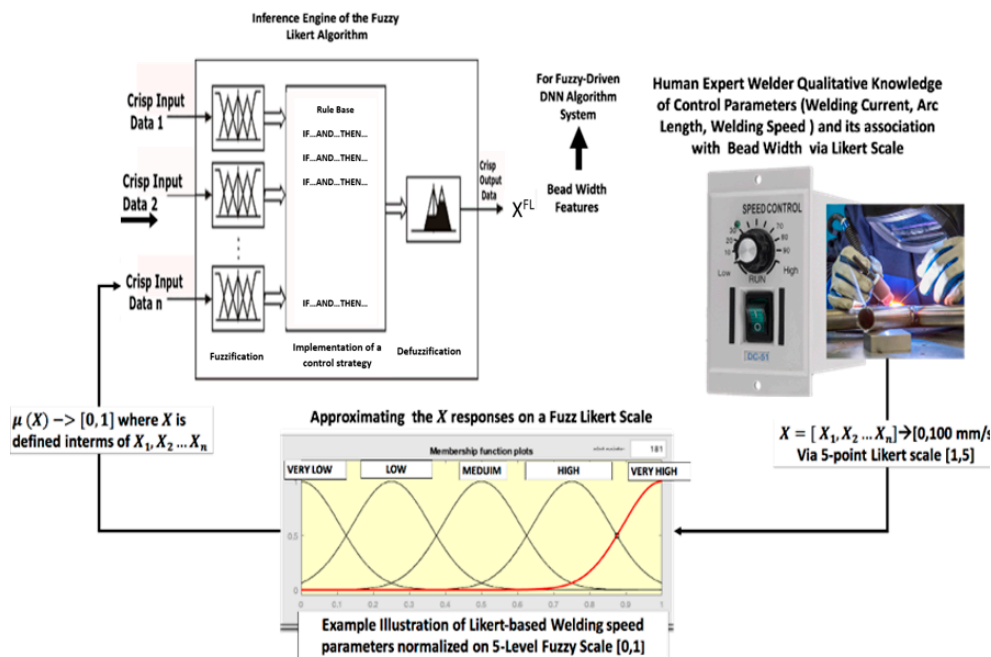
Figure 6. Fuzzy logic-based Likert inference.

The strength of the fuzzy logic-based Likert algorithm is that it helps to re-scale the raw data X from the human expert on a psychometric scale using traditional Likert scaling, which is then transformed into a fuzzy-driven feature denoted as X^{FL} as depicted in Figure 6. This is the engine for transforming an input variable X to obtain its fuzzy representations called fuzzy-driven Likert features, X^{FL}.

This transformation creates a data space with interval details so that additional data can be collected via data augmentation for training the fuzzy-driven DNN model as shown in Figure 5.

Mathematically, it is expressed as in Equation (1):

$$X^{FL} = f(X) \tag{1}$$

where X^{FL} is the target and X is the predictor of the target. So, the goal is to find a function, f that maps X and X^{FL} using fuzzy logical rules. Using a 6-point Likert scale, six fuzzy rules were defined to model the fuzzy Likert Inference engine. The extreme ends of the rule are as follows:

Rule 1: If X is Very Low THEN It is corresponding X^{FL} is also Very Low;

Rule 2: If X is Low THEN It is corresponding X^{FL} is also Low;

Rule 3: If X is Medium Low THEN It is corresponding X^{FL} is also Medium Low;

Rule 4: If X is Medium High THEN It is corresponding X^{FL} is Medium High;

Rule 5: If X is High THEN It is corresponding X^{FL} is High;

Rule 6: If X is Very High THEN It is corresponding X^{FL} is Very High.

Having defined the rule function $f(X)$ that maps X and X^{FL}, the fuzzy logic-based Likert algorithm was built using the information in Table 3.

Table 3. Description of features (Control variables) and labels (Outcome), their Likert values and corresponding fuzzy Likert crisp values for degree of truth.

Features and Labels	Linguistic Terms for Parameters	Fuzzy Likert Range,	Likert Value, X	Corresponding Fuzzy Range of Fuzzy Likert, X^{FL}
	Very Low	0	0	0–0.1704
	Low	17.1–30.4	23.75	0.171–0.304
Current (A)	Medium Low	31.0–50.4	40.7	0.31–0.504
0 to 100 A	Medium High	51.0–67.04	59.02	0.51–0.6704
	High	68.0–83.04	75.52	0.68–0.8304
	Very High	84.0–100	100	0.84–1
	Decrease greatly	0–1.704	0	0–0.1704
	Decrease	1.71–3.04	2.375	0.171–0.304
Arc Length (mm)	Slightly decrease	3.1–5.04	4.07	0.31–0.504
0 to 10 mm	Slightly Increase	5.1–6.704	5.902	0.51–0.6704
	Increase	6.8–8.304	7.552	0.68–0.8304
	Increase Greatly	8.4–10	10	0.84–1
	Very Low	0	0	0–0.1704
	Low	17.1–30.4	23.75	0.171–0.304
Speed (mm/s)	Medium Low	31.0–50.4	40.7	0.31–0.504
0 to 100 mm/s	Medium High	51.0–67.04	59.02	0.51–0.6704
	High	68.0–83.04	75.52	0.68–0.8304
	Very High	84.0–100	100	0.84–1
	Narrower	0–1.704	0	0–0.1704
	Narrow	1.71–3.04	2.375	0.171–0.304
Bead Width (mm)	Fairly Wide	3.1–5.04	4.07	0.31–0.504
0 to 10 mm	Moderately Wide	5.1–6.704	5.902	0.51–0.6704
	Fairly Wide	6.8–8.304	7.552	0.68–0.8304
	Wider	8.4–10	10	0.84–1

As indicated in Table 3, X was modelled with a 6-point Likert scale and X^{FL} was modelled with a six-level fuzzy membership function.

The fuzzy logic-based Likert algorithm was then applied to the rules in Table 4 to estimate their system boundaries (maximum and minimum data space). This technique helped re-write the experts rule as shown with an example using Rule 1 in Table 4.

Table 4. Modified expert rules using a fuzzy Likert algorithm.

Rules and Variables	If … (Premise)			Then (Conclusion)
Parameters	**Current**	**Arc Length**	**Speed**	**Bead Width**
Rule:1 $\rightarrow X$	Low	Decrease	Very High	Narrow
Rule:1 $\rightarrow X^{FL}$	17.1–30.4	1.71–3.04	84.0–100	Narrow (2.375)

Data augmentation was then carried between the data space of the control parameters. A big experimental dataset amounting to 24,012 training datasets was then extracted to train a fuzzy-driven DNN model as indicated in Figure 5. The idea of data augmentation is that many application domains do not have access to big data as in this case. Therefore, in machine learning, data augmentation is a form of data space solution to the problem of limited data. It encompasses a suite of techniques that enhance the size and quality of training datasets such that better deep learning models can be built [19]. As indicated in Table 4, no data augmentation was performed on the target behavior (weld bead) but rather the mean score of its system boundary is used as labels for the augmented features of the control variables. This was done to mitigate the model vulnerability to the course of dimensionality. With this understanding, the next section presents the training phase of the fuzzy-driven DNN model with the X^{FL} big data features extracted using the data augmentation technique.

3.1.2. Training, Validating and Testing the Fuzzy-Driven DNN Model

As shown in the AI TIG Welding process model in Figure 5, after the fuzzy-driven Likert features X^{FL} have been obtained for all the control variables and their corresponding labels, the next step is training the fuzzy-driven DNN model. The DNN model was implemented using the Keras deep learning library with Google TensorFlow backend using the Python language. Table 5 shows the experimental setting and model architecture.

Table 5. Experimental setting of the proposed DNN-based TIG Welding algorithm.

Learner Type	Neural Networks
Number of output nodes	3 classes with 6 sub-classes (see Figure 6 and Table 3)
Loss function	Categorical cross-entropy
Hidden layer	8-layer network with 6 hidden layers
	Total number of neurons: 188
Maximum number of training iterations	Epochs: 176 and Batch size: 122
Activation function	Rectified linear unit (ReLu)
Optimization algorithm	Stochastic gradient descent
Early stopping rule	Manual stopping by observation in loss in generality
Pre-training	No pre-trained model. The models were trained from scratch
	Dropout
Regularization	Dropout was applied to 6th and 7th layer with 0.05 and 0.55, respectively
	Training sample: 14,407
Dataset for training and validation	Validation sample: 9593
	Data split rule: 60/40
Dataset for testing: objective evaluation	27 experiments
Learning rate	0.003

As indicated in the experimental setting in Table 5, the proposed AI TIG Welding algorithm was built using neural networks and ReLU as an activation function. The expected output is theoretically in three classes but to capture more detailed information about the class labels, it was mathematically sub-divided into six subclasses using fuzzy mathematics, as shown in Figure 7, in line with Table 3.
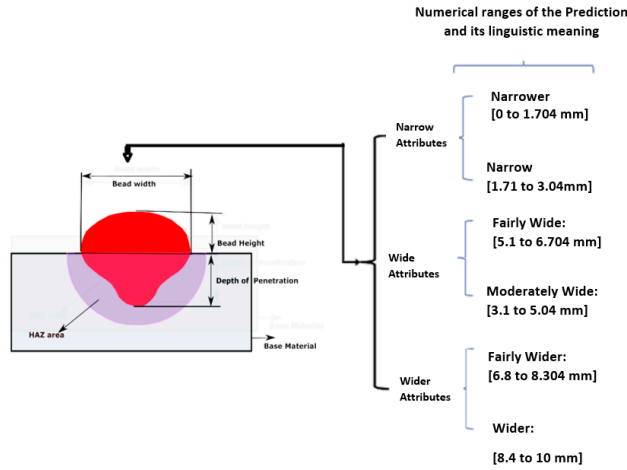
Figure 7. Number of output nodes of the model: 3 classes with 6 sub-classes.

The model parameters were tuned (optimized) using stochastic gradient descent. Dropout regularization technique was applied to the modeling to prevent the model from over-fitting into the training data since over-fitting affects the model's performance in generalizing to unseen cases. As indicated in the experimental setting, the algorithm was not built using a pre-trained model; it was trained from scratch. During the training, the model was monitored in addition to making necessary manual stops and the model's weights were recorded. In the experiment setting, the model was trained and validated with 24,000 experimental big data using 60/40 rules. Using this data split rule, the algorithm randomly used about 14,407 training datasets for training and 9593 for validation. Running the simulation at 176 epochs with a batch size of 122, we obtained a validation accuracy of 95.30%. To offer an objective evaluation of the model, we tested the model with independent data using a TIG process for a real-life experiment shared by Narang [20]. The next section gives a brief description of the experiment and reports the results that emerged when the model was applied to independent data.

3.2. Objective Evaluation of the AI TIG Welding Algorithm

Experiment: A structural steel specimen was welded with TIG welding processes using direct current straight polarity (DCSP), which was integrated with an arc image magnifying system. The length, width and thickness of the mild steel plates used for the experiments were 180 mm, 65 mm and 8 mm. The structural steel plates were cleaned properly to avoid unwanted scaling that can cause weld defects. During the welding process, shielding gas flow rate and diameter of the TIG electrode were kept constant. The chemical composition of the structural steel is given in Table 6.

Table 6. Chemical composition of the structural steel.

C %	Si %	Mn %	P %	S %	Ni %	Cr %	Fe %
0.16	0.178	0.45	0.18	0.07	0.13	0.016	98.84

The experimental setup of the TIG welding procedure integrated with a linear variable displacement transformer (LVDT) is illustrated in Figure 8. The LVDT was used during the experiments to set the gap between the electrode tip and workpiece. Trial runs were undertaken for the bead-on-plate welds to set the levels of three welding inputs of the process: welding current, traverse speed and arc length. In all, 27 test experiments of bead-on-plate welds were carried out and the results are shown in Table 7. Figure 9 shows the polished and etched TIG weldment cross-sections with different process parameters.
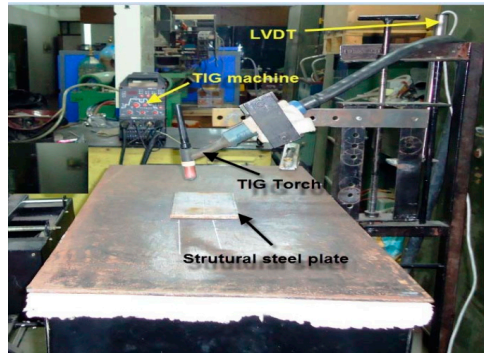
Figure 8. Experimental set-up of the TIG welding process.

Table 7. Test data for 27 test experiments of bead-on-plate welds.

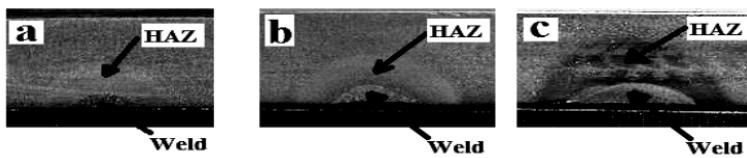| Serial Number (S.N)	Current (A)	Arc Length (mm)	Welding Speed (mm/s)	Bead Width (mm)	Depth of Penetration (mm)	Depth of HAZ (mm)	Width of HAZ (mm)
1	55	2	15	5.46	1.59	1.73	1.83
2	55	2	30	4.71	1.25	1.19	1.35
3	55	2	45	4.16	1.04	1.02	1.13
4	55	2.5	15	5.77	1.76	1.94	2.20
5	55	2.5	30	4.93	1.38	1.33	1.63
6	55	2.5	45	4.46	1.18	1.16	1.33
7	55	3	15	6.09	1.91	2.13	2.45
8	55	3	30	5.03	1.42	1.51	1.84
9	55	3	45	4.55	1.23	1.23	1.46
10	75	2	15	6.12	1.99	2.48	2.25
11	75	2	30	5.13	1.39	1.46	1.72
12	75	2.5	45	4.59	1.16	1.22	1.39
13	75	2.5	15	6.59	2.06	2.65	2.41
14	75	2.5	30	5.26	1.50	1.65	1.89
15	75	2.5	45	4.85	1.32	1.34	1.57
16	75	3	15	7.07	2.18	2.72	2.79
17	75	3	30	5.45	1.65	1.86	2.02
18	75	3	45	5.16	1.45	1.58	1.79
19	95	2	15	6.65	2.17	3.04	2.7
20	95	2	30	5.38	1.51	1.81	1.94
21	95	2	45	4.75	1.23	1.49	1.52
22	95	2.5	15	7.19	2.23	3.32	2.89
23	95	2.5	30	6.16	1.63	1.97	2.15
24	95	2.5	45	5.2	1.32	1.56	1.75
25	95	3	15	7.64	2.51	3.21	3.15
26	95	3	30	6.31	1.74	2.15	2.70
27	95	3	45	5.11	1.41	1.74	2.16

Figure 9. TIG welds polished and etched showing the weldments and HAZ with different process parameters. Current, arc length and traverse speeds are: (**a**) 55 A, 2 mm, 15 mm/s; (**b**) 75 A, 2.5 mm 30 mm/s; and (**c**) 95 A, 3 mm, 45 mm/s, respectively [20].

To obtain the same data structure used in modeling the AI TIG Welding algorithm, we pre-processed the bead width with the fuzzy logic-based Likert Inference engine in Figure 6 to obtain fuzzy Likert labels within the six classes in Table 3. The AI TIG Welding algorithm was then queried with the 27 unseen experiments. After approximately five seconds of running the simulation, the simulation results presented in Table 8 were obtained.

Table 8. Simulation experiment results when the class labels of the predicted values were compared with the observed values from the laboratory experiment.

S.N	Observed Values of Bead Width in LAB	Class Label of Observed Value in Fuzzy Likert Terms	Fuzzy Linguistic Terms for Observed Values	Predicted Value of Bead Width with the AI TIG Welding	Class Label of Predicted Values in Fuzzy Likert Terms
1	5.46	5.1–6.704	Fairly wide	5.1–6.704	Fairly wide
2	4.71	3.1–5.04	Moderately wide	3.1–5.04	Moderately wide
3	4.16	3.1–5.04	Moderately wide	3.1–5.04	Moderately wide
4	5.77	5.1–6.704	Fairly wide	5.1–6.704	Fairly wide
5	4.93	3.1–5.04	Moderately wide	3.1–5.04	Moderately wide
6	4.46	3.1–5.04	Moderately wide	3.1–5.04	Moderately wide
7	6.09	5.1–6.704	Fairly wide	5.1–6.704	Fairly wide
8	5.03	3.1–5.04	Moderately wide	3.1–5.04	Moderately wide
9	4.55	3.1–5.04	Moderately wide	3.1–5.04	Moderately wide
10	6.12	5.1–6.704	Fairly wide	5.1–6.704	Fairly wide
11	5.13	5.1–6.704	Fairly wide	5.1–6.704	Fairly wide
12	4.59	3.1–5.04	Moderately wide	3.1–5.04	Moderately wide
13	6.59	5.1–6.704	Fairly wide	5.1–6.704	Fairly wide
14	5.26	5.1–6.704	Fairly wide	5.1–6.704	Fairly wide
15	4.85	3.1–5.04	Moderately wide	3.1–5.04	Moderately wide
16	7.07	6.8–8.304	Fairly wider	6.8–8.304	Fairly wider
17	5.45	5.1–6.704	Fairly wide	5.1–6.704	Fairly wide
18	5.16	5.1–6.705	Fairly wide	3.1–5.04	Moderately wide
19	6.65	5.1–6.706	Fairly wide	6.8–8.304	Fairly wider
20	5.38	5.1–6.704	Fairly wide	5.1–6.704	Fairly wide
21	4.75	3.1–5.04	Moderately wide	3.1–5.04	Moderately wide
22	7.19	6.8–8.304	Fairly wider	6.8–8.304	Fairly wider
23	6.16	5.1–6.704	Fairly wide	5.1–6.704	Fairly wide
24	5.2	5.1–6.704	Fairly wide	5.1–6.704	Fairly wide
25	7.64	6.8–8.304	Fairly wider	6.8–8.304	Fairly wider
26	6.31	5.1–6.704	Fairly wide	5.1–6.704	Fairly wide
27	5.11	5.1–6.704	Fairly wide	5.1–6.704	Fairly wide

4. Result and Discussion

In this paper, the objective was to design an artificial intelligence (AI) TIG Welding algorithm to enhance the capability of the human welder to select appropriate input parameters to achieve good welding quality in the welding process. Using current, arc length and welding speed as case features (control variables), an AI-powered TIG Welding algorithm based on the architecture of a hybrid fuzzy deep neural network algorithm was trained. To offer an objective evaluation of the model, it was tested with experimental data from 27 welds. After training and validation, a validation accuracy of 95.30% was obtained by the AI-powered TIG welding architecture. The model was then empirically tested with new test data. Running the test simulation on the 27 real-life experimental data, we obtained the results in Table 6. As shown in the experimental results, the AI TIG welding algorithm exhibited 92.59% predictive accuracy. Out of 27 targets, it predicted 25 correctly with two mistakes (Experiments 18 and 19). As shown in the experimental results, the algorithm gave a hint on the maximum and minimum control range in which the human welder can operate to obtain the desired output. For example, using Experiment 1 as a case, in reference to Table 3, the algorithm suggested that if the current is regulated within 51 to 67.04 A and the arc length is selected within 1.71 to 3.04 mm and the welding speed is set up to a maximum of 17.04 mm/s or less, a moderately high weld bead width of approximately 5.1 to 6.704 can be achieved. This prediction is consistent with the real-life case in the experiment in Table 6, where

a current of 55 A was applied, and 2 mm arc length and 15 mm/s welding speed were set as control parameters. As indicated in the real-life case, a weld bead of 5.46 mm was recorded in the experiment, which is within the predictive range of the algorithm. This performance demonstrates the feasibility of our proposed method in supporting the human welder in automatic selection of control parameters to obtain the desired weld bead without going through a time-consuming trial-and-error approach.

In future work, the aim is to test the system with more experimental cases and expand its knowledge development to cover the depth of penetration, depth of the heat-affected zone (HAZ) and the width of the HAZ. The model should be tested in different domains of welding on best practices to improve the knowledge base of the proposed system to progress the field.

Author Contributions: M.A.K. performed the investigations, analyzed the data, and wrote the manuscript; E.B. ran the simulation test; H.H. supervised the investigation. G.K.A. discussed, edited and reviewed the manuscript. All authors have read and agreed to the published version of the manuscript.

Conflicts of Interest: The authors declare no conflicts of interest.

References

1. Harold, F.; Giles, Jr.; John, R.; Wagner, Jr. *Extrusion: The Definitive Processing Guide*, 2nd ed.; Willian Andrews Publications: Wayne, PA, USA, 2014.
2. Yung, W.K.C.; Ralph, B.; Lee, W.B.; Fenn, R. An investigation into welding parameters affecting the tensile properties of titanium welds. *J. Mater. Process. Technol.* **1997**, *63*, 759–764. [CrossRef]
3. Dutta, P.; Pratihar, D.K. Modeling of TIG welding process using conventional regression analysis and neural network-based approaches. *J. Mater. Process. Technol.* **2007**, *184*, 56–68. [CrossRef]
4. Buah, E.; Linnanen, L.; Wu, H. Emotional responses to energy projects: A new method for modeling and prediction beyond self-reported emotion measure. *Energy* **2020**, *190*, 116210. [CrossRef]
5. Torrisi, M.; Pollastri, G.; Le, Q. Deep learning methods in protein structure prediction. *Comput. Struct. Biotechnol. J.* **2020**, *521*, 436–444. [CrossRef]
6. Deng, L.; Yu, D. Deep Learning: Methods and Applications. *Found. Trends Signal Process.* **2014**, *7*, 197–387. [CrossRef]
7. Goodfellow, I. Deep Learning. Book in Preparation for MIT Press. 2016. Available online: http://www.deeplearningbook.org (accessed on 20 March 2020).
8. Deng, Y.; Bao, F.; Kong., Y.; Ren, Z.; Dai., Q. Deep direct reinforcement learning for financial signal representation and trading. *IEEE Trans. Neural Network Learn. Syst.* **2017**, *28*, 653–664. [CrossRef] [PubMed]
9. Deep Learning in Digital Pathology. Available online: http://www.global-engage.com/life-science/deep-learning-in-digital-pathology/ (accessed on 24 March 2020).
10. The Welding Institute. Available online: https://www.twi-global.com/technical-knowledge/job-knowledge/tungsten-inert-gas-tig-or-gta-welding-006 (accessed on 18 March 2020).
11. Larry, F.J. *Welding Principles and Applications*; Cengage Learning: Boston, MA, USA, 2002.
12. Larry, F.J. *Welding and Metal Fabrication*; Cengage Learning: Boston, MA, USA, 2002.
13. Azar, A.S.; Ås, S.; Akselsen, O.M. Determination of welding heat source parameters from actual bead shape. *Comput. Mater. Sci.* **2012**, *54*, 176–182. [CrossRef]
14. Dey, V.; Pratihar, D.K.; Datta, G.; Jha, M.N.; Saha, T.; Bapat, A. Optimization of bead geometry in electron beam welding using a Genetic Algorithm. *J. Mater. Process. Technol.* **2009**, *209*, 1151–1157. [CrossRef]
15. Anbarasan, N.; Oyyaravelu, R.; Kuppan, P. Effect of GMAW process parameters on the influence of bead geometry and HAZ area on ASTM A516 grade 70 Low alloy Pressure vessel steel. *Int. J. Technol. Chem. Res.* **2015**, *1*, 1–10.

16. Deshmukh, A.; Venkatachalam, G.; Divekar, H.; Saraf, M. Effect of Weld Penetration on Fatigue Life. *Procedia Eng.* **2014**, *97*, 783–789. [CrossRef]
17. Zadeh, L. The concept of a linguistic variable and its application to approximate reasoning—II. *Inf. Sci.* **1975**, *8*, 301–357. [CrossRef]
18. Bonanno, D.; Nock, K.; Smith, L.; Elmore, P.; Petry, F. An approach to explainable deep learning using fuzzy inference. Next-Generation Analyst V. *Proc. SPIE* **2017**, *10207*, 102070D.
19. Shorten, C.; Khoshgoftaar, T.M. A survey on Image Data Augmentation for Deep Learning. *J. Big Data* **2019**, *6*, 60. [CrossRef]
20. Narang, H.; Singh, U.; Mahapatra, M.; Jha, P. Prediction of the weld pool geometry of TIG arc welding by using fuzzy logic controller. *Int. J. Eng. Sci. Technol.* **2011**, *3*, 77–85. [CrossRef]

ACTA UNIVERSITATIS LAPPEENRANTAENSIS

934. XIN, YAN. Knowledge sharing and reuse in product-service systems with a product lifecycle perspective. 2020. Diss.

935. PALACIN SILVA, VICTORIA. Participation in digital citizen science. 2020. Diss.

936. PUOLAKKA, TIINA. Managing operations in professional organisations – interplay between professionals and managers in court workflow control. 2020. Diss.

937. AHOLA, ANTTI. Stress components and local effects in the fatigue strength assessment of fillet weld joints made of ultra-high-strength steels. 2020. Diss.

938. METSOLA, JAAKKO. Good for wealth or bad for health? Socioemotional wealth in the internationalisation process of family SMEs from a network perspective. 2020. Diss.

939. VELT, HANNES. Entrepreneurial ecosystems and born global start-ups. 2020. Diss.

940. JI, HAIBIAO. Study of key techniques in the vacuum vessel assembly for the future fusion reactor. 2020. Diss.

941. KAZARNIKOV, ALEXEY. Statistical parameter identification of reaction-diffusion systems by Turing patterns. 2020. Diss.

942. SORMUNEN, PETRI. Ecodesign of construction and demolition waste-derived thermoplastic composites. 2020. Diss.

943. MANKONEN, ALEKSI. Fluidized bed combustion and humidified gas turbines as thermal energy conversion processes of the future. 2020. Diss.

944. KIANI OSHTORJANI, MEHRAN. Real-time efficient computational approaches for hydraulic components and particulate energy systems. 2020. Diss.

945. PEKKANEN, TIIA-LOTTA. What constrains the sustainability of our day-to-day consumption? A multi-epistemological inquiry into culture and institutions. 2021. Diss.

946. NASIRI, MINA. Performance management in digital transformation: a sustainability performance approach. 2021. Diss.

947. BRESOLIN, BIANCA MARIA. Synthesis and performance of metal halide perovskites as new visible light photocatalysts. 2021. Diss.

948. PÖYHÖNEN, SANTERI. Variable-speed-drive-based monitoring and diagnostic methods for pump, compressor, and fan systems. 2021. Diss.

949. ZENG, HUABIN. Continuous electrochemical activation of peroxydisulfate mediated by single-electron shuttle. 2021. Diss.

950. SPRINGER, SEBASTIAN. Bayesian inference by informative Gaussian features of the data. 2021. Diss.

951. SOBOLEVA, EKATERINA. Microscopy investigation of the surface of some modern magnetic materials. 2021. Diss.

952. MOHAMMADI ASL, REZA. Improved state observers and robust controllers for non-linear systems with special emphasis on robotic manipulators and electro-hydraulic servo systems. 2021. Diss.

953. VIANNA NETO, MÁRCIO RIBEIRO. Synthesis and optimization of Kraft process evaporator plants. 2021. Diss.

954. MUJKIC, ZLATAN. Sustainable development and optimization of supply chains. 2021. Diss.

955. LYYTIKÄINEN, JOHANNA. Interaction and barrier properties of nanocellulose and hydrophobically modified ethyl(hydroxyethyl)cellulose films and coatings. 2021. Diss.

956. NGUYEN, HOANG SI HUY. Model based design of reactor-separator processes for the production of oligosaccharides with a controlled degree of polymerization. 2021. Diss.

957. IMMONEN, HEIKKI. Application of object-process methodology in the study of entrepreneurship programs in higher education. 2021. Diss.

958. KÄRKKÄINEN, HANNU. Analysis of theory and methodology used in determination of electric motor drive system losses and efficiency. 2021. Diss.

959. KIM, HEESOO. Effects of unbalanced magnetic pull on rotordynamics of electric machines. 2021. Diss.

960. MALYSHEVA, JULIA. Faster than real-time simulation of fluid power-driven mechatronic machines. 2021. Diss.

961. SIEVINEN, HANNA. Role of the board of directors in the strategic renewal of later-generation family firms. 2021. Diss.

962. MENDOZA MARTINEZ, CLARA. Assessment of agro-forest and industrial residues potential as an alternative energy source. 2021. Diss.

963. OYEWO, AYOBAMI SOLOMON. Transition towards decarbonised power systems for sub-Saharan Africa by 2050. 2021. Diss.

964. LAHIKAINEN, KATJA. The emergence of a university-based entrepreneurship ecosystem. 2021. Diss.

965. ZHANG, TAO. Intelligent algorithms of a redundant robot system in a future fusion reactor. 2021. Diss.

966. YANCHUKOVICH, ALEXEI. Screening the critical locations of a fatigue-loaded welded structure using the energy-based approach. 2021. Diss.

967. PETROW, HENRI. Simulation and characterization of a front-end ASIC for gaseous muon detectors. 2021. Diss.

968. DONOGHUE, ILKKA. The role of Smart Connected Product-Service Systems in creating sustainable business ecosystems. 2021. Diss.

969. PIKKARAINEN, ARI. Development of learning methodology of additive manufacturing for mechanical engineering students in higher education. 2021. Diss.

970. HOFFER GARCÉS, ALVARO ERNESTO. Submersible permanent-magnet synchronous machine with a stainless core and unequal teeth widths. 2021. Diss.

971. PENTTILÄ, SAKARI. Utilizing an artificial neural network to feedback-control gas metal arc welding process parameters. 2021. Diss.

LUT
University